TNO Built Environment and Geosciences

Princetonlaan 6
P.O. Box 80015
3508 TA Utrecht
The Netherlands

T +31 30 256 45 32
F +31 30 256 46 05
info-BenO@tno.nl

TNO report

2007-U-R1272C

Velmod-2

Joint Industry Project

Date	November 2007
Author(s)	Drs. W. van Dalfsen, Drs. S.F. van Gessel, Drs. J.C. Doornenbal
Number of pages	97
Customer	Ascent Resources, Chevron, Cirrus Energy, EBN, Gaz de France, NAM, Northern Petroleum, Petro-Canada, PGS, Total, Vermilion and Wintershall
Projectname	Velmod-2
Projectnumber	034.62155

Contents

List of figures

Figure 20 Local velocities at borehole MDN-01 according to non-calibrated sonic data

List of tables

List of appendices (on DVD)

List of goodies

Goody	1-1	V_{int}-distribution of the layer of the North Sea Supergroup (NU+NM+NL)
Goody	1-1a	V_{int}-distribution of the layer of the Upper North Sea Group (NU)
Goody	1-1b	V_{int}-distribution of the layer of the Middle and Lower North Sea groups (NM+NL)
Goody	1-2	V_{int}-distribution of the layer of the Chalk Group (CK)
Goody	1-3	V_{int}-distribution of the layer of the Rijnland Group (KN)
Goody	1-3a	V_{int}-distribution of the layer of the Holland Formation (KNGL)
Goody	1-3b	V_{int}-distribution of the layer of the Vlieland subgroup (KNN)
Goody	1-4	V_{int}-distribution of the layer of the Schieland, Scruff and Niedersachsen groups (SL+SG+SK)
Goody	1-5	V_{int}-distribution of the layer of the Altena Group (AT)
Goody	1-6	V_{int}-distribution of the layer of the Upper and Lower Germanic Trias groups (RN+RB)
Goody	1-6a	V_{int}-distribution of the layer of the Upper Germanic Trias Group (RN)
Goody	1-6b	V_{int}-distribution of the layer of the Lower Germanic Trias Group (RB)
Goody	1-8	V_{int}-distribution of the layer of the Upper Rotliegend Group (RO)
Goody	1-9	V_{int}-distribution of the layer of the Limburg Group (DC)
Goody	2-1	Kriging standard deviation of V_{int} for the layer of the North Sea Supergroup (NU+NM+NL)
Goody	2-1a	Kriging standard deviation of V_{int} for the layer of the Upper North Sea Group (NU)
Goody	2-1b	Kriging standard deviation of V_{int} for the layer of the Middle and Lower North Sea groups (NM+NL)

Goody	2-2	Kriging standard deviation of V_{int} for the layer of the Chalk Group (CK)
Goody	2-3	Kriging standard deviation of V_{int} for the layer of the Rijnland Group (KN
Goody	2-3a	Kriging standard deviation of V_{int} for the layer of the Holland Formation (KNGL)
Goody	2-3b	Kriging standard deviation of V_{int} for the layer of the Vlieland subgroup (KNN)
Goody	2-4	Kriging standard deviation of V_{int} for the layer of the Schieland, Scruff and Niedersachsen groups (SL+SG+SK)
Goody	2-5	Kriging standard deviation of V_{int} for the layer of the Altena Group (AT)
Goody	2-6	Kriging standard deviation of V_{int} for the layer of the Upper and Lower Germanic Trias groups (RN+RB)
Goody	2-6a	Kriging standard deviation of V_{int} for the layer of the Upper Germanic Trias Group (RN)
Goody	2-6b	Kriging standard deviation of V_{int} for the layer of the Lower Germanic Trias Group (RB)
Goody	2-8	Kriging standard deviation of V_{int} for the layer of the Upper Rotliegend Group (RO)
Goody	2-9	Kriging standard deviation of V_{int} for the layer of the Limburg Group (DC)
Goody	3-1	Variogram model of the V_{int}-values for the North Sea Supergroup
Goody	3-1a	Variogram model of the V_{int} -values for the Upper North Sea Group
Goody	3-1b	Variogram model of the V_{int} -values for the Middle and Lower North Sea groups
Goody	3-2	Variogram model of the V_{int} -values for the Chalk Group
Goody	3-3	Variogram model of the V_{int} -values for the Rijnland Group
Goody	3-3a	Variogram model of the V_{int} -values for the Holland Formation

Goody 3-3b	Variogram model of the V_{int} -values for the Vlieland subgroup
Goody 3-4	Variogram model of the V_{int} -values for the Schieland, Scruff and Niedersachsen groups
Goody 3-5	Variogram model of the V_{int} -values for the Altena Group
Goody 3-6	Variogram model of the V_{int} -values for the Upper and Lower Germanic Trias groups
Goody 3-6a	Variogram model of the V_{int} -values for the Upper Germanic Trias Group
Goody 3-6b	Variogram model of the V_{int} -values for the Lower Germanic Trias Group
Goody 3-8	Variogram model of the V_{int} -values for the Upper Rotliegend Group
Goody 3-9	Variogram model of the V_{int} -values for the Limburg Group

1 Introduction

TNO, eleven E&P companies in the Netherlands and an oilfield service company were engaged in VELMOD-2, the building of a comprehensive seismic velocity model (on a grid of 1 km x 1 km) that covers Dutch territory, both onshore and offshore, in its entirety. TNO's partners in the VELMOD-2 Joint Industry Project (JIP) were: Ascent Resources, Chevron, Cirrus Energy, EBN, Gaz de France, NAM, Northern Petroleum, Petro-Canada, PGS, Total, Vermilion and Wintershall.

VELMOD-2 is the successor of VELMOD-1, a seismic velocity model that was built in a previous JIP (Van Dalfsen et al., 2006a; Van Dalfsen et al., 2006b). Both models have been based on sonic logs to which had been assigned depth markers of lithostratigraphic layer boundaries.

In comparison with its predecessor, VELMOD-2 had at its disposal more digital sonic data of much more boreholes. Enlargement of the digital sonics database was effected by E&P companies making available digital or digitized sonic data, checkshot data and borehole deviation data. Also, the layer cake model of VELMOD-2 includes more layers, as three layers of VELMOD-1 were each split into two sublayers.

In reading this report on VELMOD-2, one should resort time and again to the Appendices 1 and 2 (on DVD in this report) . In these appendices, all essential data of VELMOD-2 have been conveniently arranged.

2 Data

Sonics data

Borehole sonics datafiles available to VELMOD-2 are listed in the first column of Appendix 1. The datafiles are contained in Appendix 7. There are three types of files.

First, files of digital or digitized composite sonic logs. Usually these files contain slowness data as a function of depth measured along the borehole path. Exceptionally, files contain instantaneous (local) sonic velocities instead of slowness values.

Second, digital files with densely sampled traveltime (T)-depth (Z) pairs. The TZ-pairs resulted from sonic log calibration with checkshot data.

Third, V_{int}-Z_{mid} pairs taken from analogous composite sonic logs. Determination and inventory of these pairs was accomplished in SNET, a previous seismic velocity modeling project of TNO (Doornenbal, 2001).

The second column of Appendix 1 lists the shortnames of the boreholes in which the sonics data have been obtained. These shortnames conform to the borehole names in the National Geo-data Centre of the Netherlands – DINO, accessible through the 'NL Olie- en Gasportaal' at www.nlog.nl.

It is noted that several sonics datafiles are available for most boreholes. The sonic data on the files for one and the same borehole are not necessarily all the same. This is due to differently executed manipulations on sonic data in the workflow that turns a number of sonic logs, run on different depth sections of a borehole, into a composite (calibrated) log. Differences in composite sonic logs of a borehole may be traced to the way log analysts and geophysiscists have performed data editing, processing, interpretation and calibration.

Deviation data

Apart from the borehole deviation data already available from DINO, E&P companies also provided deviation data for VELMOD-2. For boreholes with several files of deviation data, files were ranked and the file with highest ranking was qualified as default deviation file in DINO.

Lithostratigraphic marker data

Borehole lithostratigraphic marker data needed for VELMOD-2 were retrieved from DINO. These markers are those assigned and used by TNO. Lithostratigraphy conforms to the standard stratigraphic nomenclature of the Netherlands (Van Adrichem Boogaert & Kouwe, 1993-1997). The way stratigraphic data are used at deviated boreholes, is described in Chapter 3

3 Layer cake model.

General model

In VELMOD, the velocity model is of the so-called layer cake type: seismic velocity is modeled per lithostratigraphic layer. The layers involved in VELMOD-2 are presented in Figure 1.

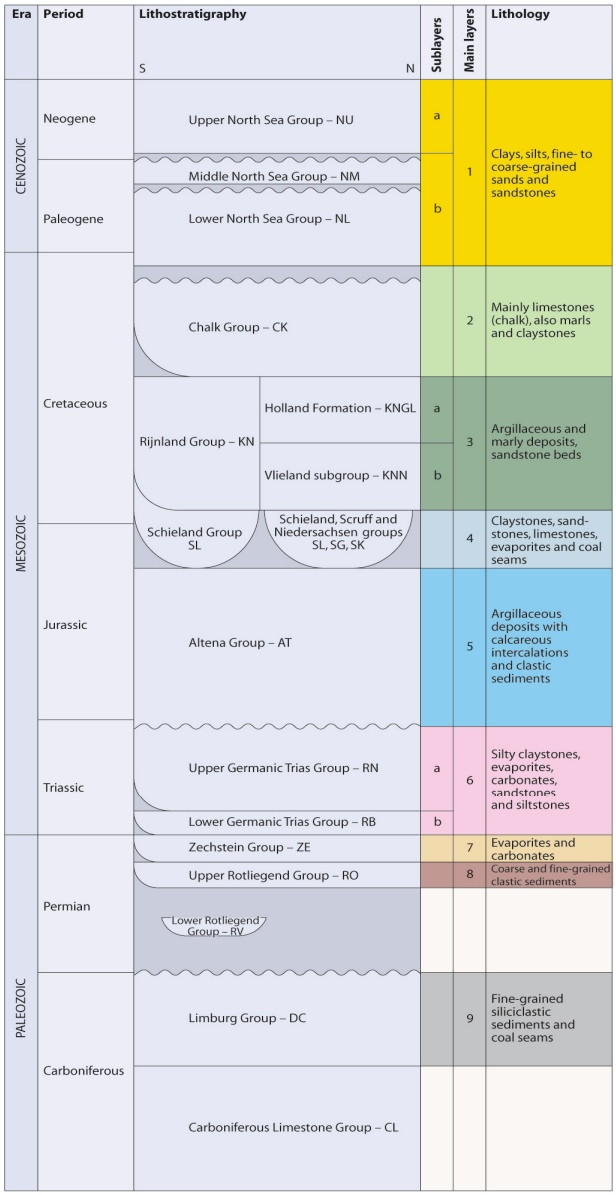

Figure 1 Layer cake model of VELMOD-2 based on lithostratigraphy after Van Adrichem Boogaert and Kouwe (1993-1997)

There are two layer cakes: the main one of nine layers, also applied in VELMOD-1, and a layer cake with three main layers (numbers 1, 3 and 6) each split into two sublayers (Figure 1).

Determination and processing of layer data at boreholes

Determination and processing of layer data is straightforward at vertical boreholes. The procedure for processing layer parameters in case of a deviated borehole is clarified in Figure 2.

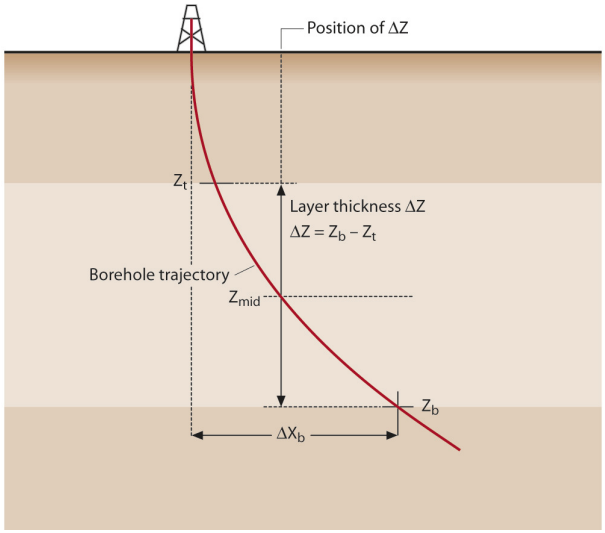

Figure 2 Assignment of layer data to a deviated borehole

ΔX_b is a component of the borehole deviation at the base of a layer. The layer parameters Z_t, Z_{mid}, Z_b and ΔZ are assigned to the position of Z_{mid}. It is noted that these layer parameters are less accurate at boreholes where the layer boundaries deviate from horizontal. Data columns of the parameters Z_{mid} and ΔZ have been included in Appendix 1; depths are stated with reference to the standard datum level of the Netherlands. It is to be noted that the ΔZ-values for the lowermost layer (that of the Limburg Group) do not, as a rule, represent the thickness of this layer, but only a fraction of it. The mere reason for this is that only a few boreholes in the Netherlands perforate the layer of the Limburg Group. TZ-data are compiled in Appendix 6.

Local sonic velocities per lithostratigraphic layer at boreholes

All digital sonic data of VELMOD-2 can be viewed in the form of local (or instantaneous) velocities plotted against true vertical depth with reference to standard datum. Figure 3 shows local velocities in borehole L08-G-01. The local velocity graphs are coloured per lithostratigraphic layer, with layer base depths (Z_b) and layer base deviations from the vertical (ΔX_b and ΔY_b) listed in columns. Appendix 2 contains all local velocity graphs of VELMOD-2, including a column of sonic traveltime data (ΔT) and columns of the layerwise local velocity parameters (v_0 and k). The latter parameters are described in Chapter 4.

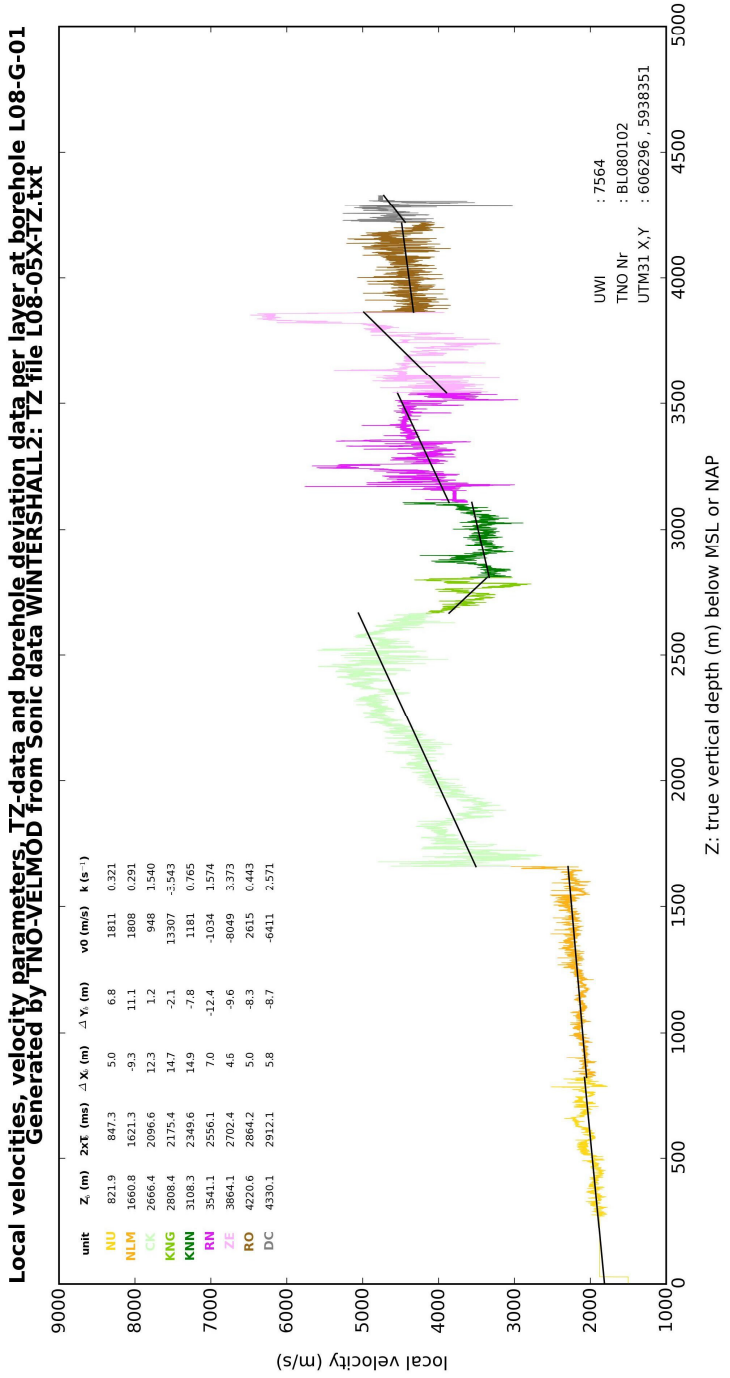

Figure 3 Local velocities, velocity parameters, TZ-data and borehole deviation data per lithostratigraphic layer at borehole L08-G-01

4 VELMOD velocity models for compacting layers

Models with linear depth dependency of velocity

Except the layer of the Zechstein Group, all layers of the layer cake model (Figure 1) have been subjected to considerable compaction due to sediment loading during burial phases. This compaction resulted in an increase of compressional wave velocity of layer sediments with burial depth.

For the compacting layers, we adopt model velocities that increase linearly with depth. A velocity model of this type is completely described by only two parameters.

In VELMOD-2, we present two different models with linear depth dependency of model velocity. First a local velocities based model, and second a model based on the V_{int} - Z_{mid} method (Robein, 2003) combined with parameter calibration through the layer traveltimes (ΔT) at boreholes. Both models are described below.

Local velocities based model

In this model, local (or instantaneous) velocities at boreholes are approximated with model velocities with parametrization:

$$v\,(X,Y,Z) = v_0(X,Y) + k(X,Y) \bullet Z$$

Here v is model velocity, whereas v_0 and k are position dependent model parameters. Figure 3 shows the results of the model applied to the local velocities of borehole L08-G-01. All v_0- and k-values of VELMOD-2 are presented in Appendices 1 and 2.

V_{int} - Z_{mid} method based model with calibration on ΔT

In this model, model velocities V(X,Y,Z) are parameterized as:

$$V(X,Y,Z) = V_0\,(X,Y) + K \bullet Z$$

K is determined according to the V_{int} - Z_{mid} method applied to collections of V_{int} - Z_{mid} pairs. All selected V_{int} - Z_{mid} pairs of VELMOD-2 are preceded by the x-sign in Appendix 1.

For most layers, one K-value applies for the entire Dutch territory, both onshore and offshore. For some layers this territory is subdivided in regions. This applies for the layer of the Schieland, Scruff and Niedersachsen groups (main layer 4), and the layer of the Altena Group (main layer 5). The subdivision of the Dutch territory into regions for the above layers is shown in Figure 4. These regions conform to regional structures or structural elements as presented in Duin et al. (2006).

Linear regressions for the determination of the K-values are shown in Figure 5 for the compacting main layers, and in Figure 6 for the sublayers. K-values, together with other regression data, are listed in Tables 1 and 2.

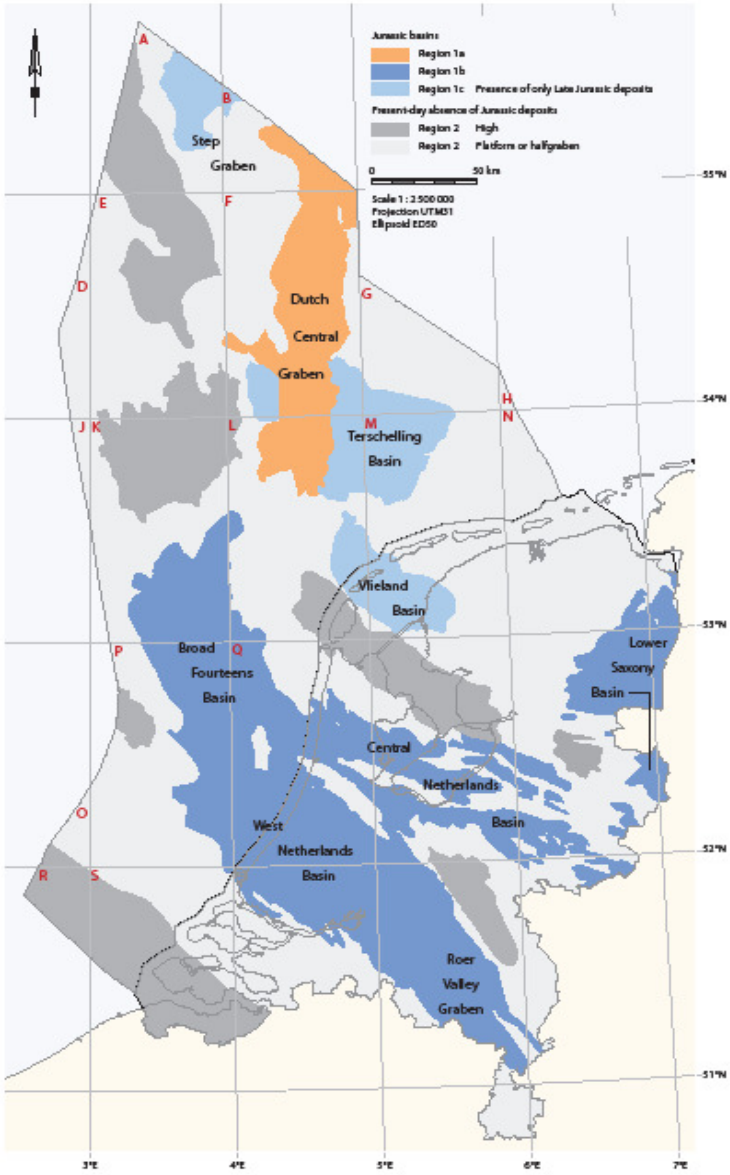

Figure 4 Regional subdivision of K for the layers with Jurassic sediments

Table 1 K-values and other linear V_{int} - Z_{mid} regression data for compacting main layers of VELMOD-2

Main layer	Litho-code	Area	# Boreholes	K (s^{-1})	V_0^{area} (m/s)	Correlation coefficient r
1	NU+NM+NL	Dutch territory	598	0.321	1757	0.849
2	CK	Dutch territory	680	0.864	2359	0.844
3	KN	Dutch territory	756	0.508	2120	0.781
4	SL+SG+SK	Region 1a	52	0.805	1090	0.794
4	SL+SG+SK	Region 1b	127	0.635	2334	0.705
4	SL+SG+SK	Region 1c	41	0.854	1209	0.819
5	AT	Region 1a	17	0.601	1559	0.880
5	AT	Region 1b	165	0.484	2221	0.783
6	RN+RB	Dutch territory	498	0.367	3143	0.571
8	RO	Dutch territory	456	0.354	2979	0.654
9	DC	Dutch territory	295	0.273	3400	0.701

Table 2 K-values and other linear V_{int} - Z_{mid} regression data for sublayers of VELMOD-2

Sub-layer	Litho-code	Area	# Boreholes	K (s^{-1})	V_0^{area} (m/s)	Correlation coefficient r
1a	NU	Dutch territory	265	0.429	1742	0.737
1b	NM+NL	Dutch territory	373	0.198	1833	0.551
3a	KNGL	Dutch territory	679	0.637	1985	0.877
3b	KNN	Dutch territory	596	0.441	2174	0.653
6a	RN	Dutch territory	353	0.374	3185	0.578
6b	RB	Dutch territory	466	0.417	3087	0.582

The local parameter V_0 is determined at borehole locations by the following calibration formula (Japsen, 1993):

$$V_0(X,Y) = K \bullet [Z_b - Z_t \bullet \exp(K \bullet \Delta T)] \bullet [\exp(K \bullet \Delta T) - 1]^{-1}$$

This formula makes traveltime according to the V_{int} - z_{mid} method equal to the vertical traveltime ΔT according to the sonic data. The ΔT-values of VELMOD-2 are listed in Appendix 1. V_0-values are listed in Appendix 5-1.

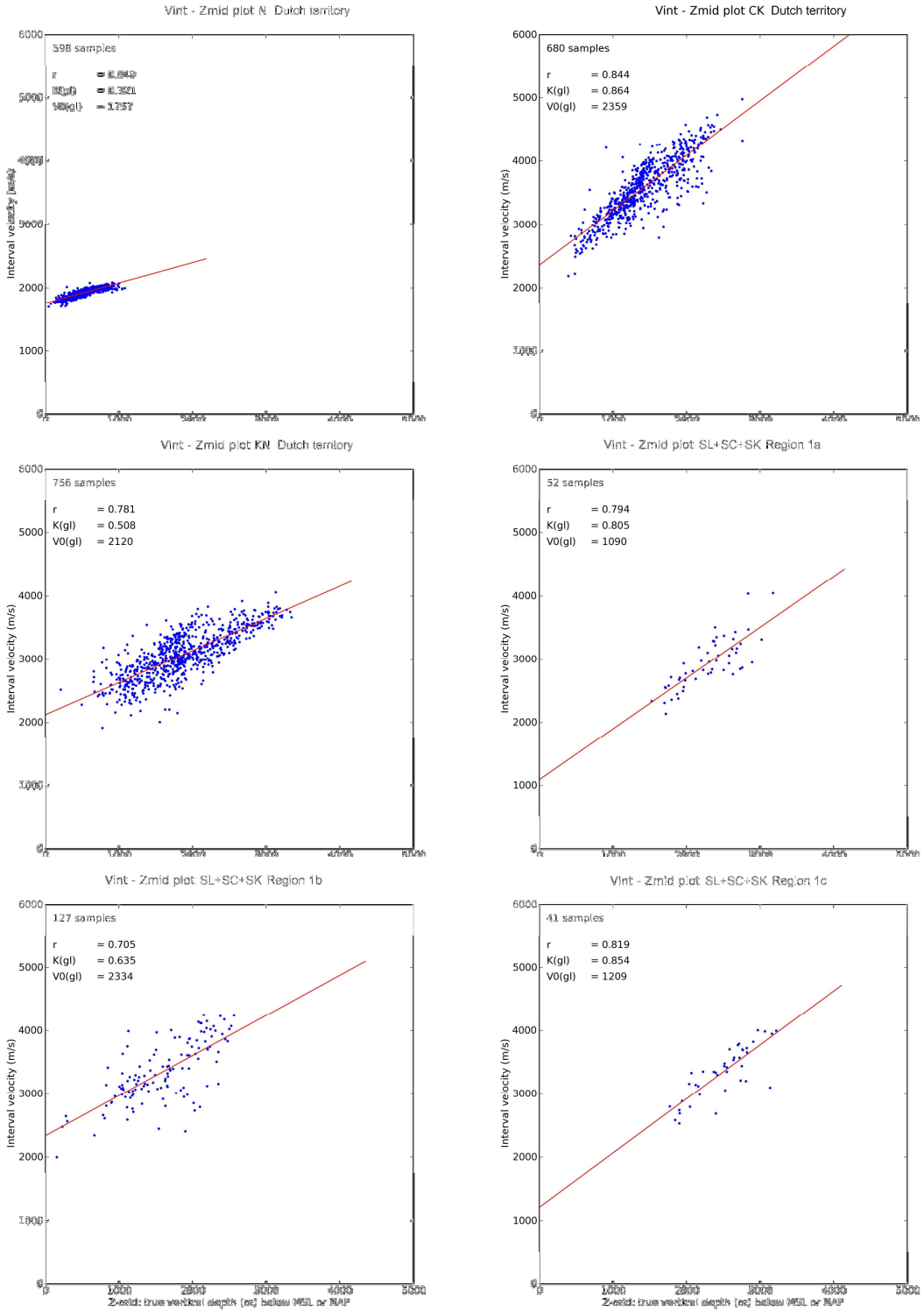

Figure 5 Linear least squares relation between V_{int} and Z_{mid} for the compacting main layers of VELMOD-2

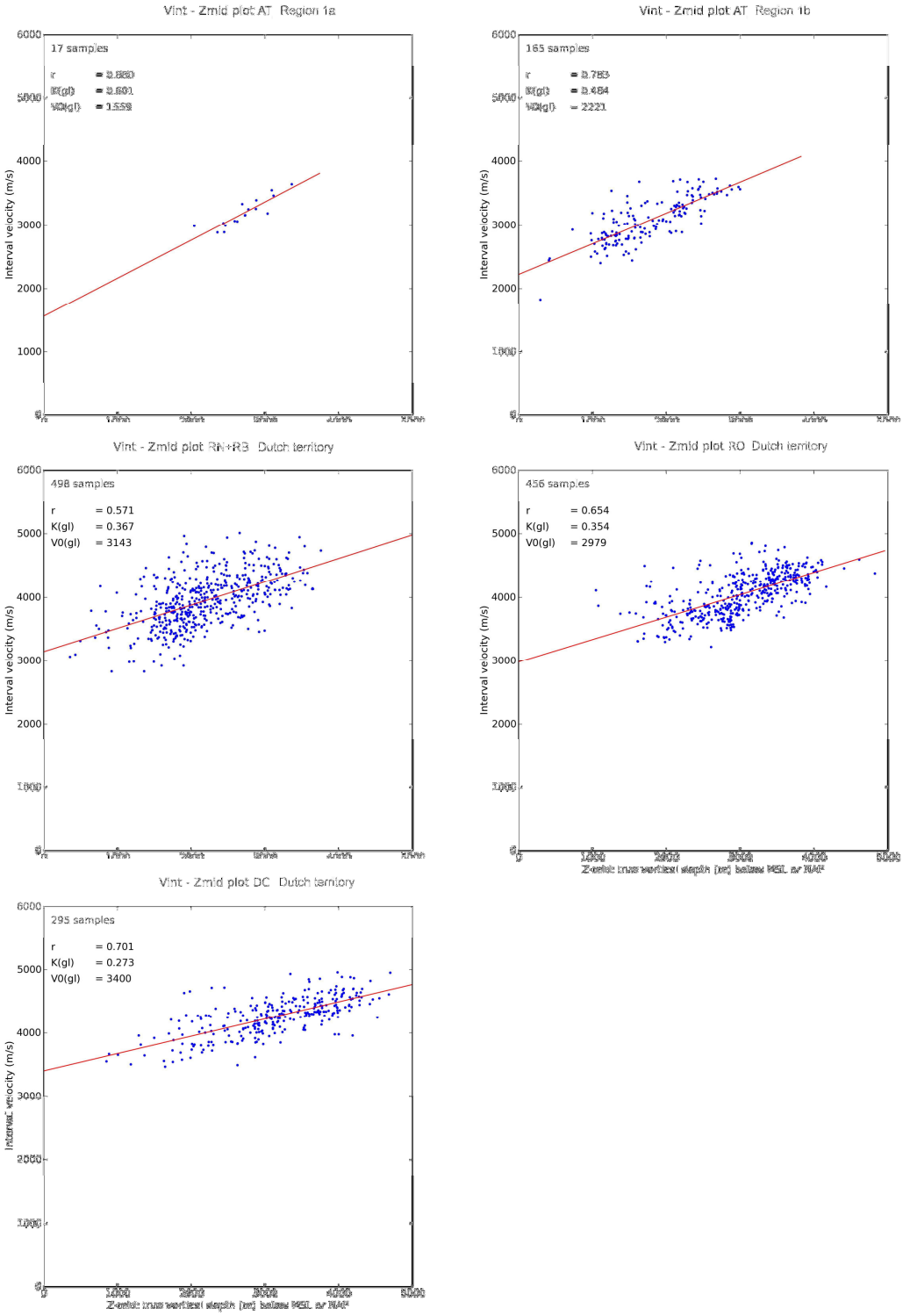

Figure 5 Linear least squares relation between V_{int} and Z_{mid} for the compacting main layers of VELMOD-2 (continued)

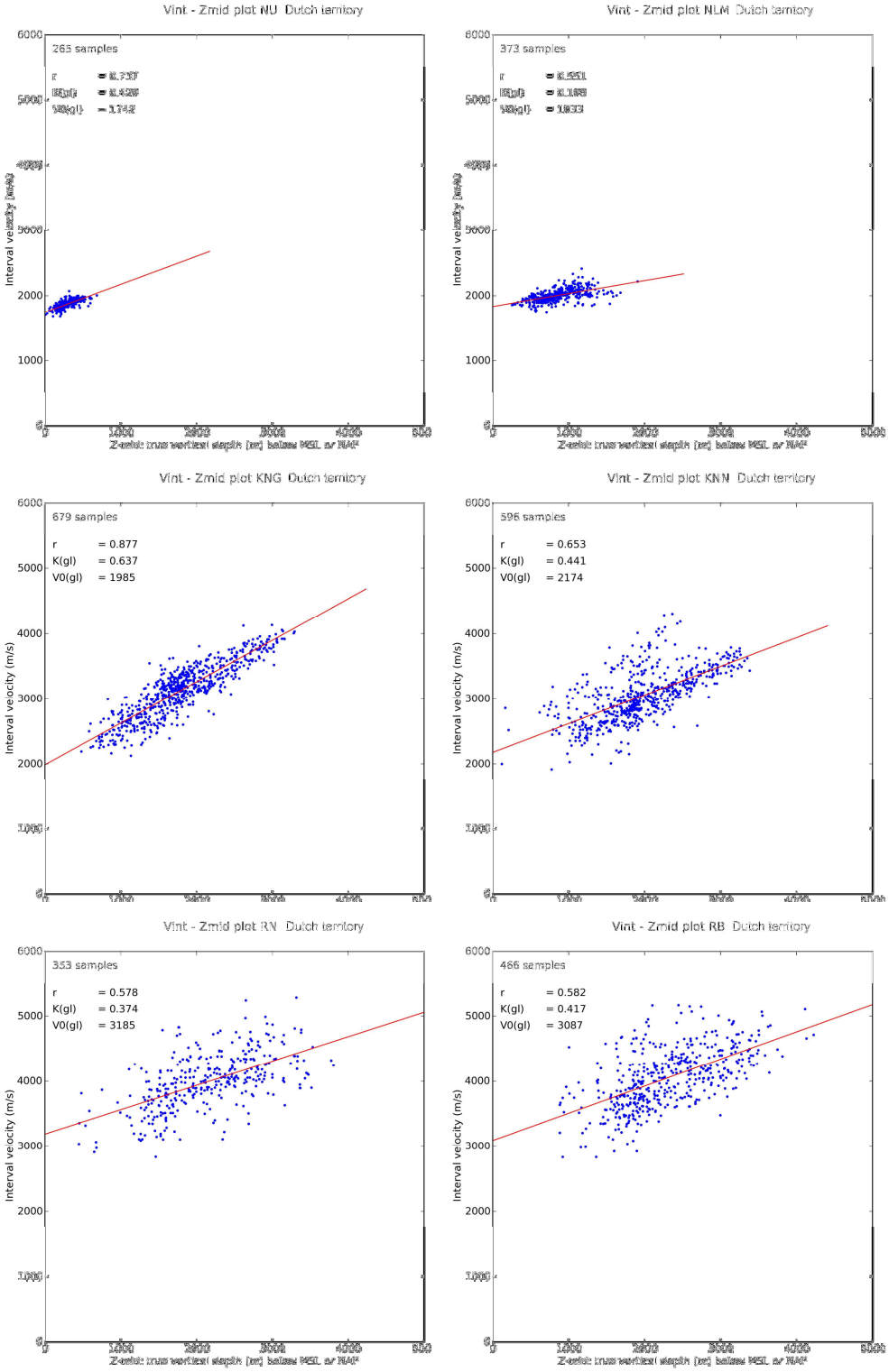

Figure 6 Linear least squares relation between V_{int} and Z_{mid} for the sublayers of VELMOD-2

Grids of V_0 and its kriging standard deviation

Ordinary block kriging (Goovaerts, 1997) was applied to the V_0-values at borehole locations to obtain grids of both V_0 and its kriging standard-deviation (Appendix 3). The cell size of the grids is 1 km x 1 km. The V_0-variogram models used for kriging are shown in Figures 7 and 8.

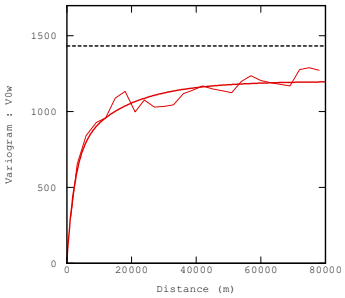

North Sea Supergroup (N)

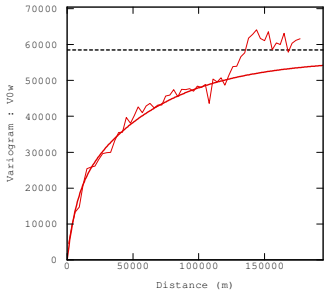

Chalk Group (CK)

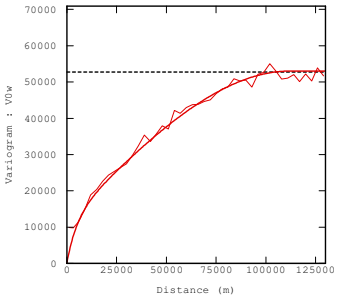

Rijnland Group (KN)

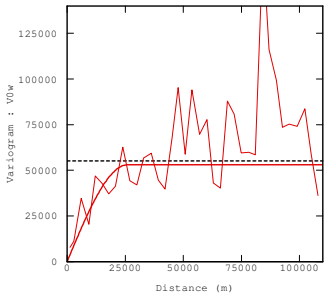

Schieland, Scruff and Niedersachsen groups (SL+SG+SK), region 1a

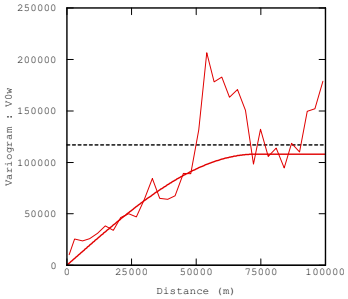

Schieland, Scruff and Niedersachsen groups (SL+SG+SK), region 1b

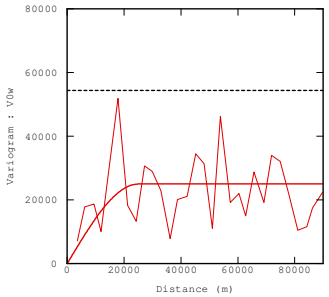

Schieland, Scruff and Niedersachsen groups (SL+SG+SK), region 1c

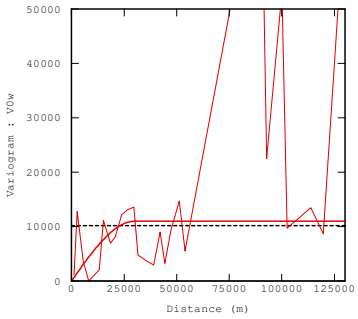

Altena Group (AT), region 1a

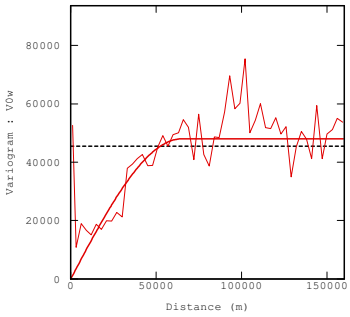

Altena Group (AT), region 1b

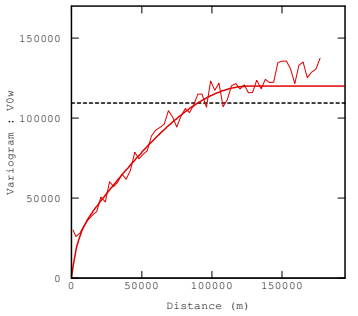

Upper and Lower Germanic Trias groups (RN+RB)

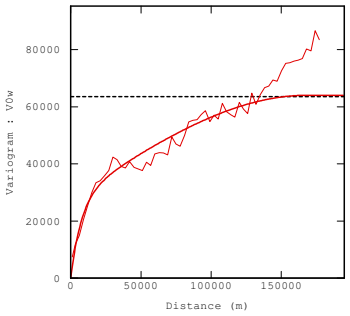

Upper Rotliegend Group (RO)

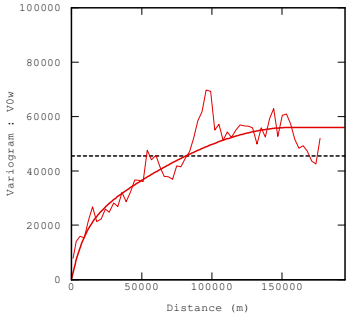

Limburg Group (DC)

Figure 7 Variogram models of the V_0-values for the compacting main layers of VELMOD-2

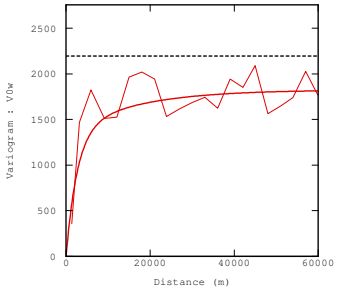

Upper North Sea Group (NU)

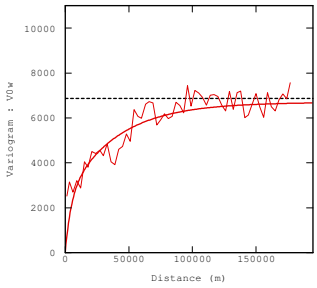

Middle and Lower North Sea Groups (NM + NL)

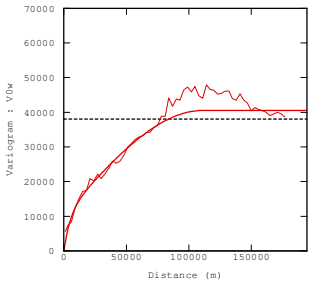

Holland Formation (KNGL)

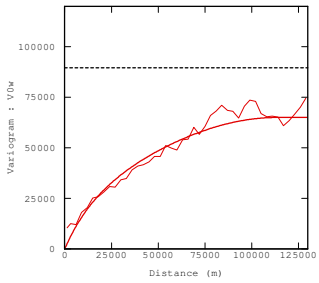

Vlieland subgroup (KNN)

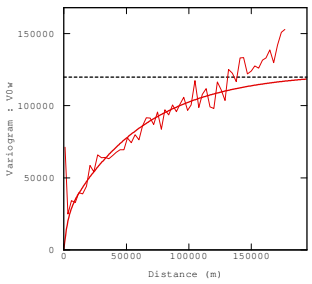

Upper Germanic Trias Group (RN)

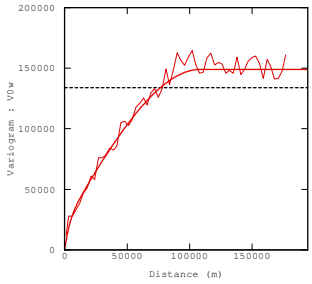

Lower Germanic Trias Group (RB)

Figure 8 Variogram models of the V_0-values for the sublayers of VELMOD-2

In Figures 9-10, maps of V_0 and its kriging standard-deviation are shown for the compacting main layers of VELMOD-2. Maps of V_0 and its kriging standard-deviation for the sublayers of VELMOD-2 are shown in Figures 11-12. The fault lines on the maps were taken from Duin et al. (2006). All kriging standard-deviations should be used with care (Dubrule, 2003). V_0-grids of all compacting layers are presented in Appendices 3.

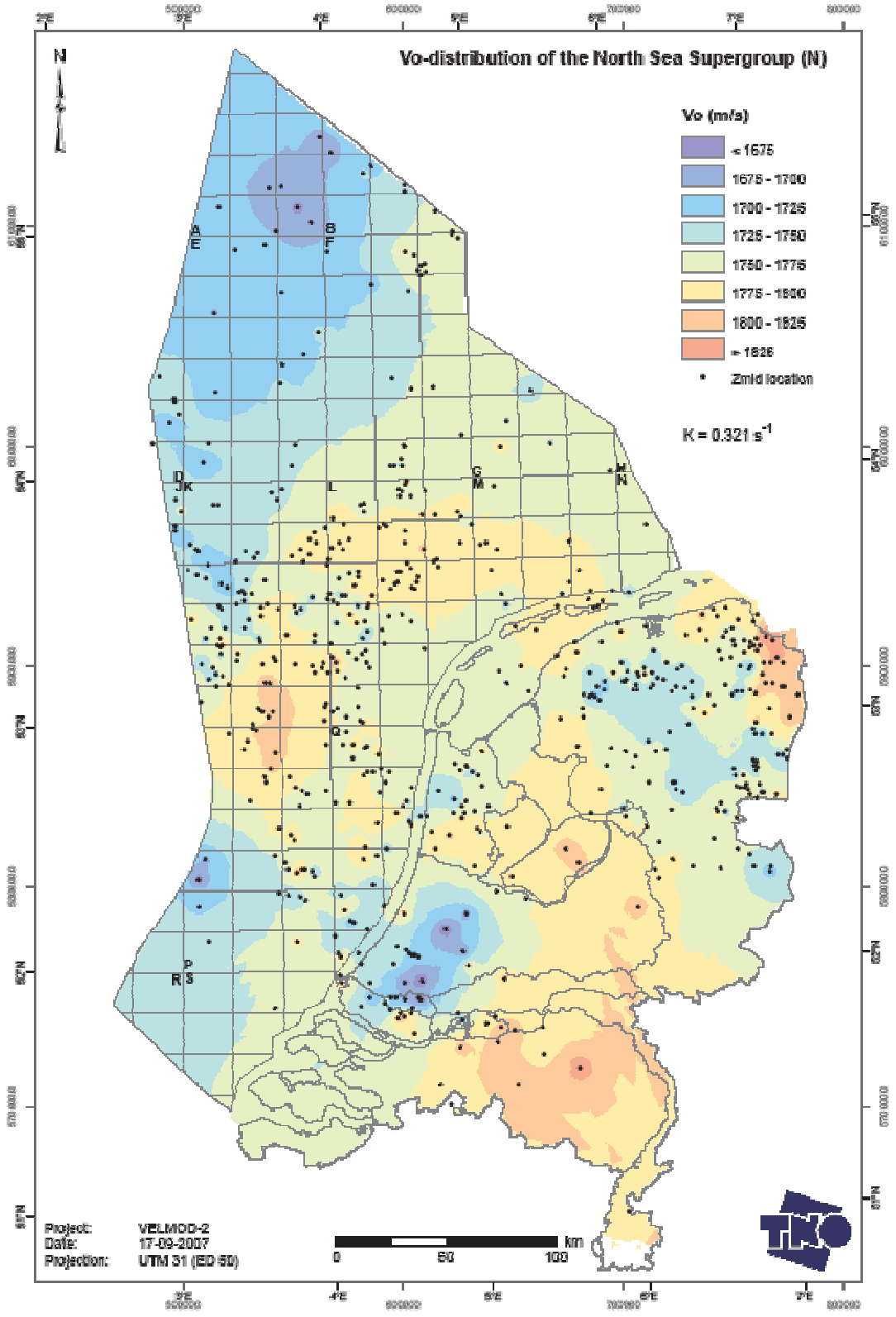

Figure 9-1 V_0-distribution of the layer of the North Sea Supergroup (N)

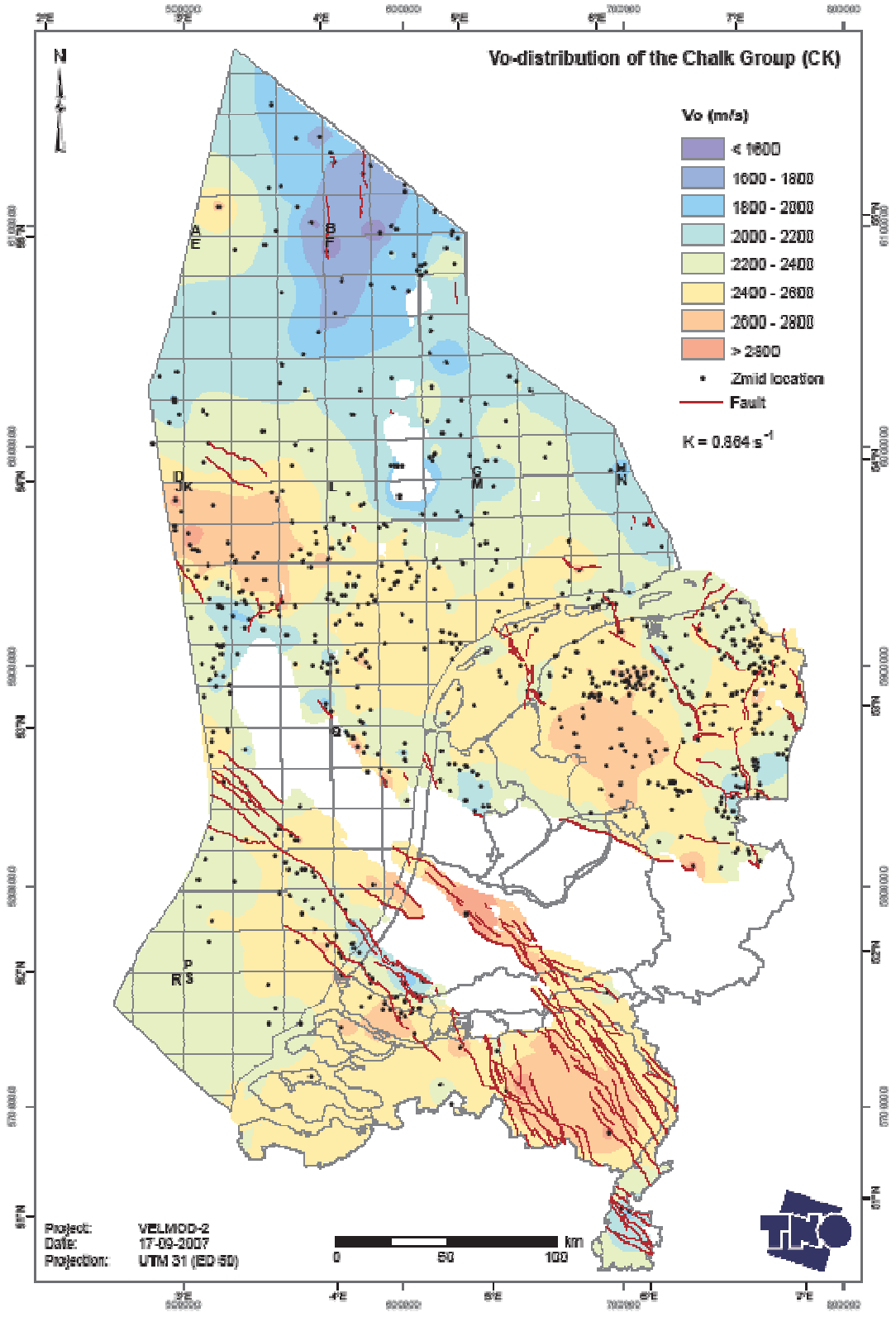

Figure 9-2 V_0-distribution of the layer of the Chalk Group (CK)

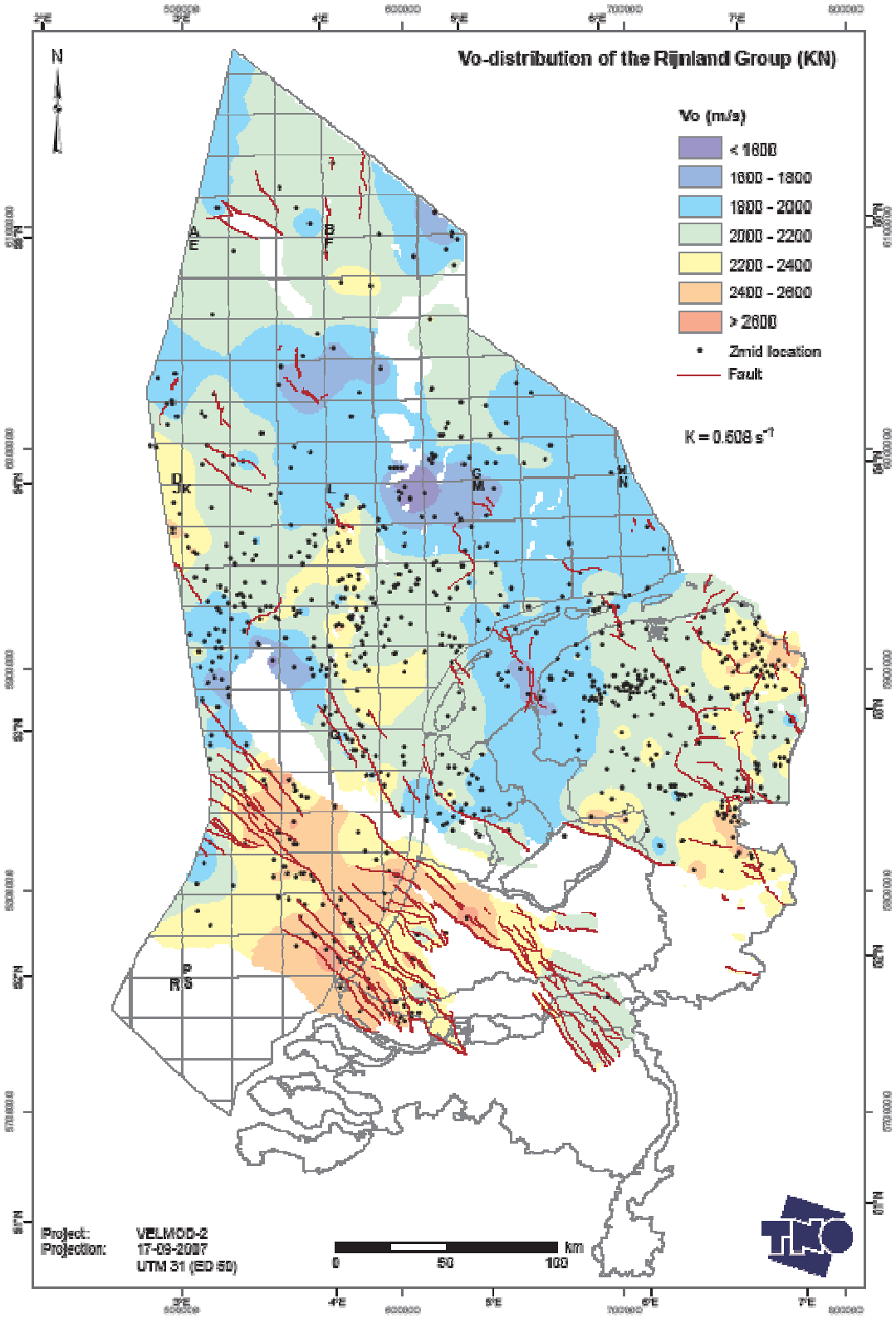

Figure 9-3 V_0-distribution of the layer of the Rijnland Group (KN)

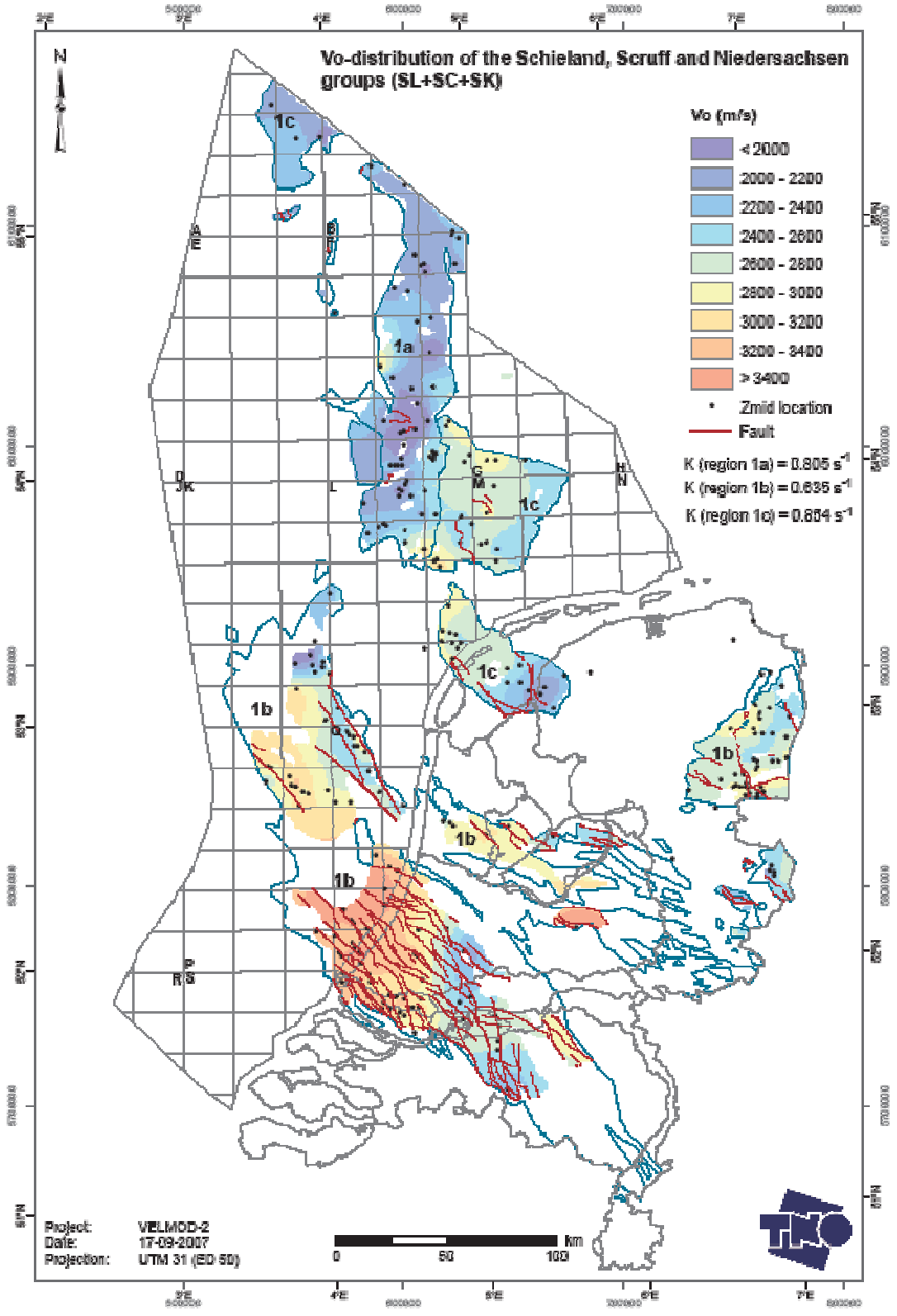

Figure 9-4 V_0-distribution of the layer of the Schieland, Scruff and Niedersachsen groups (SL+SG+SK)

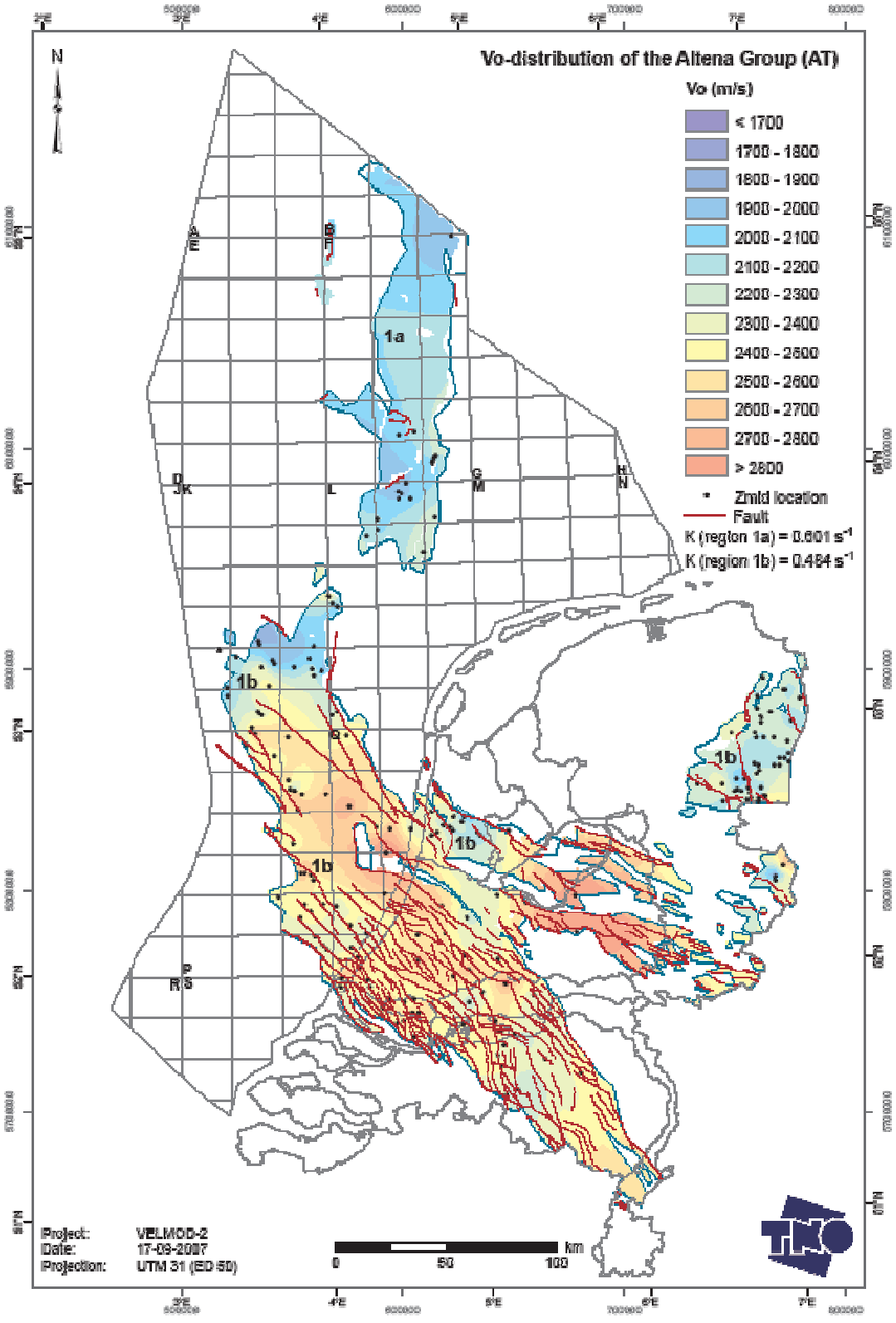

Figure 9-5 V_0-distribution of the layer of the Altena Group (AT)

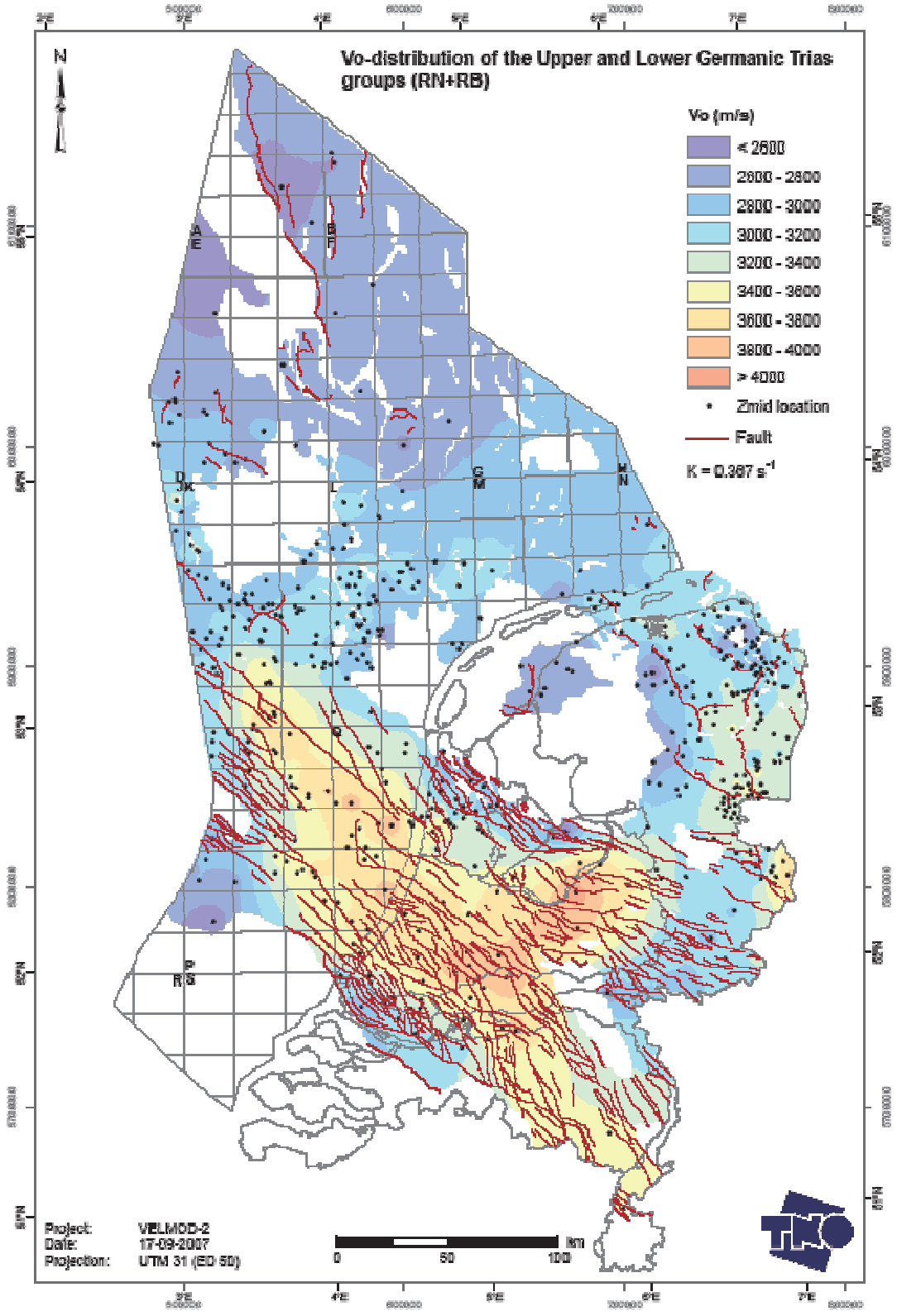

Figure 9-6 V_0-distribution of the layer of the Upper and Lower Germanic Trias groups (RN+RB)

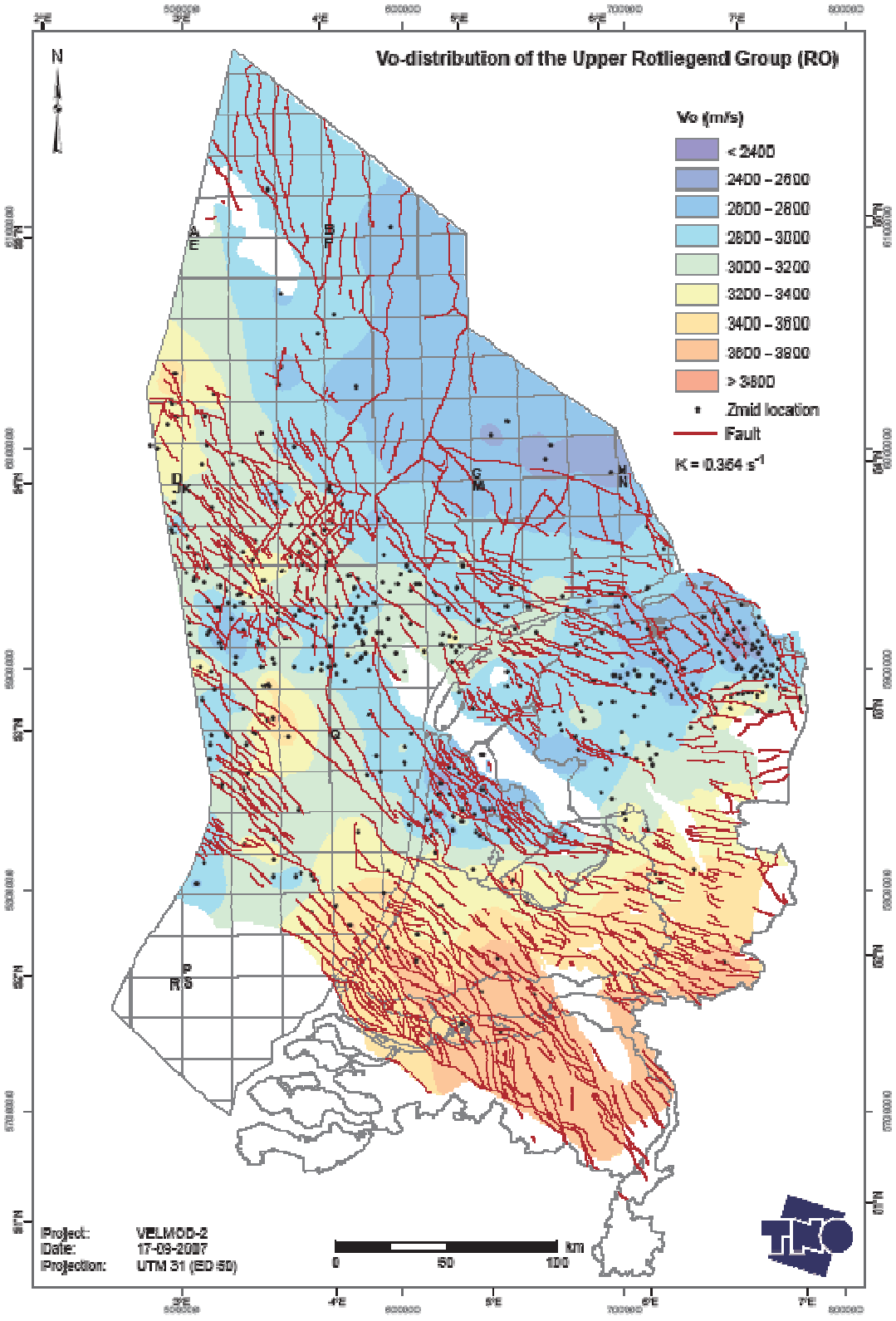

Figure 9-8 V_0-distribution of the layer of the Upper Rotliegend Group (RO)

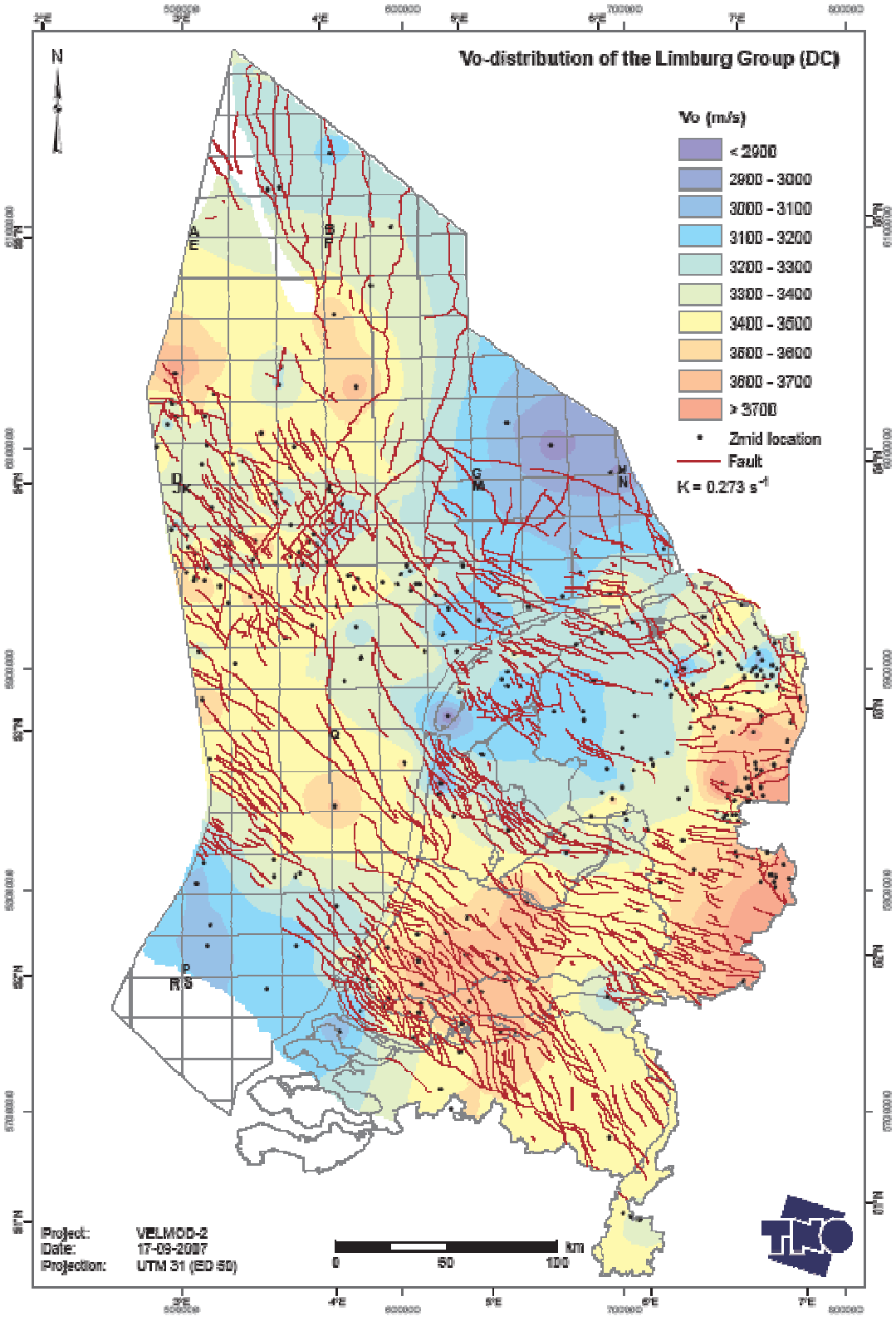

Figure 9-9 V_0-distribution of the layer of the Limburg Group (DC)

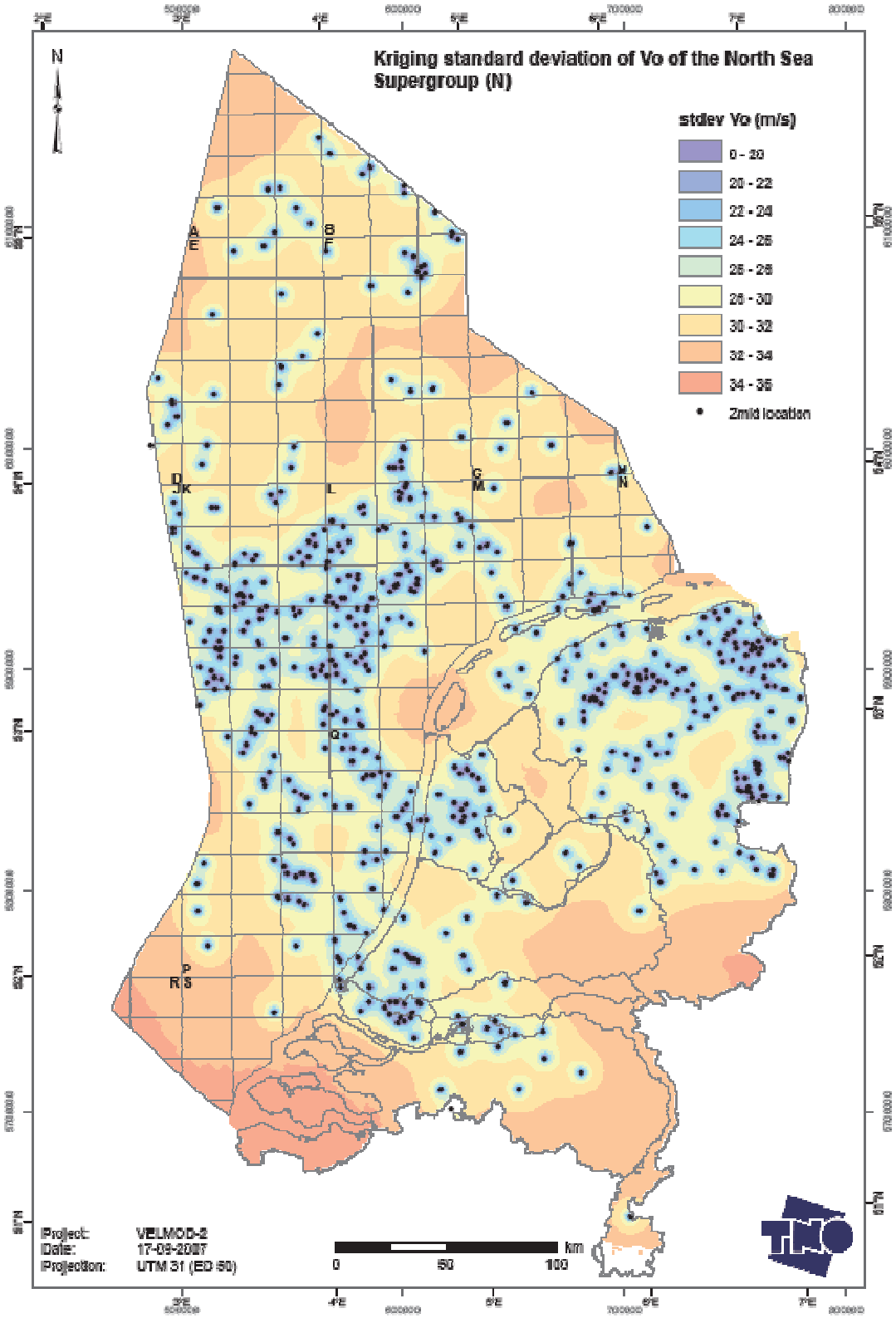

Figure 10-1 Kriging standard deviation of V_0 for the layer of the North Sea Supergroup (N)

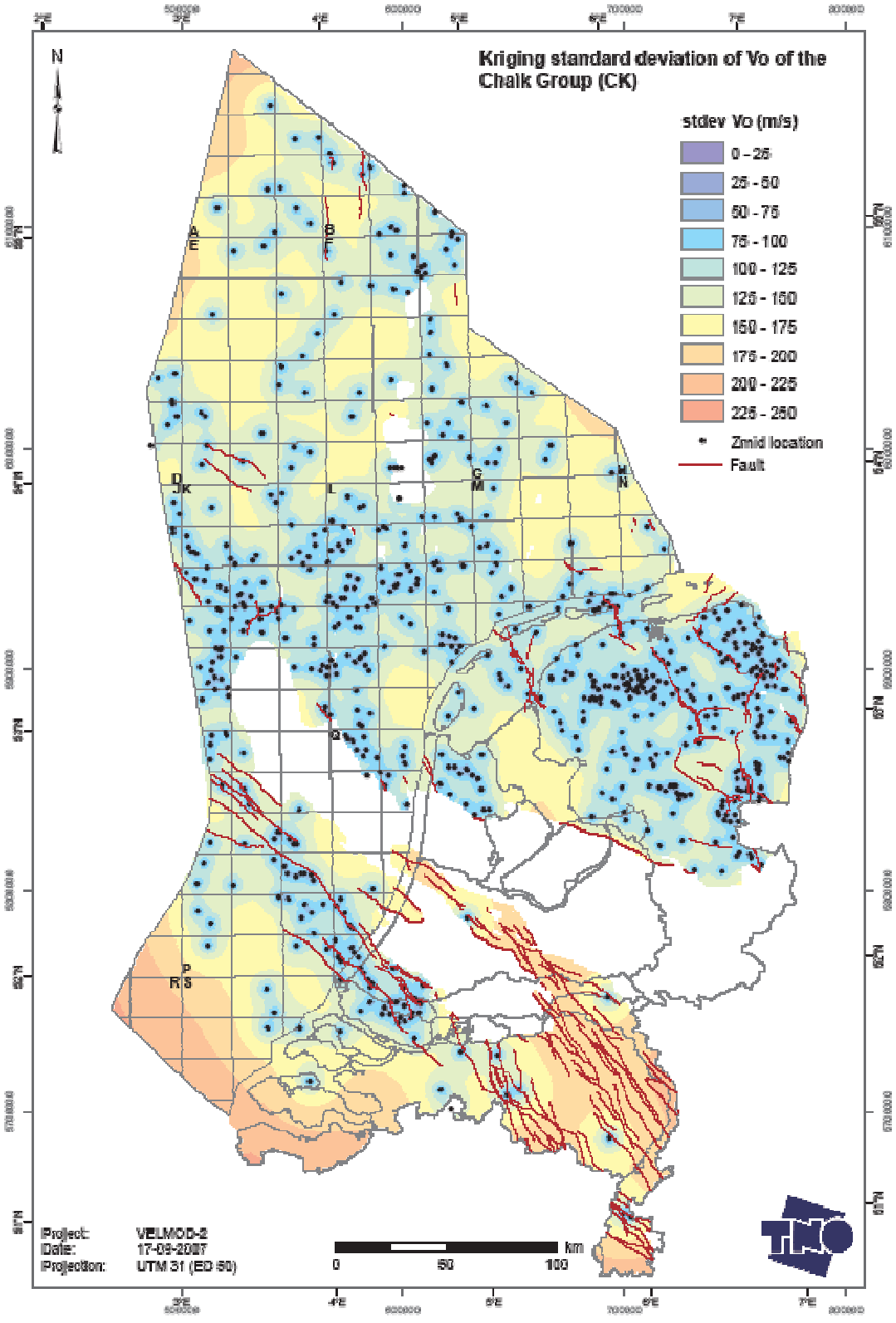

Figure 10-2 Kriging standard deviation of V_0 for the layer of the Chalk Group (CK)

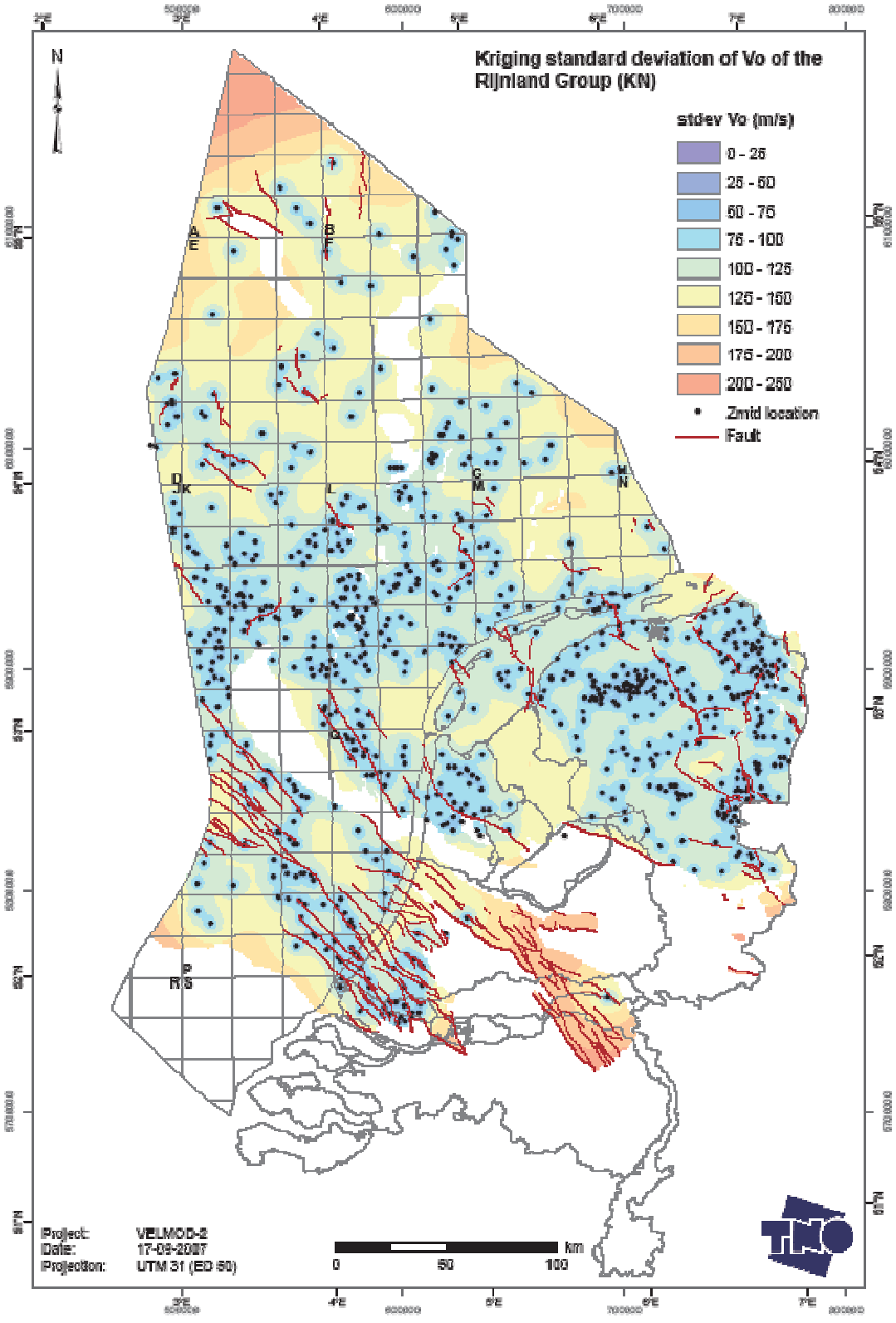

Figure 10-3 Kriging standard deviation of V_0 for the layer of the Rijnland Group (KN)

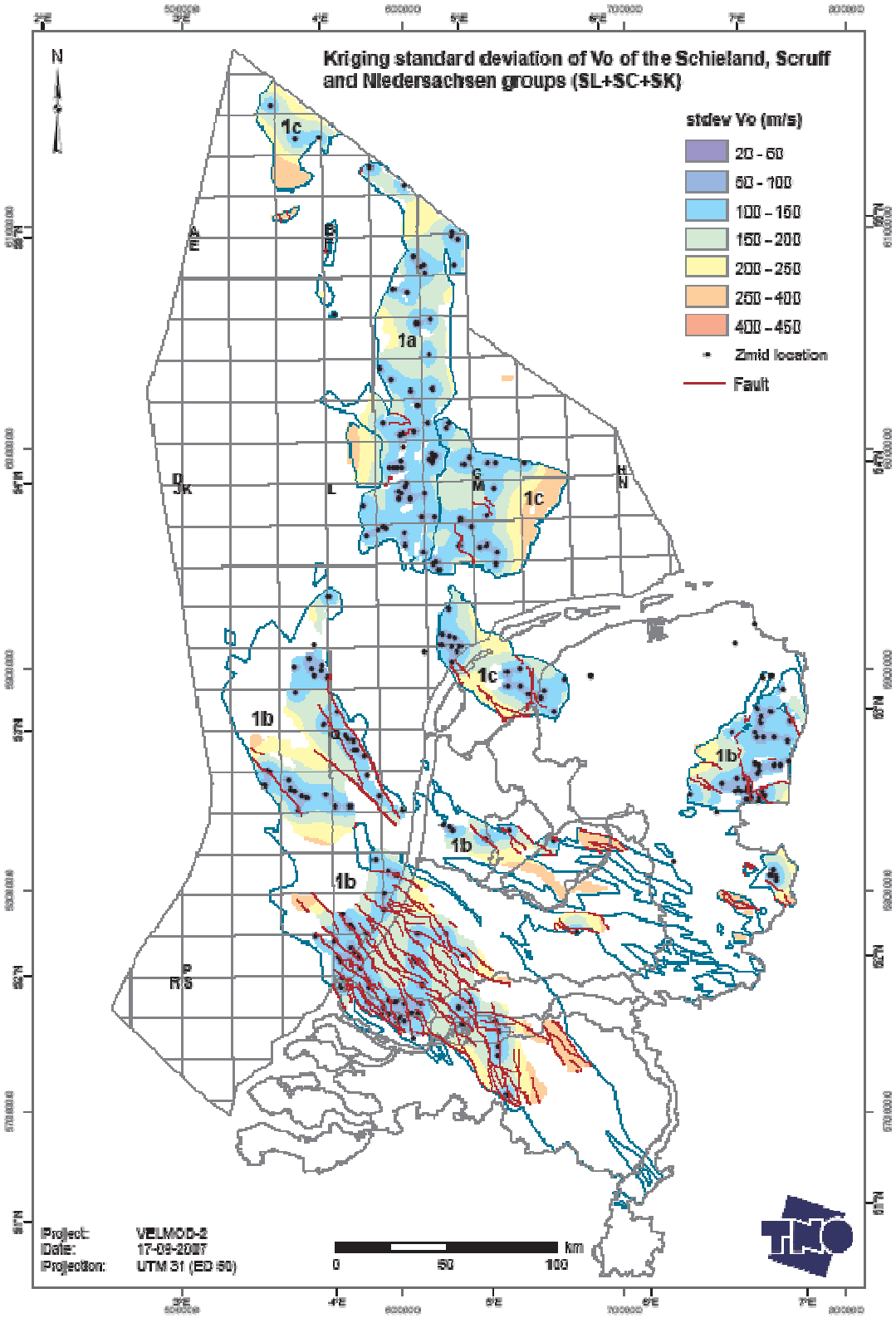

Figure 10-4 Kriging standard deviation of V_0 for the layer of the Schieland, Scruff and Niedersachsen groups (SL+SG+SK)

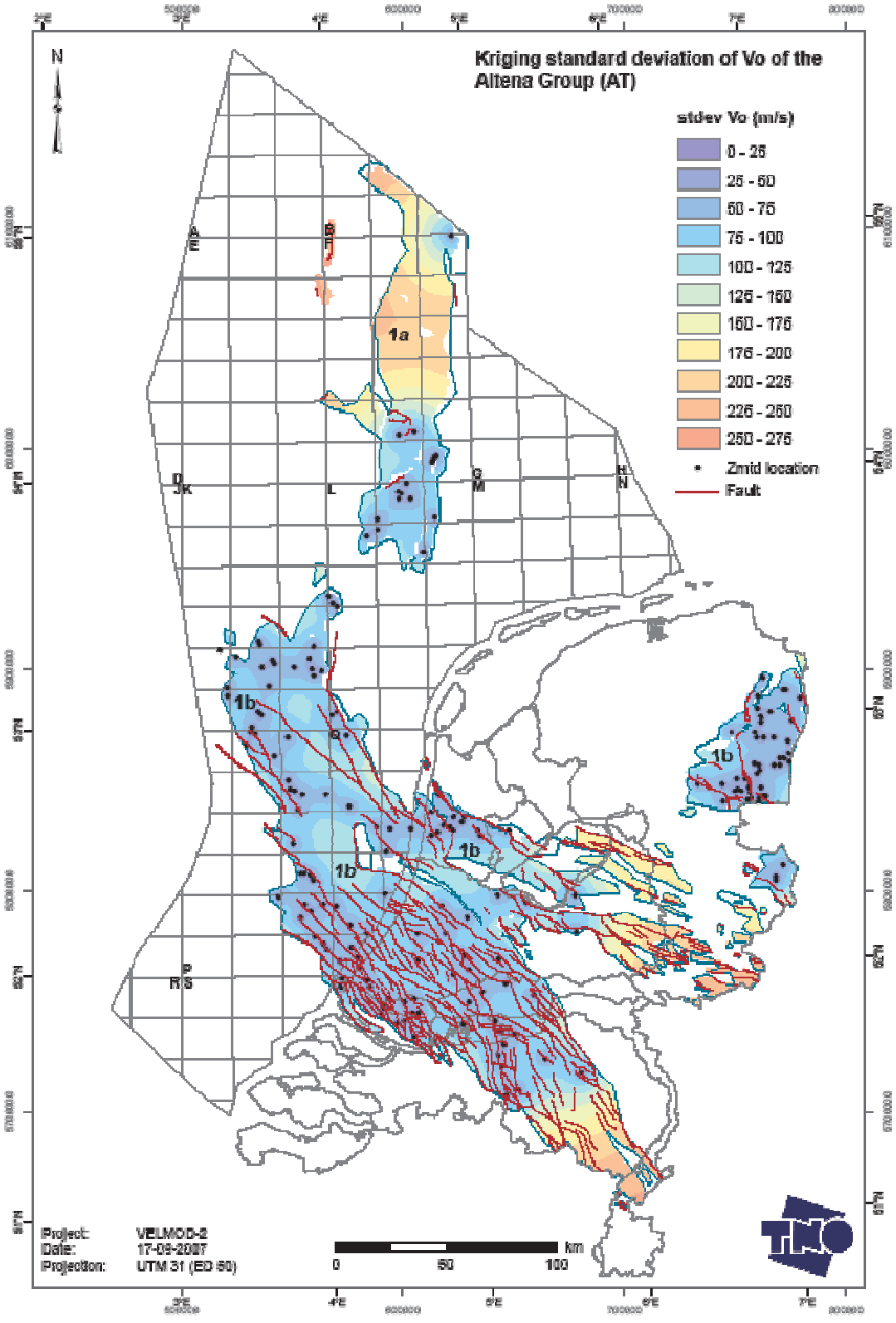

Figure 10-5 Kriging standard deviation of V_0 for the layer of the Altena Group (AT)

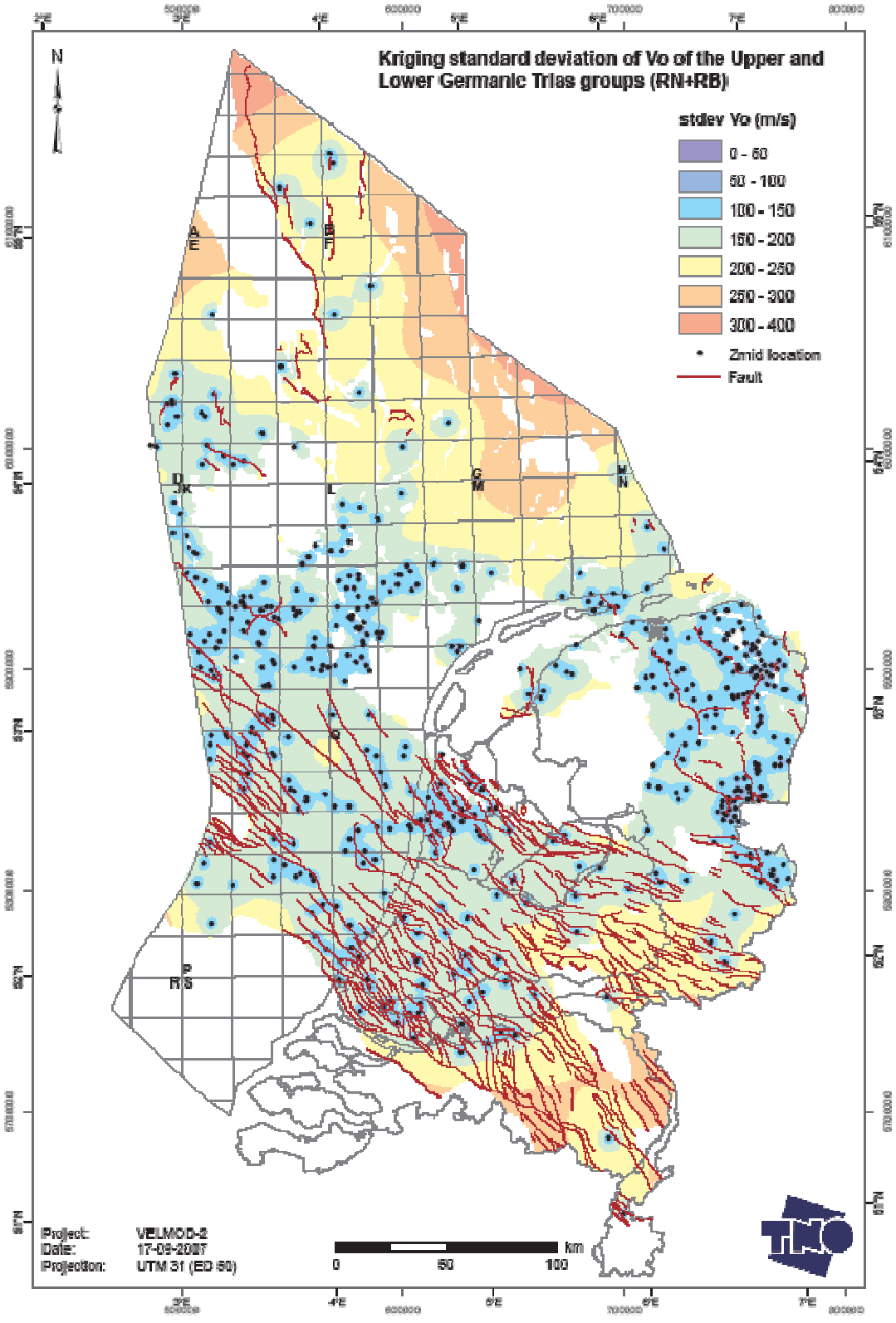

Figure 10-6 Kriging standard deviation of V_0 for the layer of the Upper and Lower Germanic Trias groups (RN+RB)

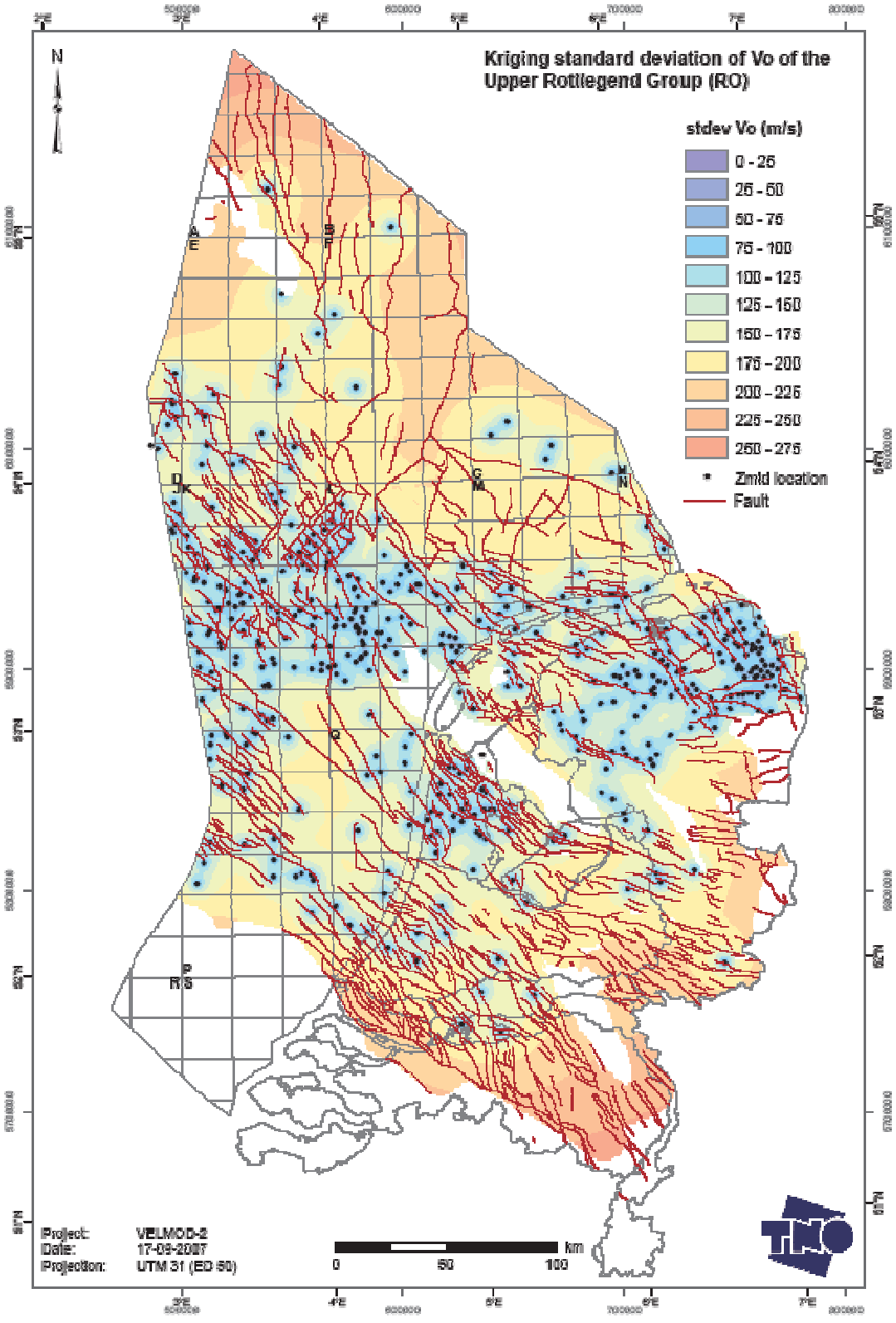

Figure 10-8 Kriging standard deviation of V_0 for the layer of the Upper Rotliegend Group (RO)

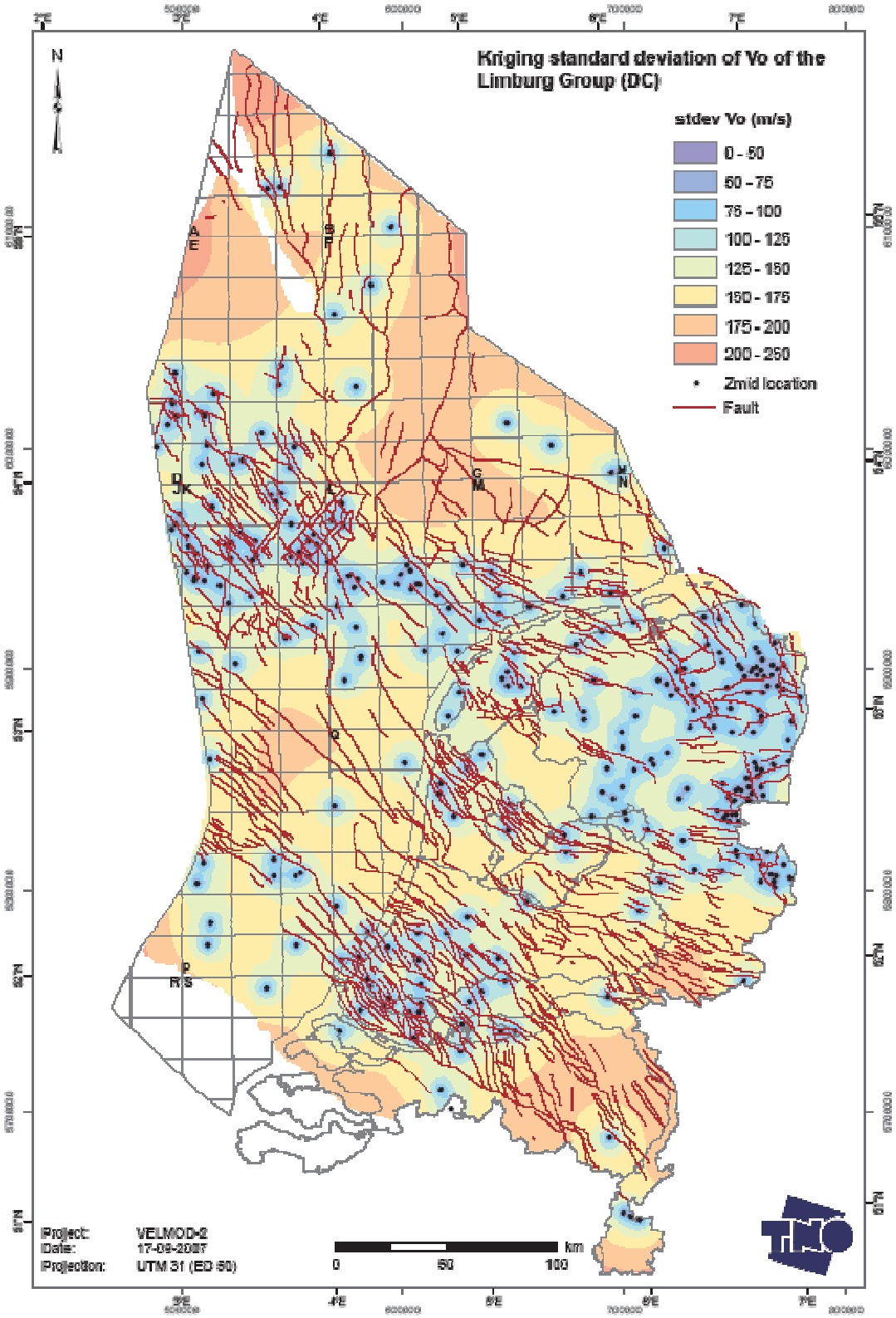

Figure 10-9 Kriging standard deviation of V_0 for the layer of the Limburg Group (DC)

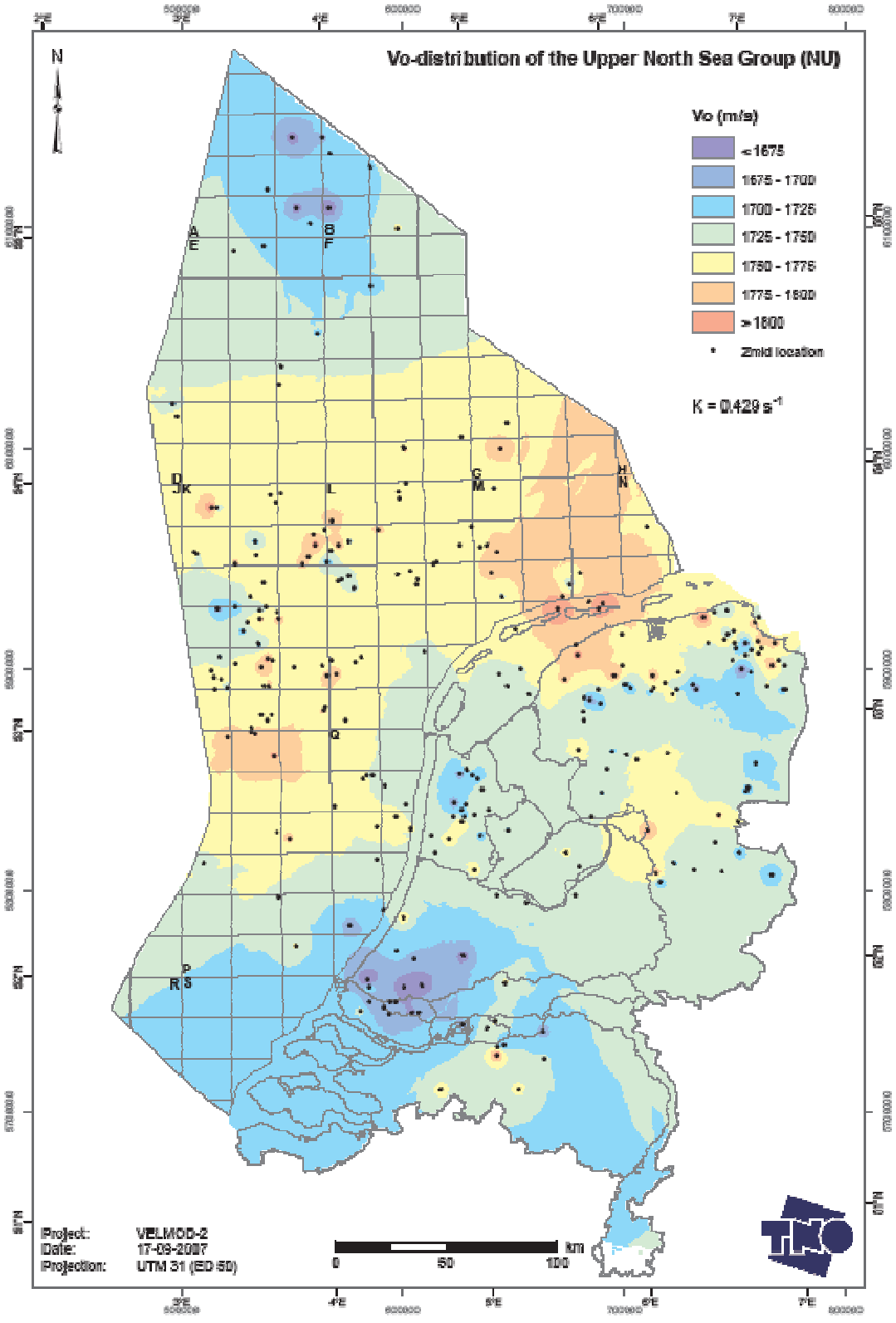

Figure 11-1a V_0-distribution of the sublayer of the Upper North Sea Group (NU)

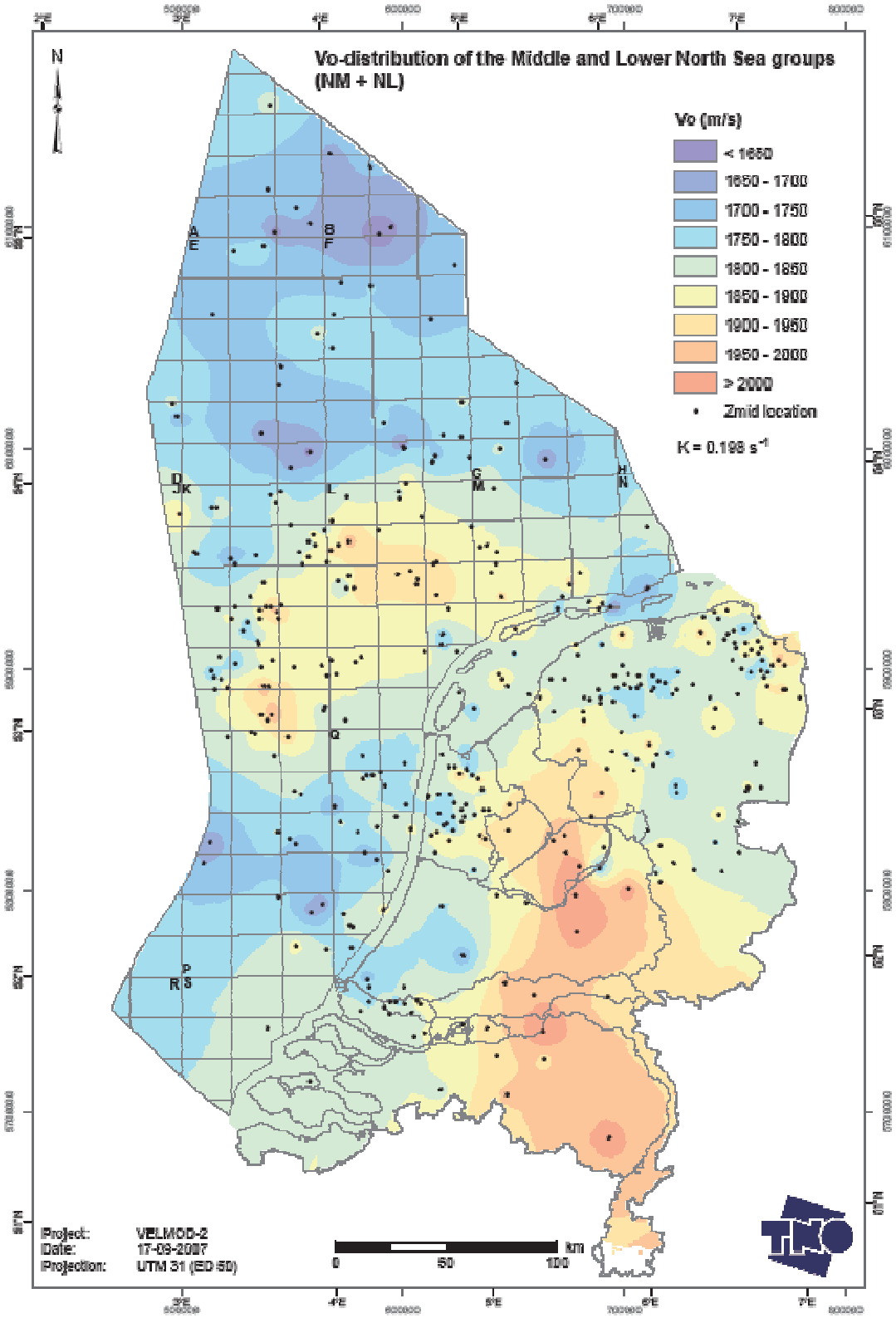

Figure 11-1b V_0-distribution of the sublayer of the Middle and Lower North Sea groups (NM+NL)

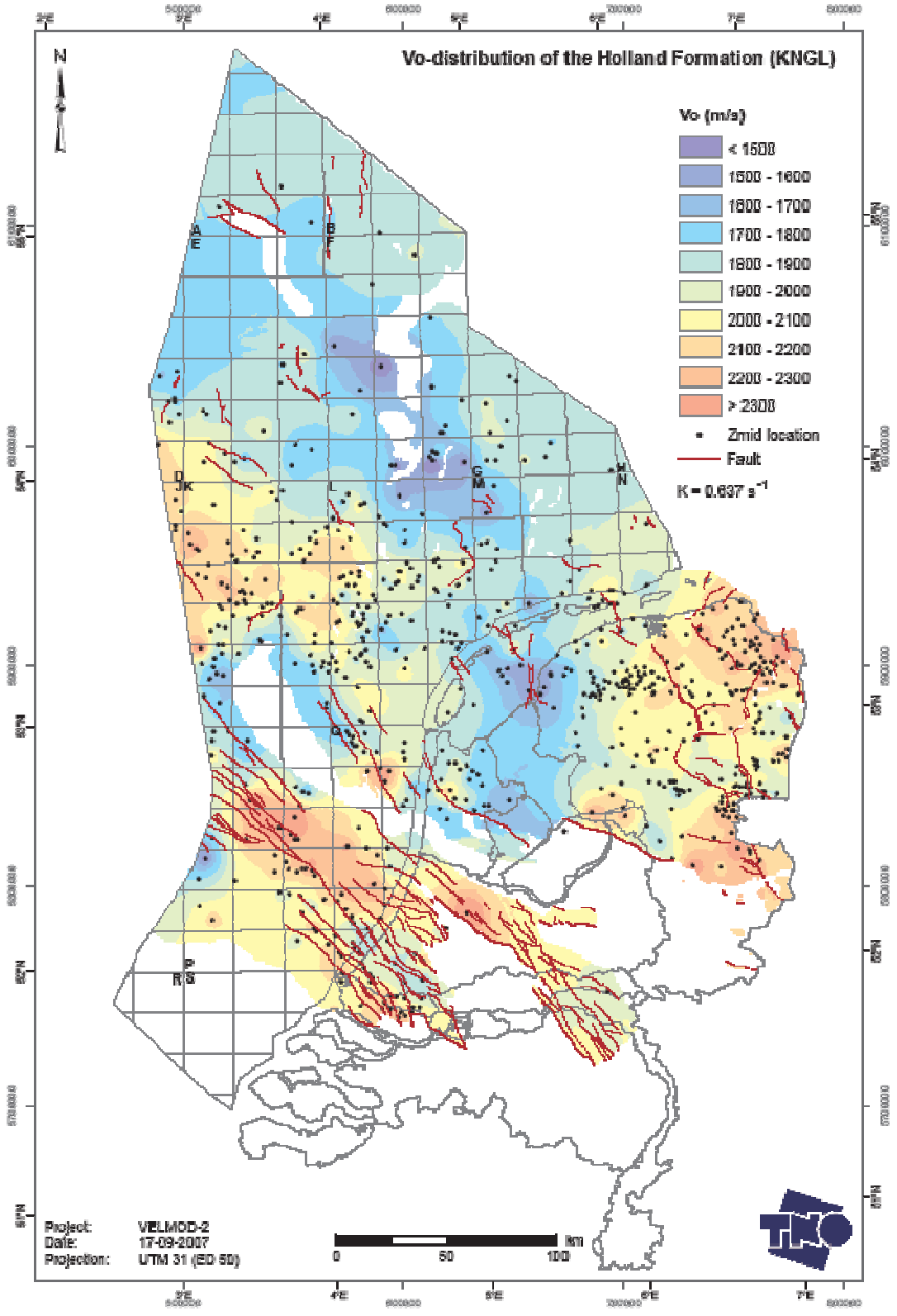

Figure 11-3a V_0-distribution of the sublayer of the Holland Formation (KNGL)

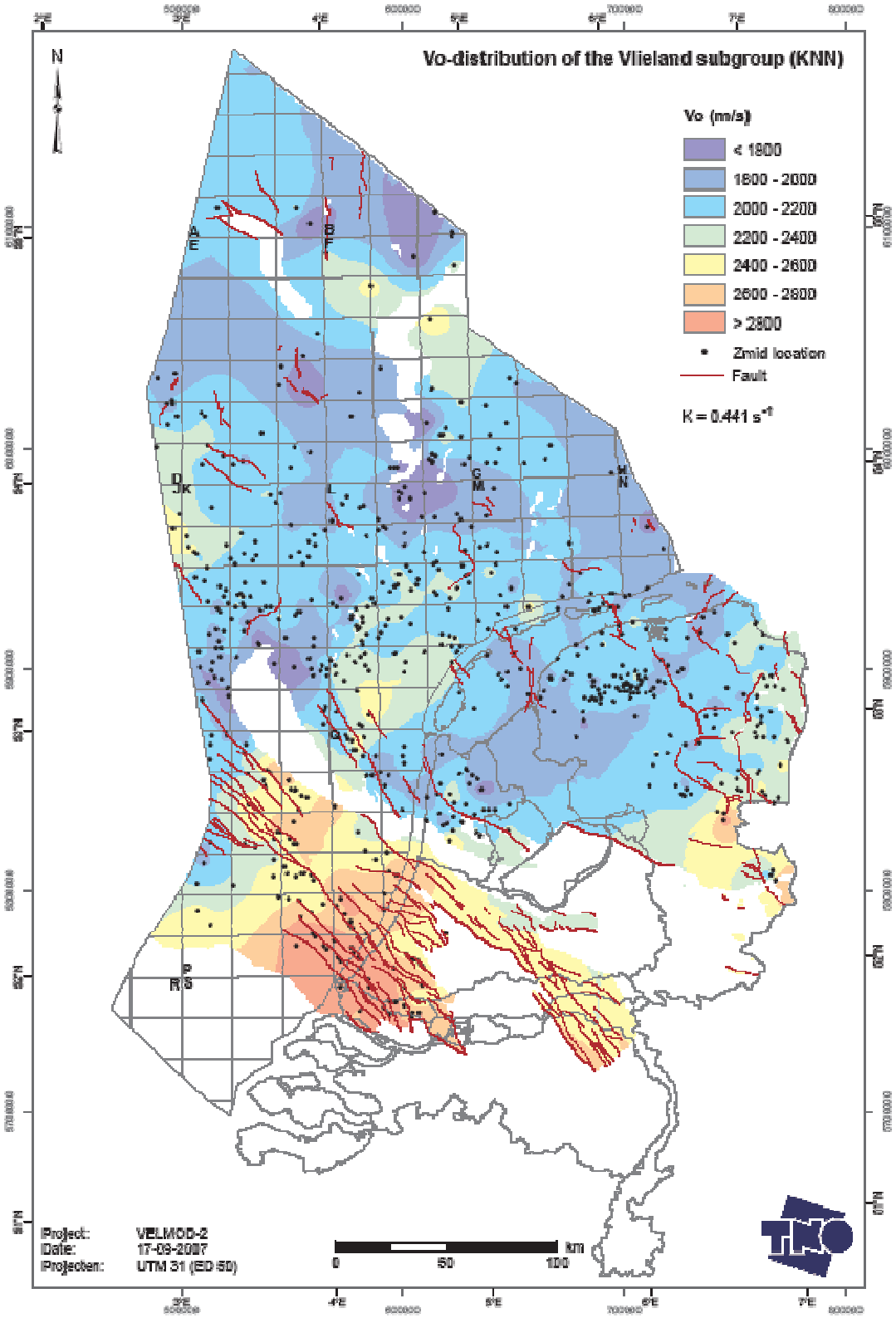

Figure 11-3b V_0-distribution of the sublayer of the Vlieland subgroup (KNN)

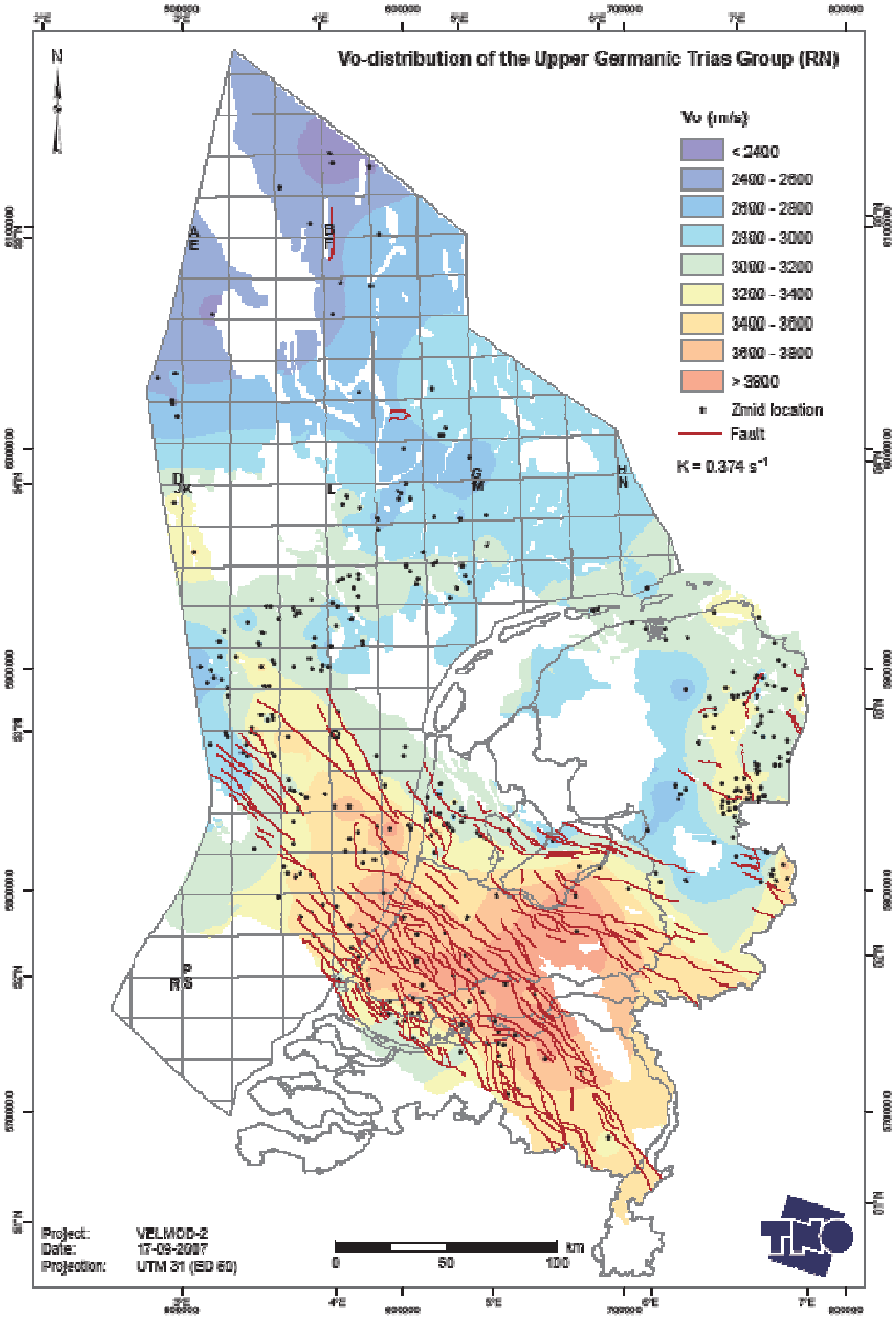

Figure 11-6a V_0-distribution of the sublayer of the Upper Germanic Trias Group (RN)

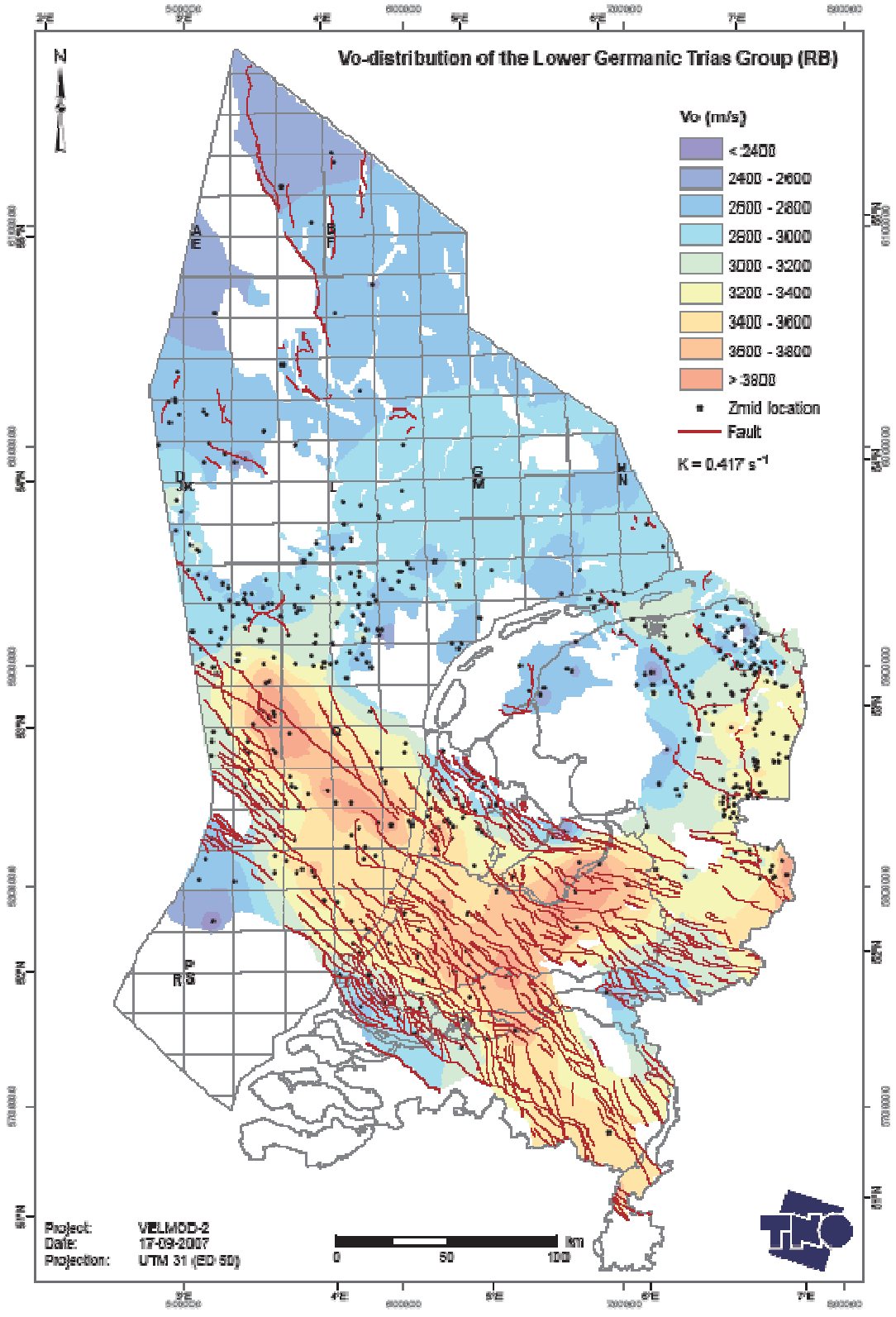

Figure 11-6b V_0-distribution of the sublayer of the Lower Germanic Trias group (RB)

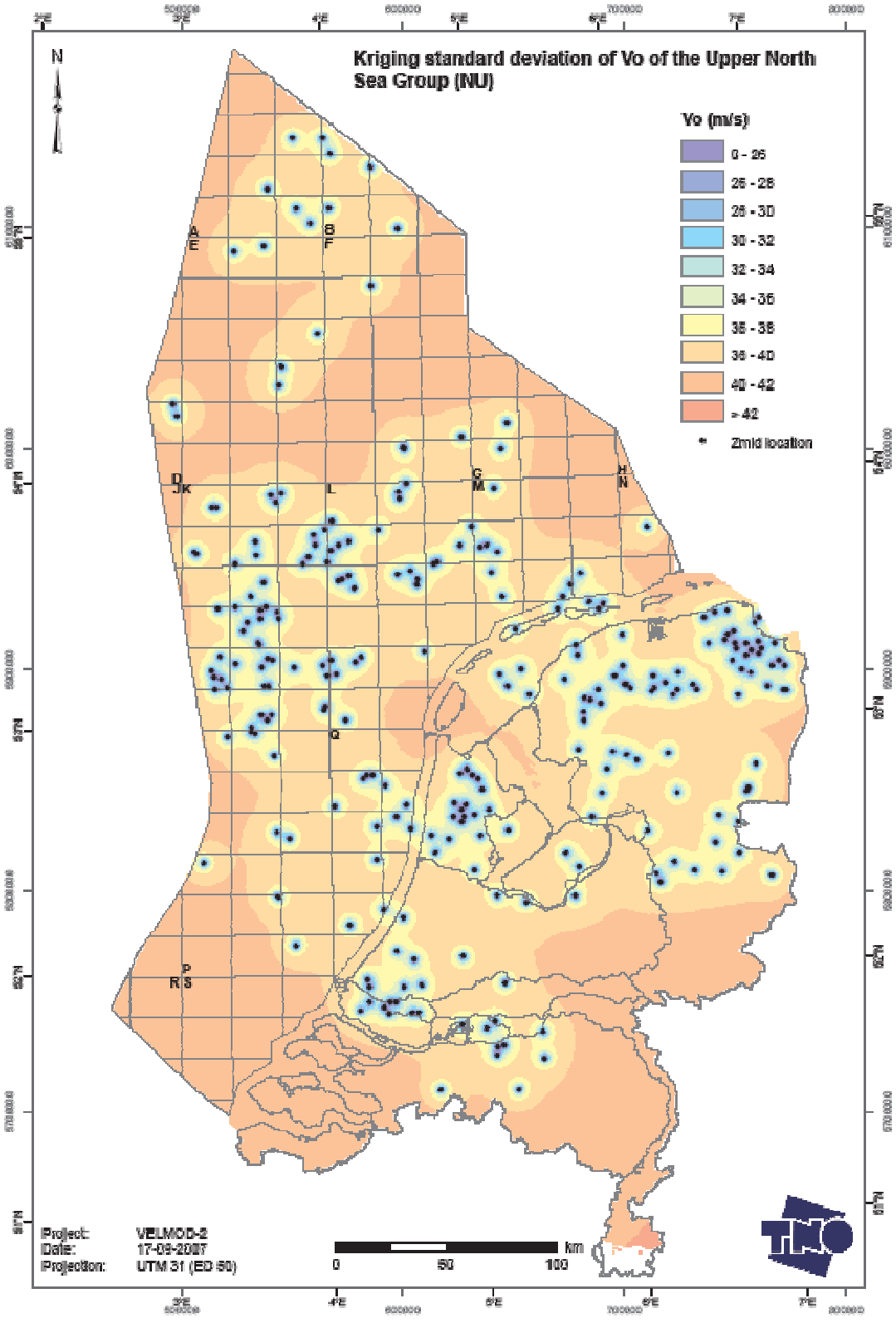

Figure 12-1a Kriging standard deviation of V_0 for the sublayer of the Upper North Sea Group (NU)

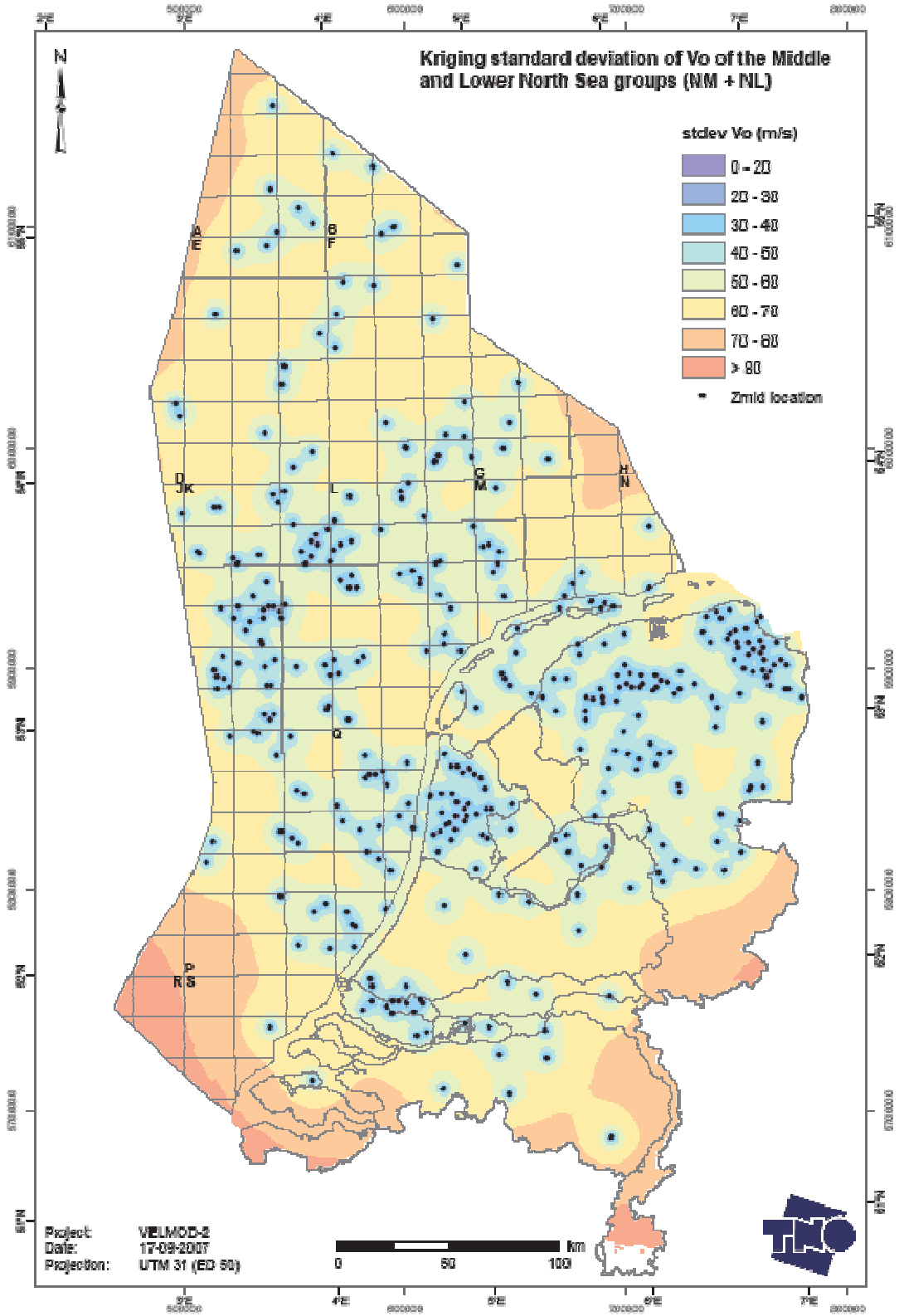

Figure 12-1b Kriging standard deviation of V_0 for the sublayer of the Middle and Lower North Sea groups (NM+NL)

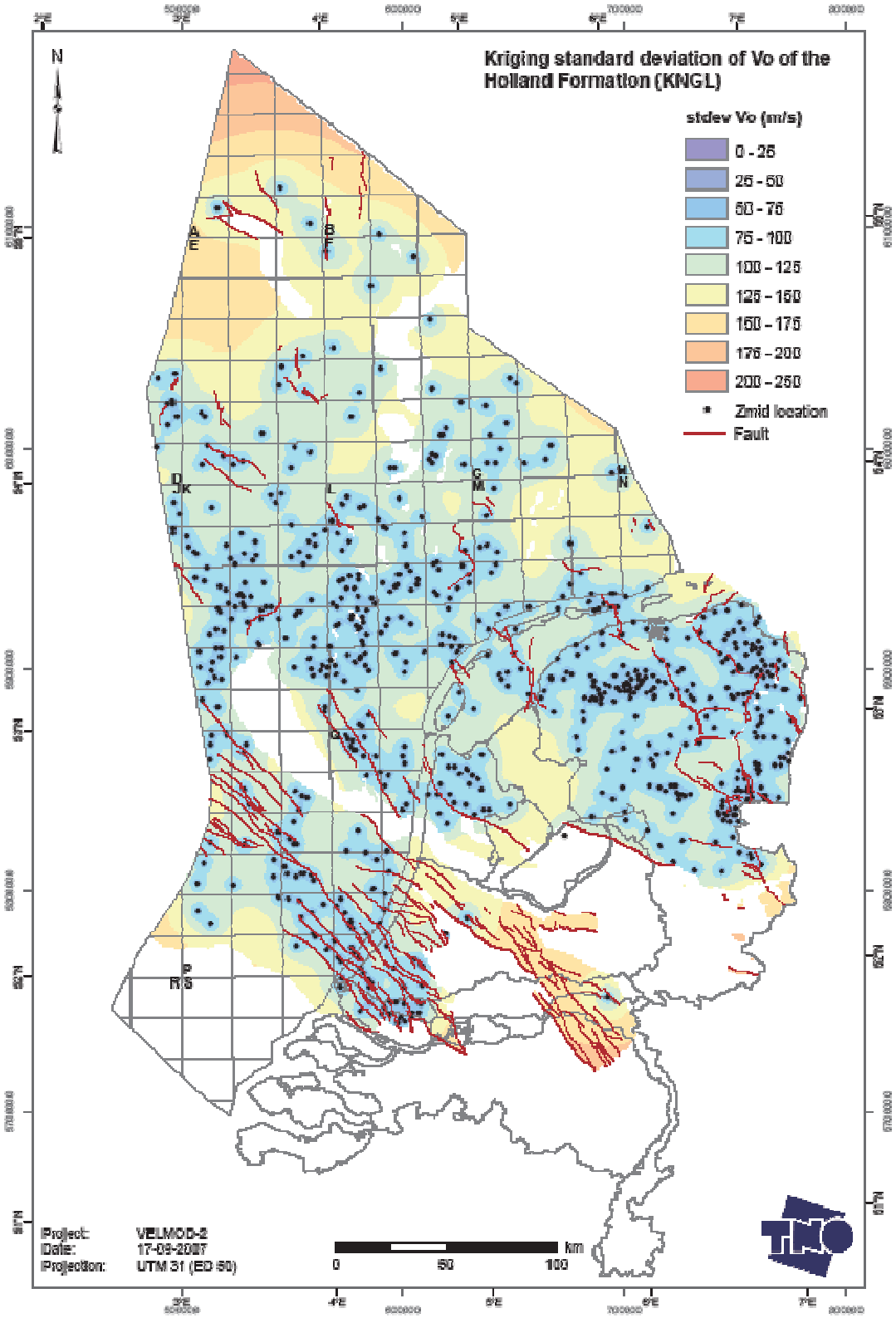

Figure 12-3a Kriging standard deviation of V_0 for the sublayer of the Holland Formation (KNGL)

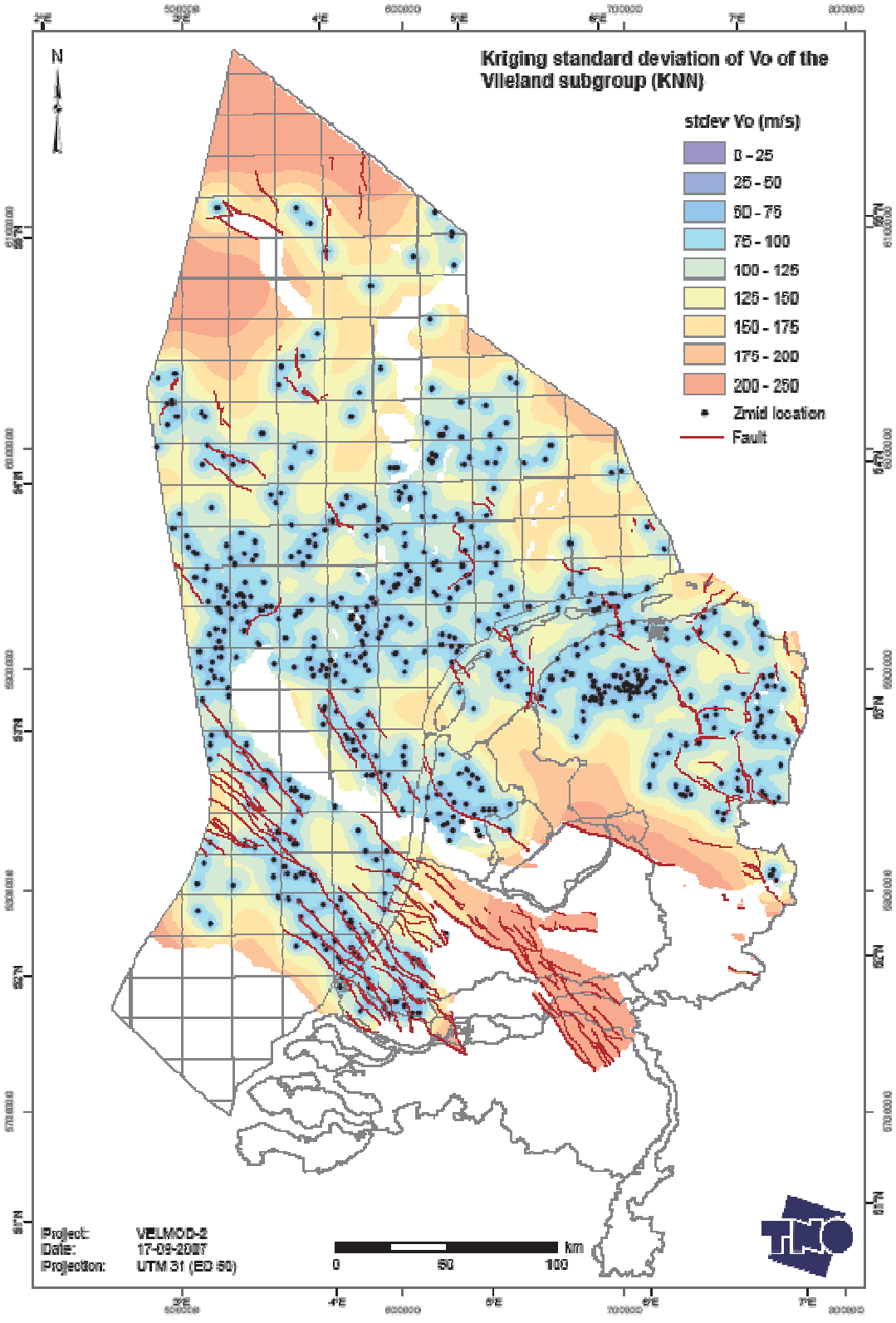

Figure 12-3b Kriging standard deviation of V_0 for the sublayer of the Vlieland subgroup (KNN)

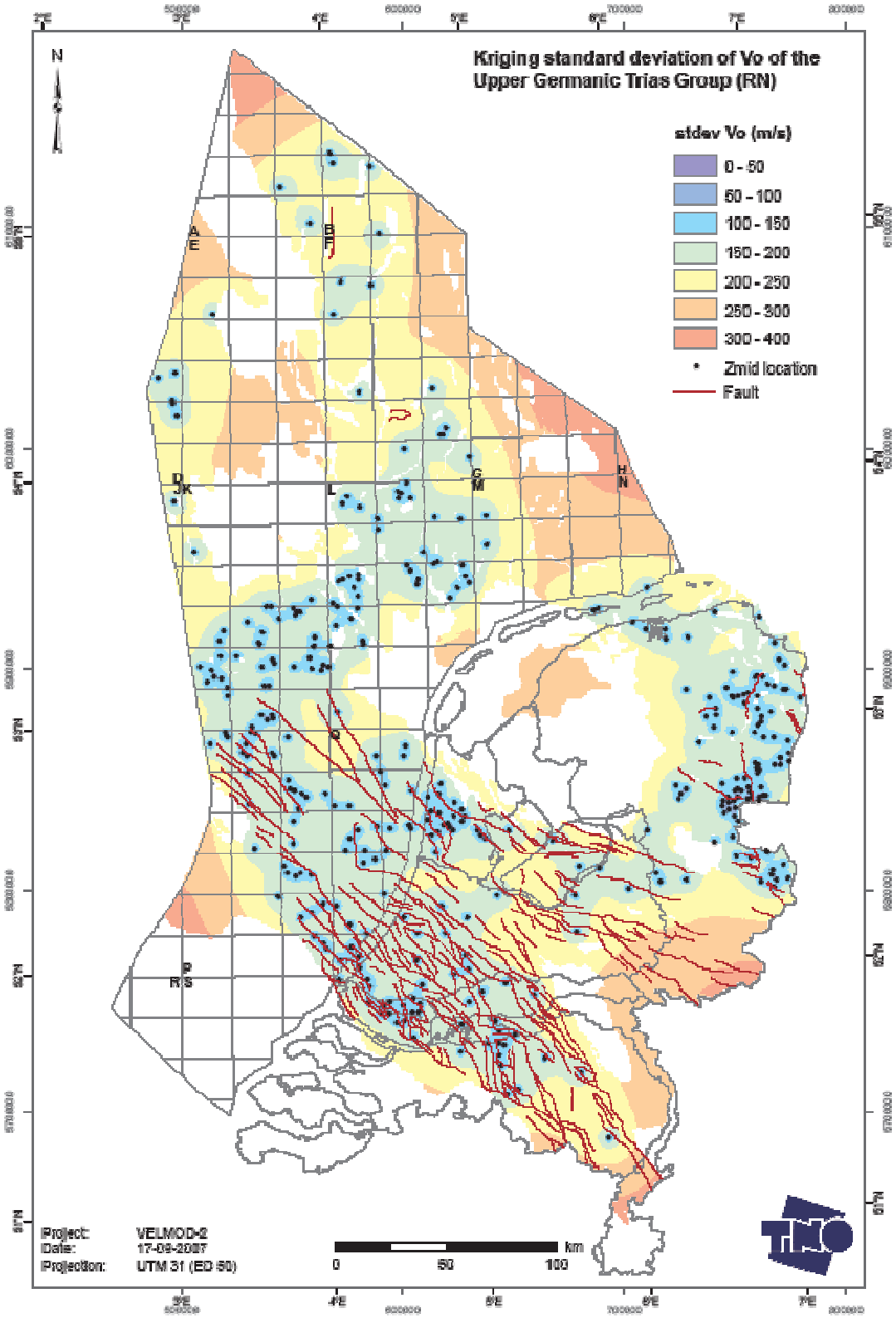

Figure 12-6a Kriging standard deviation of V_0 for the sublayer of the Upper Germanic Trias Group (RN)

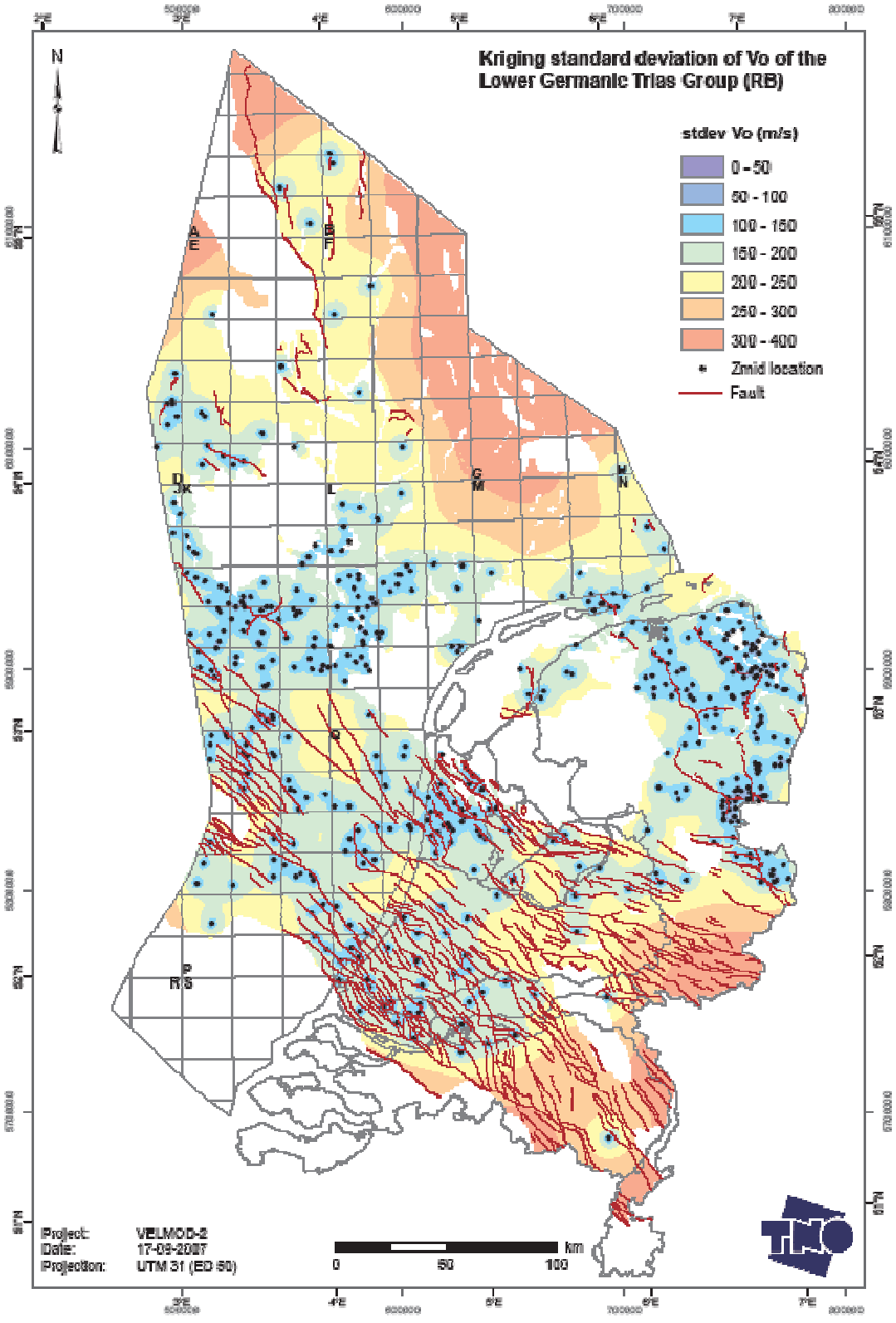

Figure 12-6b Kriging standard deviation of V_0 for the sublayer of the Lower Germanic Trias Group (RB)

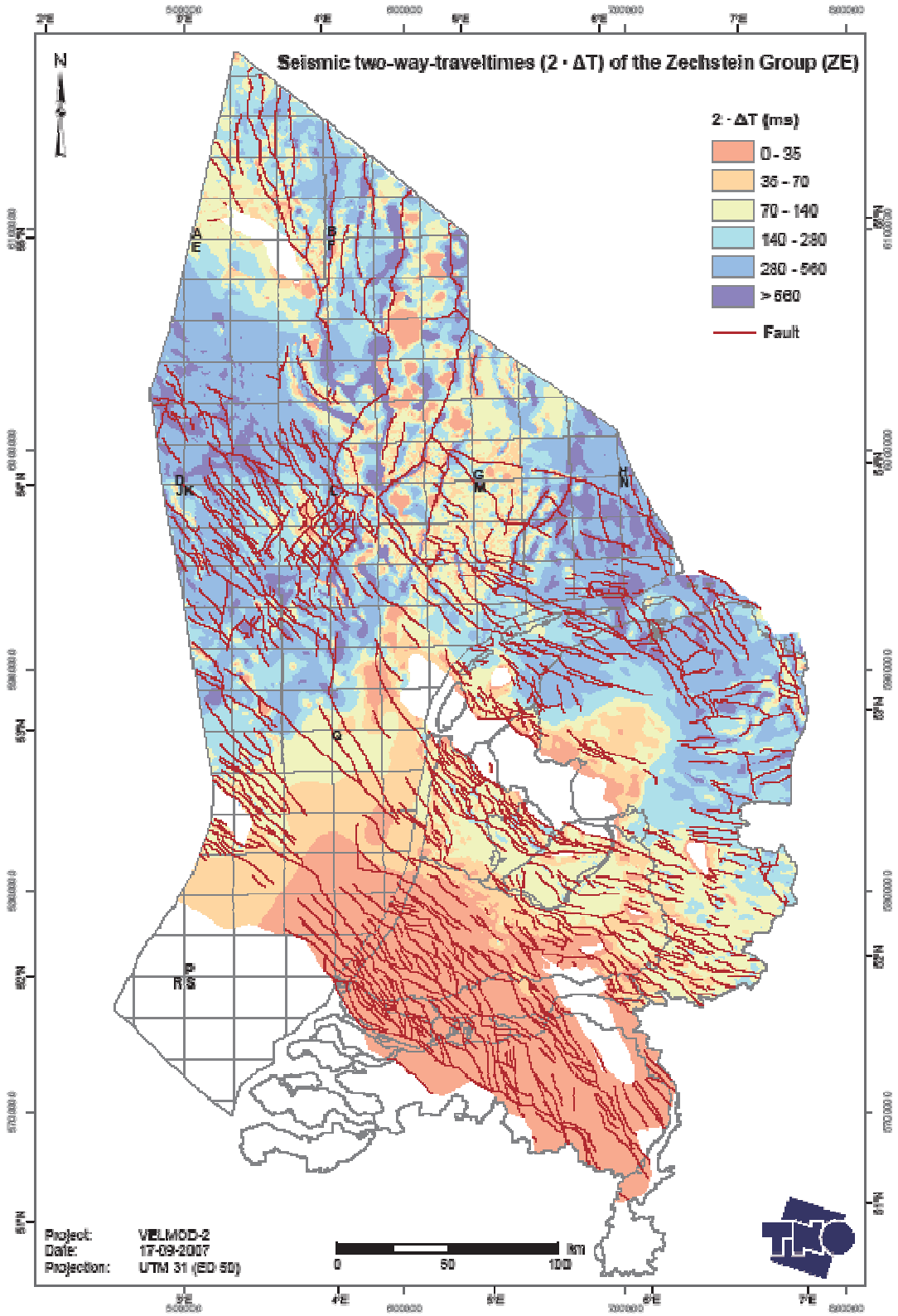

Figure 13 Isochores (two-way seismic traveltime representation) of the layer of the Zechstein Group

5 VELMOD velocity model for layer of the Zechstein Group

The model for the layer of the Zechstein Group consists of interval velocities V_{int}^{ZE}. At borehole locations the model velocity is set equal to the interval velocity V_{int} according to borehole sonics (Appendices 1 and 5-2). V_{int}^{ZE} at other locations is assumed to depend on both V_{int}-values and on the seismic traveltime ΔT^{ZE} through the layer of the Zechstein Group. For this purpose, we used seismic two-way-traveltimes according to TNO's NCP-1 mapping project (Figure 13). We took the following two steps to arrive at V_{int}^{ZE}- values.

In the first step, preliminary interval velocities V^{prelim} are introduced, which depend on ΔT^{ZE} (in ms) as formulated below:

$$V^{prelim} = 4500 \text{ m/s} \qquad \text{if } \Delta T^{ZE} \geq 150 \text{ ms}$$
$$V^{prelim} = 5500 - 6.67 \bullet \Delta T^{ZE} \text{ m/s} \qquad \text{if } \Delta T^{ZE} < 150 \text{ ms}$$

These relations reflect the predominance of halite in relatively thick layers of Zechstein Group deposits, and are derived from a graph of V_{int} against ΔT at borehole locations (Figure 14).

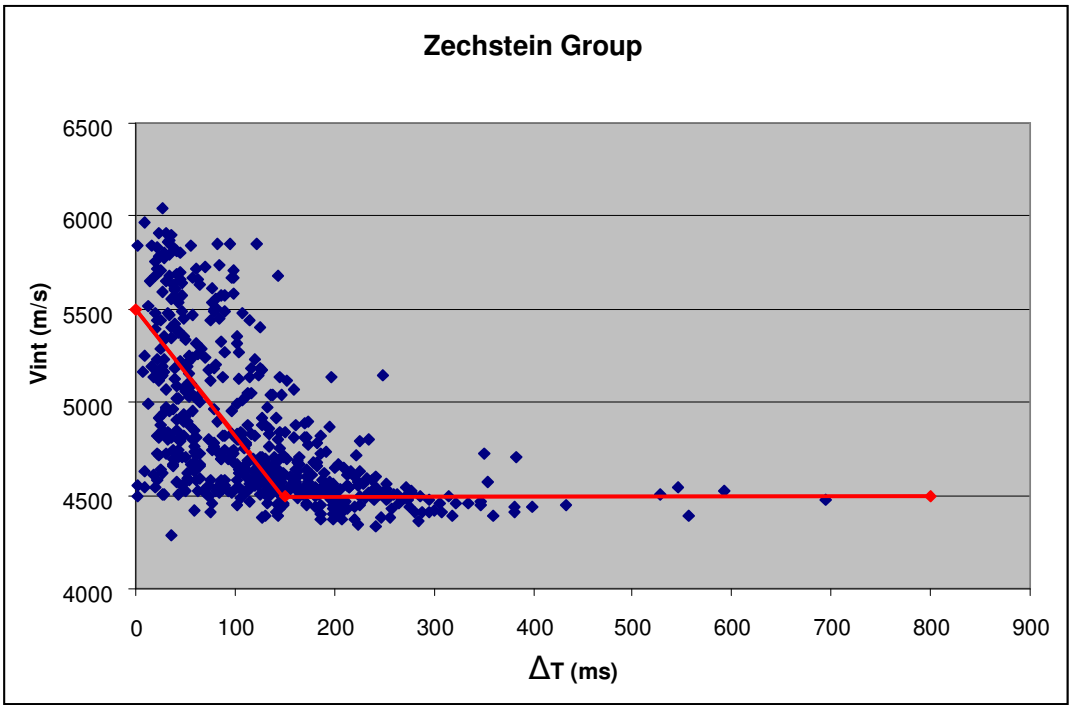

Figure 14 Schematic relation between V_{int} and ΔT at borehole locations

In the second step, the differences V^{prelim}-V_{int} at borehole locations are kriged to obtain interpolated correction values ΔV^{prelim}. The variogram for this kriging procedure is

shown in Figure 15. The resulting map is shown in Figure 16. With these correction values one arrives at V_{int}^{ZE} at no-borehole locations through:

$$V_{int}^{ZE} = V^{prelim} - \Delta V^{prelim}$$

In the above step, the V_{int}^{ZE} - values in the area of ΔT^{ZE} - values (Figure 13), are constrained to a minimum value of 4400 m/s. The final V_{int}^{ZE} - distribution is shown in Figure 17, the kriging standard deviation of V_{int}^{ZE} in Figure 18. V_{int}^{ZE}-grid values are presented in Appendix 4.

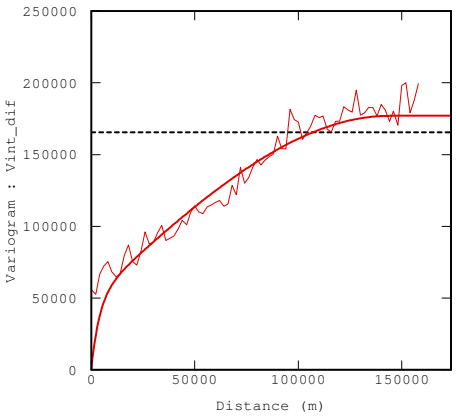

Figure 15 Variogram model of the ΔV^{prelim}-values for the layer of the Zechstein Group of VELMOD-2

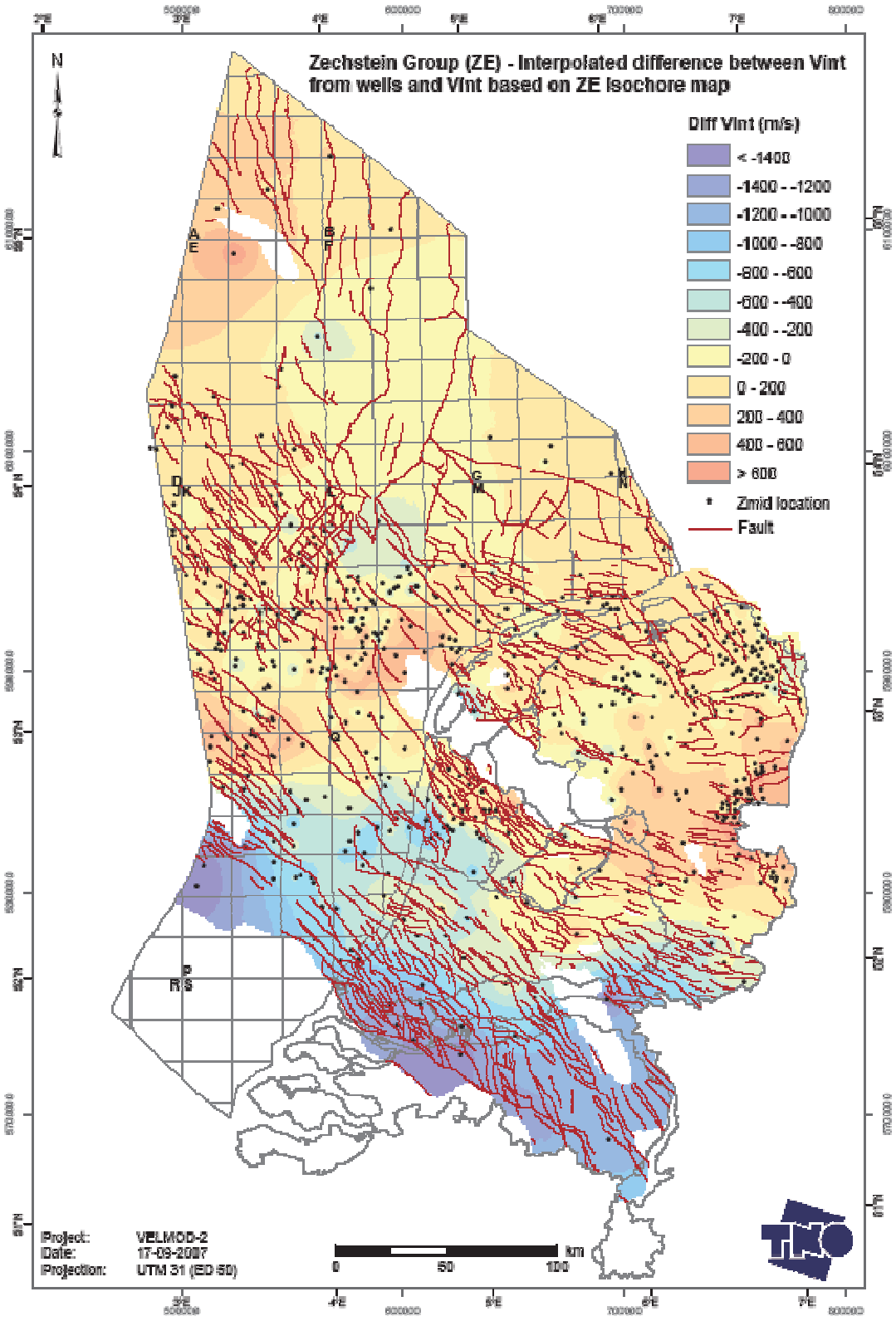

Figure 16 ΔV^{prelim} -distribution for the layer of the Zechstein Group of VELMOD-2

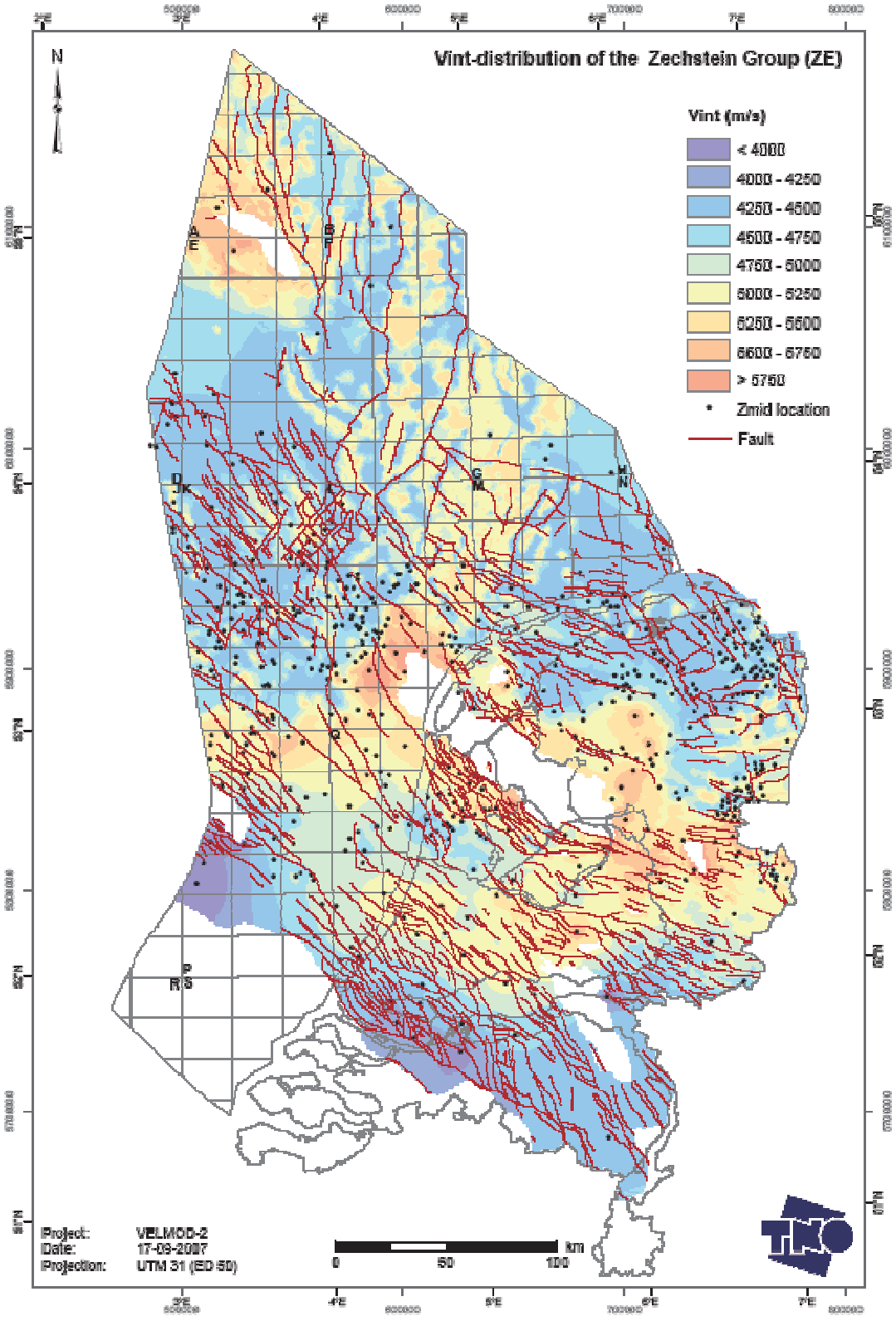

Figure 17 V_{int}-distribution of the layer of the Zechstein Group of VELMOD-2

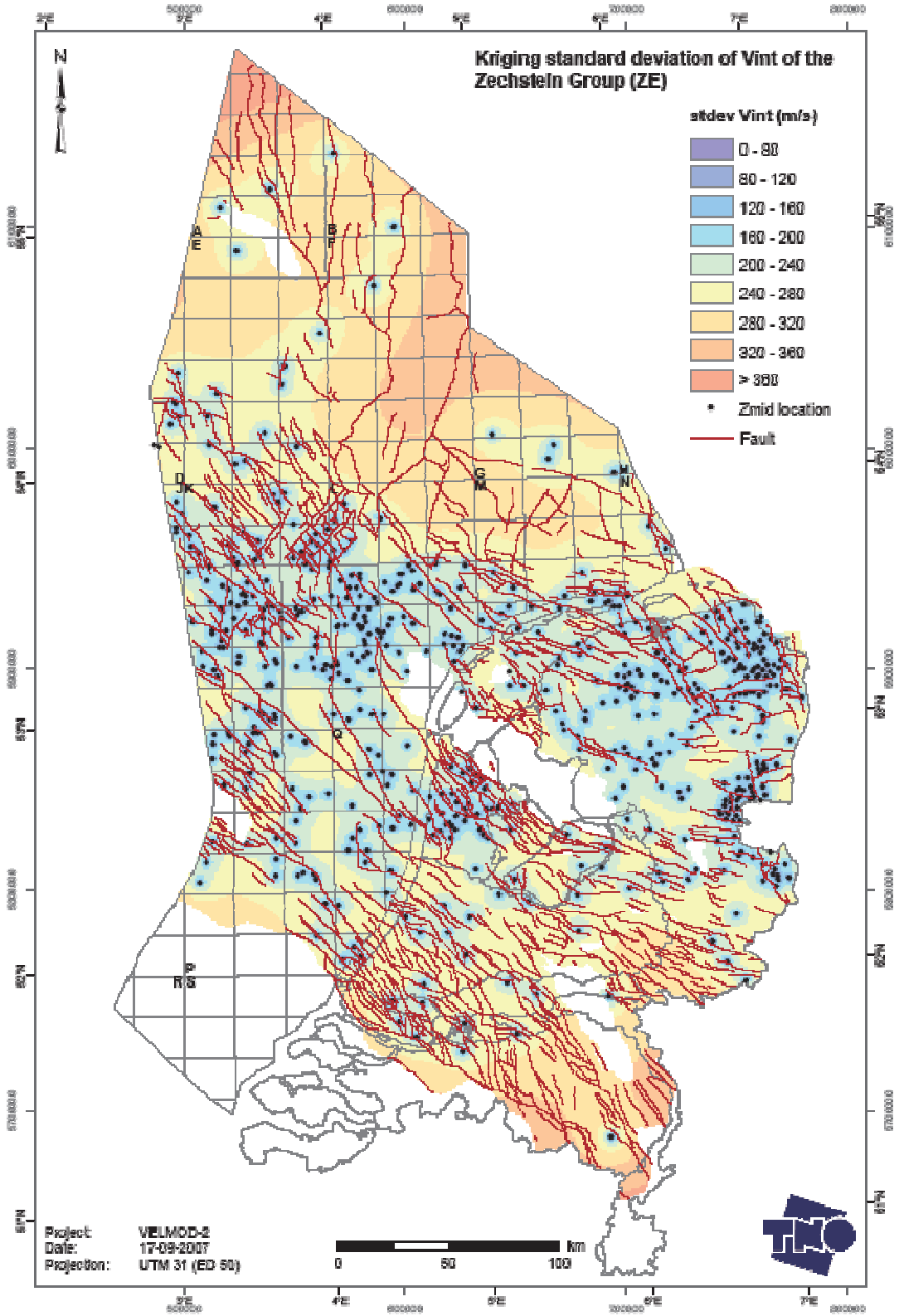

Figure 18 Kriging standard deviation of V_{int} for the layer of the Zechstein Group

6 Discussion

Geologic aspects of V_0 - distributions

The V_0-distributions for a number of layers can be interpreted in geological terms.

The relatively low V_0-values for the Mesozoic layers in the Step Graben, the Dutch Central Graben and the Terschelling Basin are attributed to overpressured pore fluids in these areas (Simmelink et al., 2005). Overpressures opposed compaction of the Mesozoic layers, resulting in lower velocities than would occur under hydrostatic equilibrium conditions. On their turn, the relatively low velocities effectuate relatively low V_0-values

The relatively high V_0-values for compacting Mesozoic and Paleozoic layers (those of the Chalk and Limburg Group excepted) in the Roer Valley Graben, the West Netherlands Basin and the Broad Fourteens Basin are attributed to the uplift of these layers. Apparent uplift in the Broad Fourteens Basin may be as large as 1600-2400 m according to an analysis of interval velocities of a Triassic claystone (Van Dalfsen, 2005). As the layer compaction, incurred at maximum burial depth, was largely irreversible during uplift, the velocities of the layer sediments, and therefore also the V_0-values, are relatively high.

Reliability of the VELMOD-2 model velocities

The reliability of VELMOD-2 is definitely higher than that of VELMOD-1, thanks to the availability of more digital sonic data of more boreholes. The availability of the local velocity graphs with lithostratigraphic markers (Appendix 2) easily allows inspection of the sonic data and detection of flaws like erroneous log data, hiatuses in log data, wrong editing and interpolation of log data, dubious log calibration and dubious stratigraphic markers. These inspections resulted in a careful acceptance of V_{int}- and z_{mid}-values, preceded by a x-sign in Appendix 1, and rejection of erroneous and dubious values.

Contrary to previous thougth, calibrated sonic data are not necessarily to be preferred above non-calibrated data. This illustrated with sonics datafiles of borehole MDN-01 (see Appendix 1). Figure 19 shows the local velocities according to non-calibrated sonic data, and Figure 20 according to TZ-data. Evidently, local velocities according to the TZ-data are erroneously high in that section of the layer of the Zechstein Group, where halite is predominantly present, as witnessed by velocities of roughly 4500 m/s according to Figure 20. What is evident for boreholes like MDN-01, is taken as a guideline for other boreholes, namely that one should be careful in preferring calibrated sonic data above non-calibrated data.

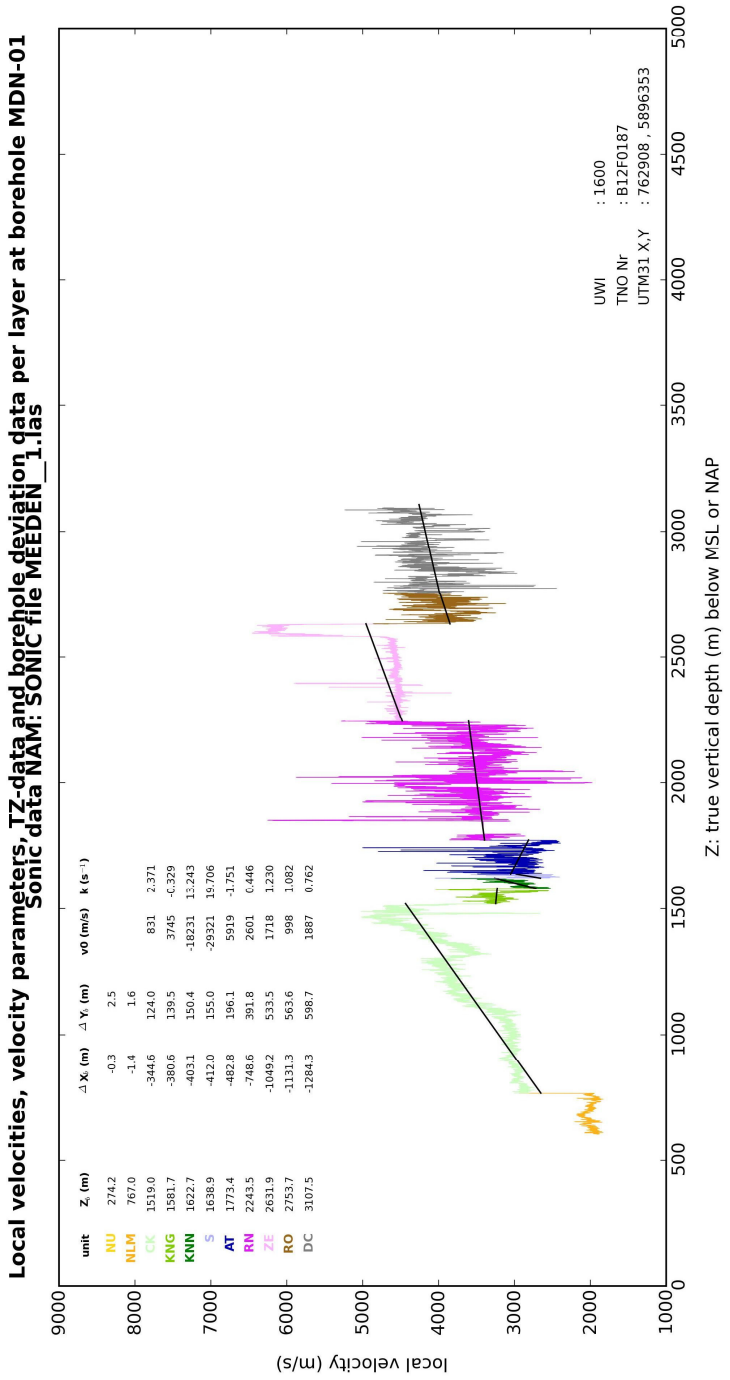

Figure 19 Local velocities at borehole MDN-01 according to TZ-data

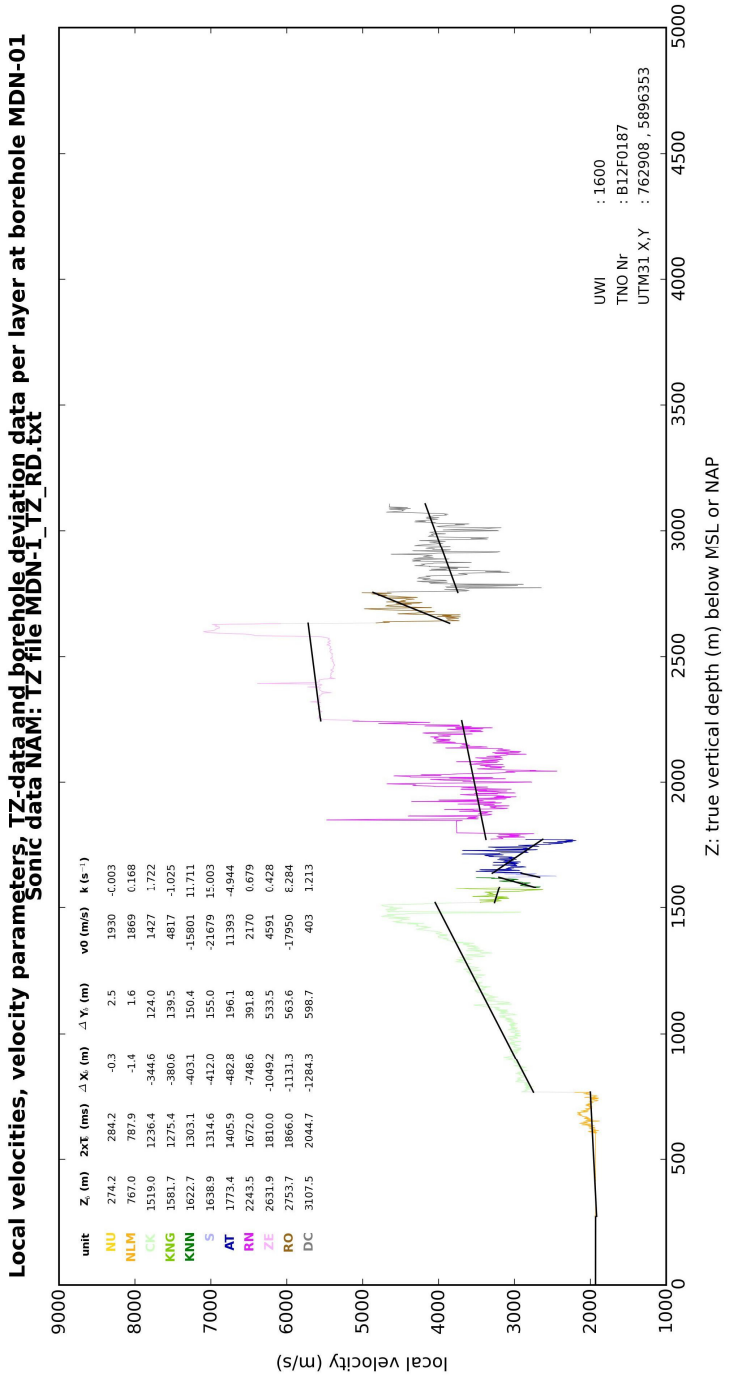

Figure 20 Local velocities at borehole MDN-01 according to non-calibrated sonic data

7 Conclusions and recommendations

Conclusions

1. The velocity model of VELMOD-2 may be expected to be more accurate than that of VELMOD-1. This is due to the availability of more digital sonic logs of more boreholes.
2. Many calibrated sonic logs, or their TZ-pairs, show flaws. Therefore one must be cautious using them in velocity modeling.
3. Several V_0-distributions can be interpreted in terms of the geologic phenomena of uplift and subsurface fluid overpressure.

Recommendations

1. Inform TNO on your companies' experiences with VELMOD-2;
2. Improve on VELMOD-2. This can be accomplished if:
   - Deficiencies in the borehole lithostratigraphic markers of the DINO database are removed;
   - Quality control of sonic data can be further improved;
   - More boreholes become available with digital sonic data.

8 References

Doornenbal, J.C., 2001. Regional velocity models of the Netherlands territory. 63rd EAGE Conference Expanded Abstracts, Paper A08.

Dubrule, O., 2003. Geostatistics for Seismic Data Integration in Earth Models. 2003 Distinguished Instructor Short Course, Distinguished Instructor Series, No. 6, EAGE.

Duin, E.J.T., Doornenbal, J.C., Rijkers, R.H.B., Verbeek, J.W. & Wong, Th.E., 2006. Subsurface structure of the Netherlands – results of recent onshore and offshore mapping. Netherlands Journal of Geosciences / Geologie en Mijnbouw 85-4: 245-276.

Goovaerts, P., 1997. Geostatistics for Natural Resources Evaluation. Oxford University Press.

Japsen, P., 1993. Influence of lithology and Neogene uplift on seismic velocities in Denmark: implications for depth conversion of maps. American Association of Petroleum Geologists Bulletin 77, No.2: 194-211.

Robein, E., 2003. Velocities, Time-imaging and Depth-Imaging in Reflection Seismics. Principles and Methods, EAGE Publications b.v.

Simmelink, E., Verweij, H., Underschultz, J. & Otto, C.J., 2005. A quality controlled pressure database and a regional hydrodynamic and overpressure assessment in the Dutch North Sea. Poster at the AAPG 2005 Annual Convention.

Van Adrichem Boogaert, H.A. & Kouwe, W.F.P., 1993-1997 (eds). Stratigraphic nomenclature of the Netherlands, revision and update by RGD and NOGEPA, Mededelingen Rijks Geologische Dienst, nr. 50.

Van Dalfsen, W., Mijnlieff, H.A. & Simmelink, E., 2005. Interval velocities of a Triassic claystone: key to burial history and velocity modeling. Poster 178 at EAGE 2005 Annual Meeting.

Van Dalfsen, W., Doornenbal, J.C., Dortland, S. & Gunnink, J.L., 2006a. VELMOD-1 Joint Industry Project, TNO report 2006-U-R0037/B.

Van Dalfsen, W., Doornenbal, J.C., Dortland, S. & Gunnink, J.L., 2006b. A comprehensive seismic velocity model for the Netherlands based on lithostratigraphic layers. Netherlands Journal of Geosciences / Geologie en Mijnbouw 85-4: 277-292.

9 Goodies

On request of participants, goodies are added to this report. These are maps of V_{int} (Goody 1) and its kriging standard-deviation (Goody 2) for all compacting main layers and sublayers, together with their variograms (Goody 3). Appendix 8 contains the grids of V_{int} and its kriging standard deviation.

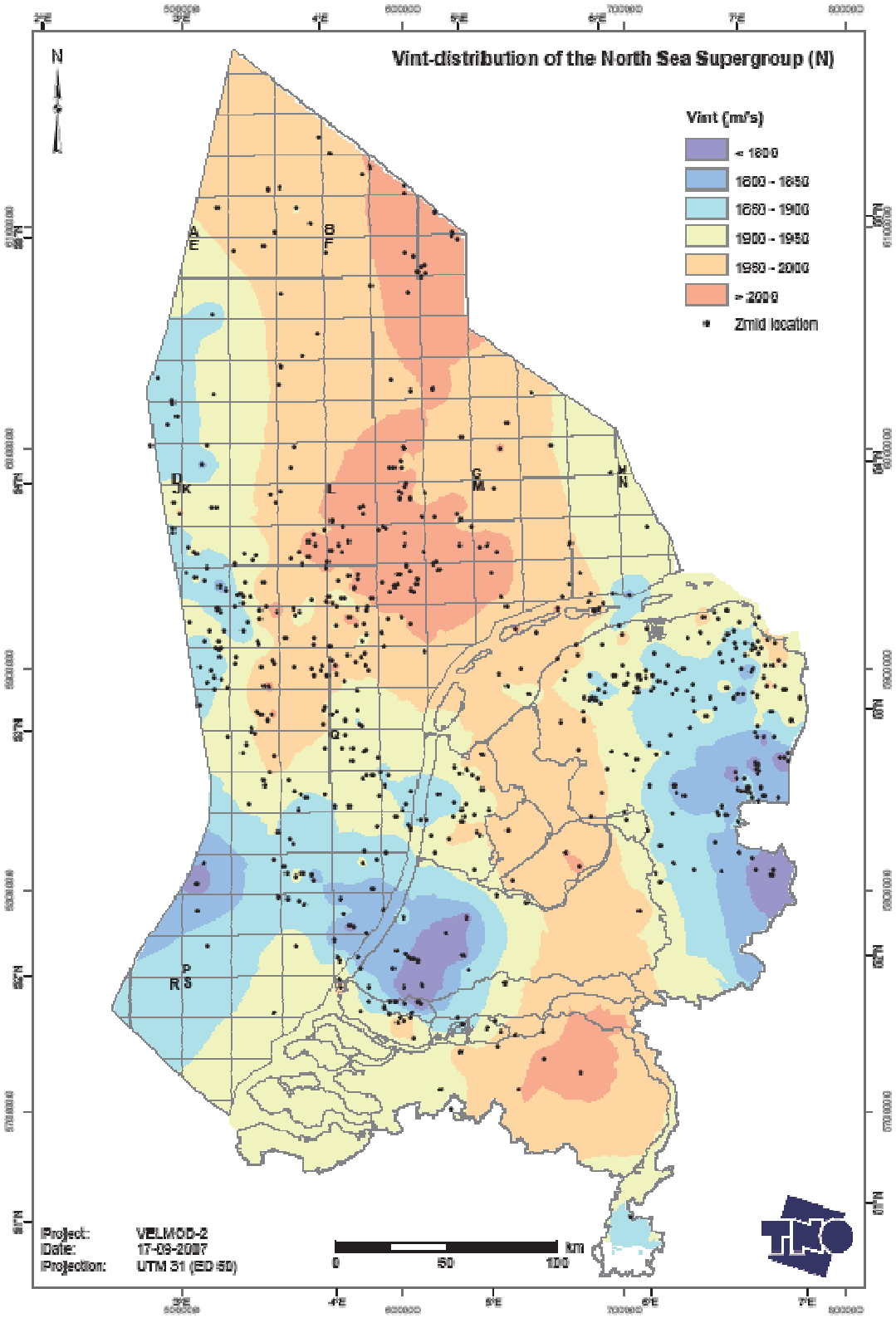

Goody 1-1 V_{int}-distribution of the layer of the North Sea Supergroup (NU+NM+NL)

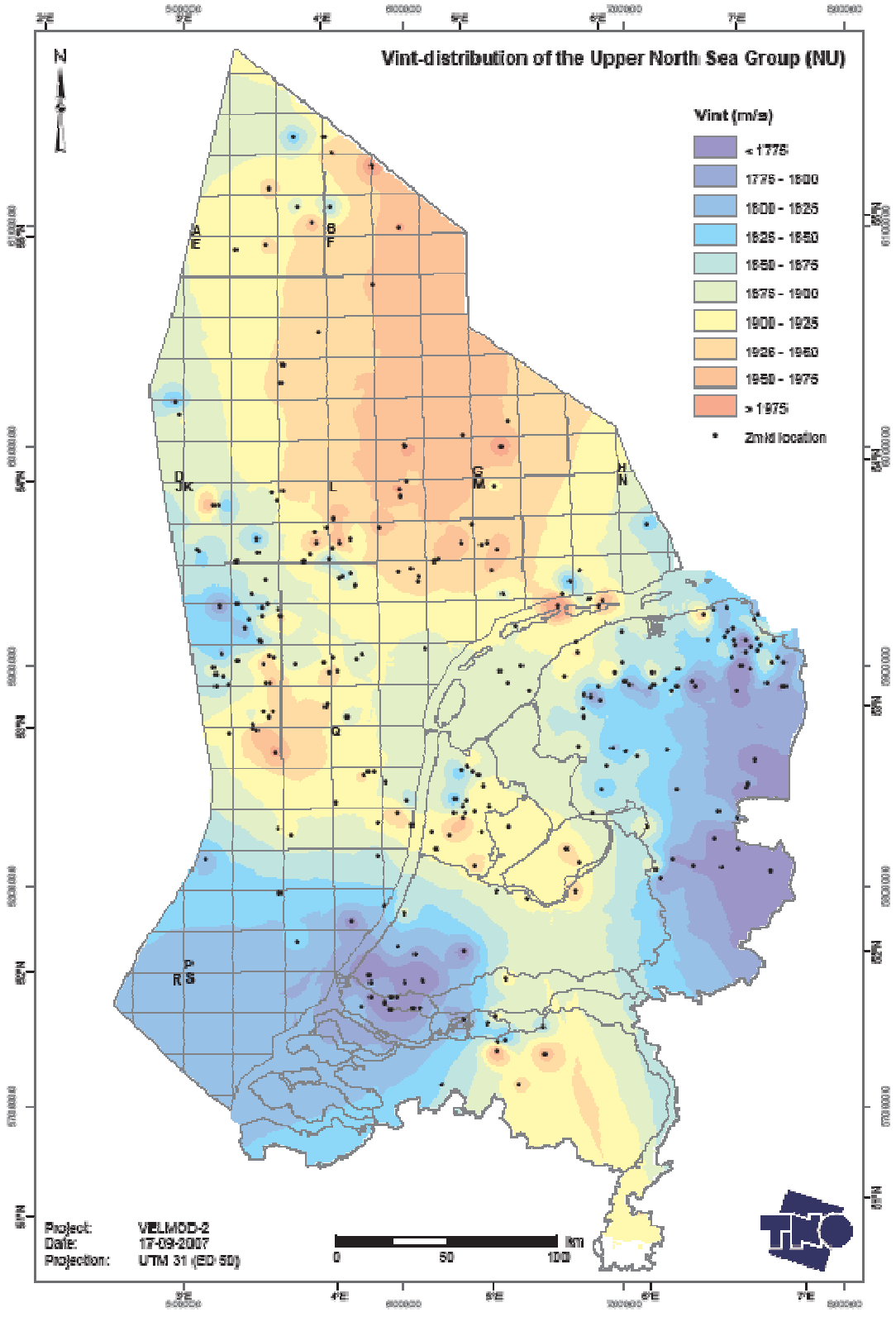

Goody 1-1a V_{int}-distribution of the layer of the Upper North Sea Group (NU)

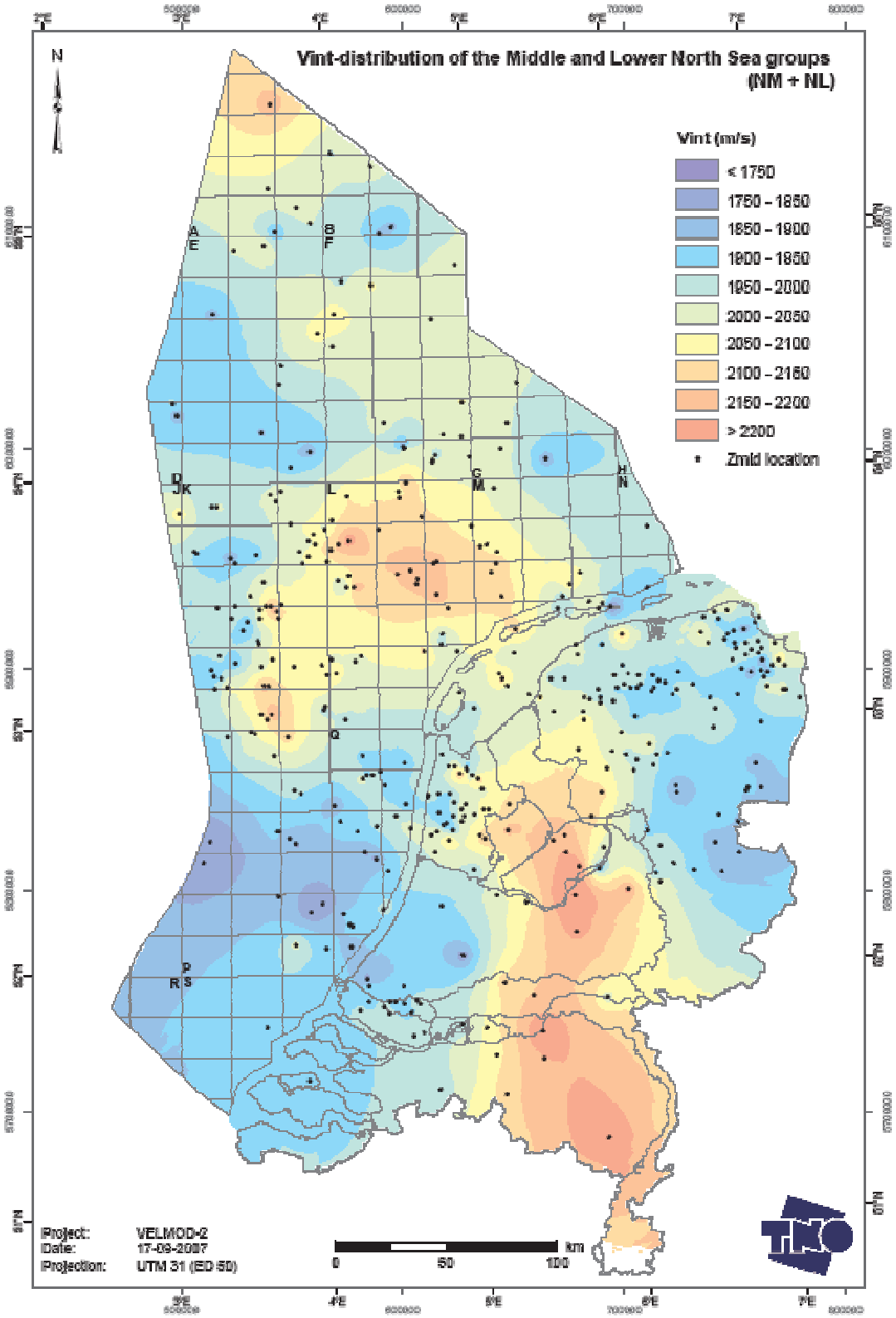

Goody 1-1b V_{int}-distribution of the layer of the Middle and Lower North Sea groups (NM+NL)

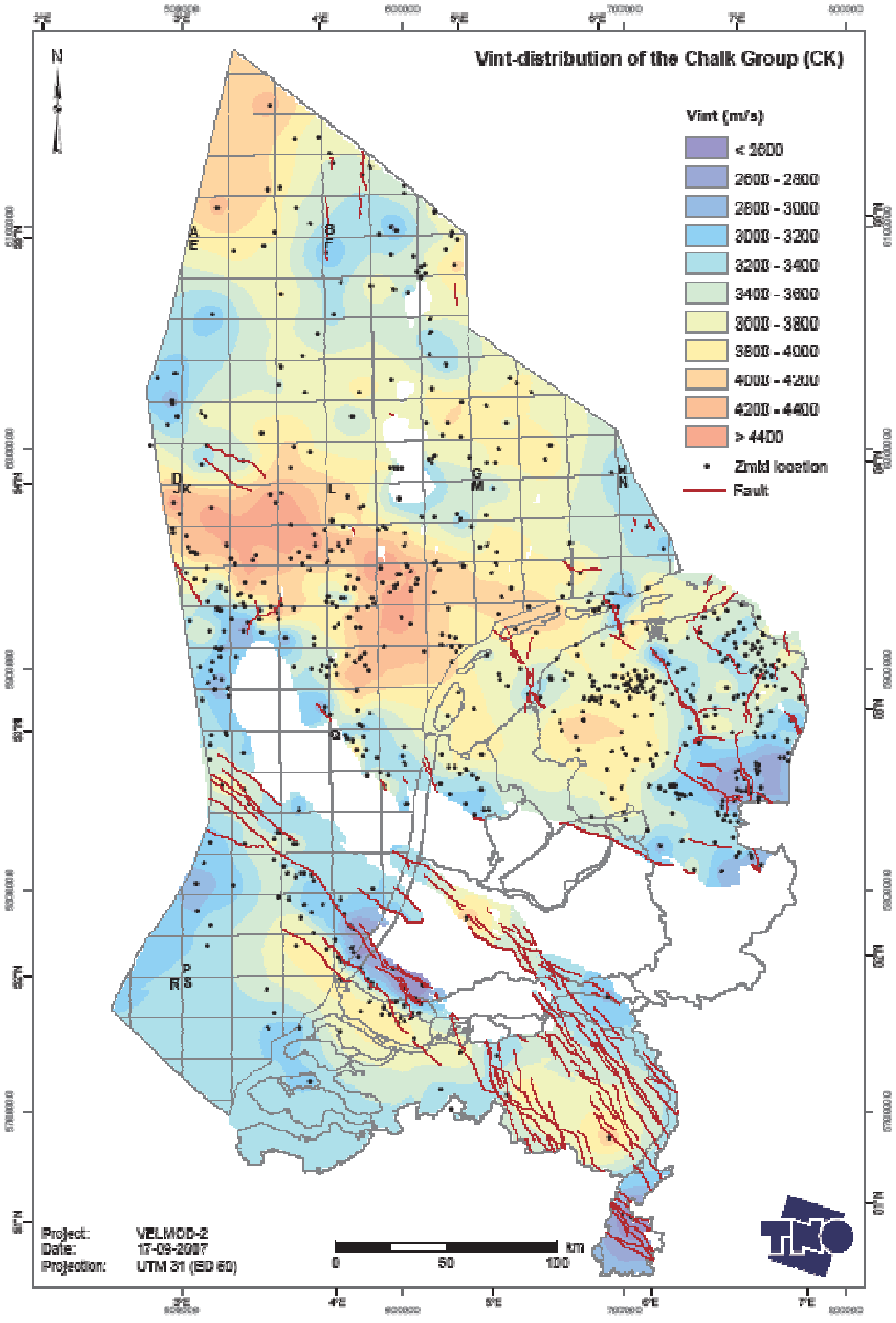

Goody 1-2 V_{int}-distribution of the layer of the Chalk Group (CK)

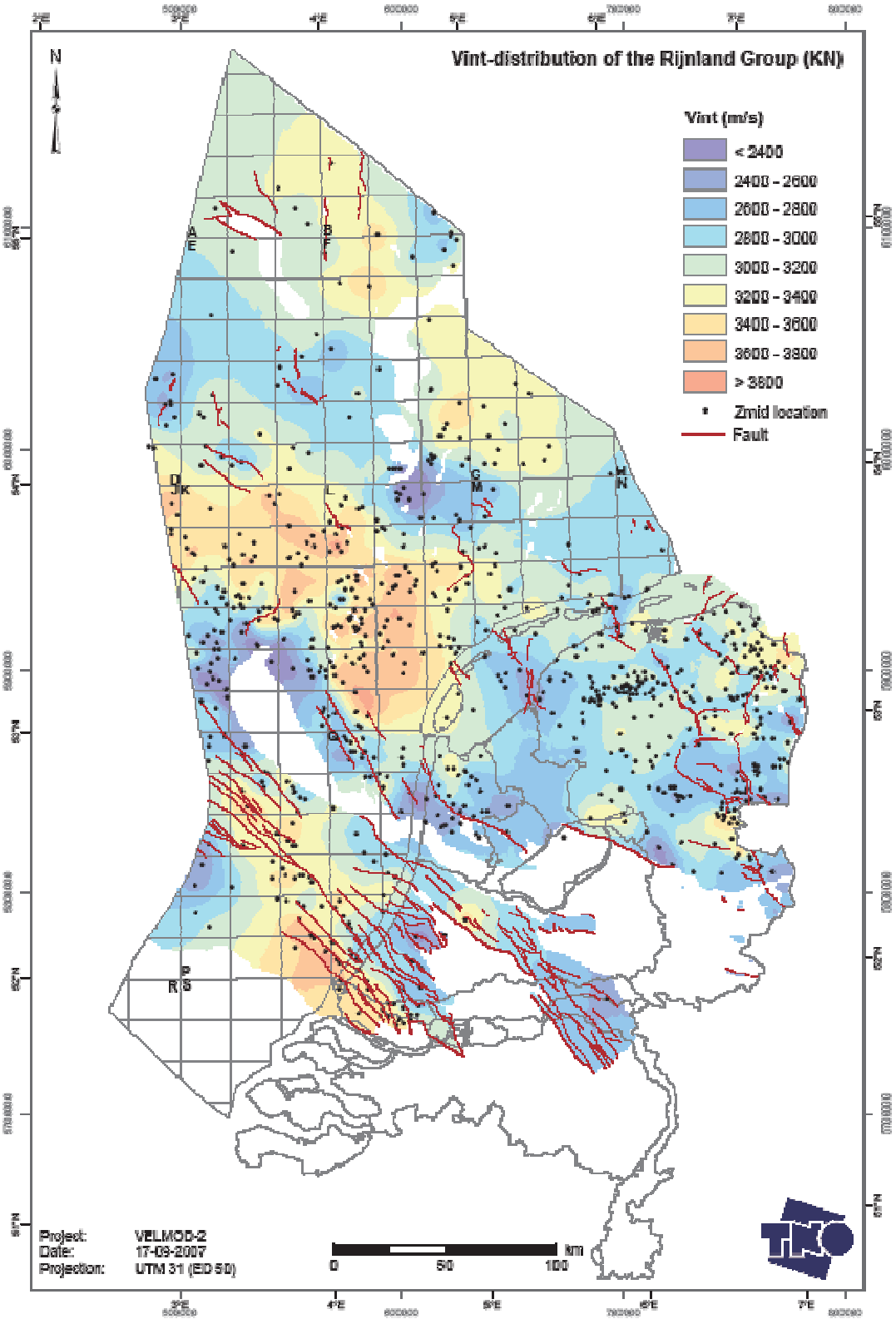

Goody 1-3 V_{int}-distribution of the layer of the Rijnland Group (KN)

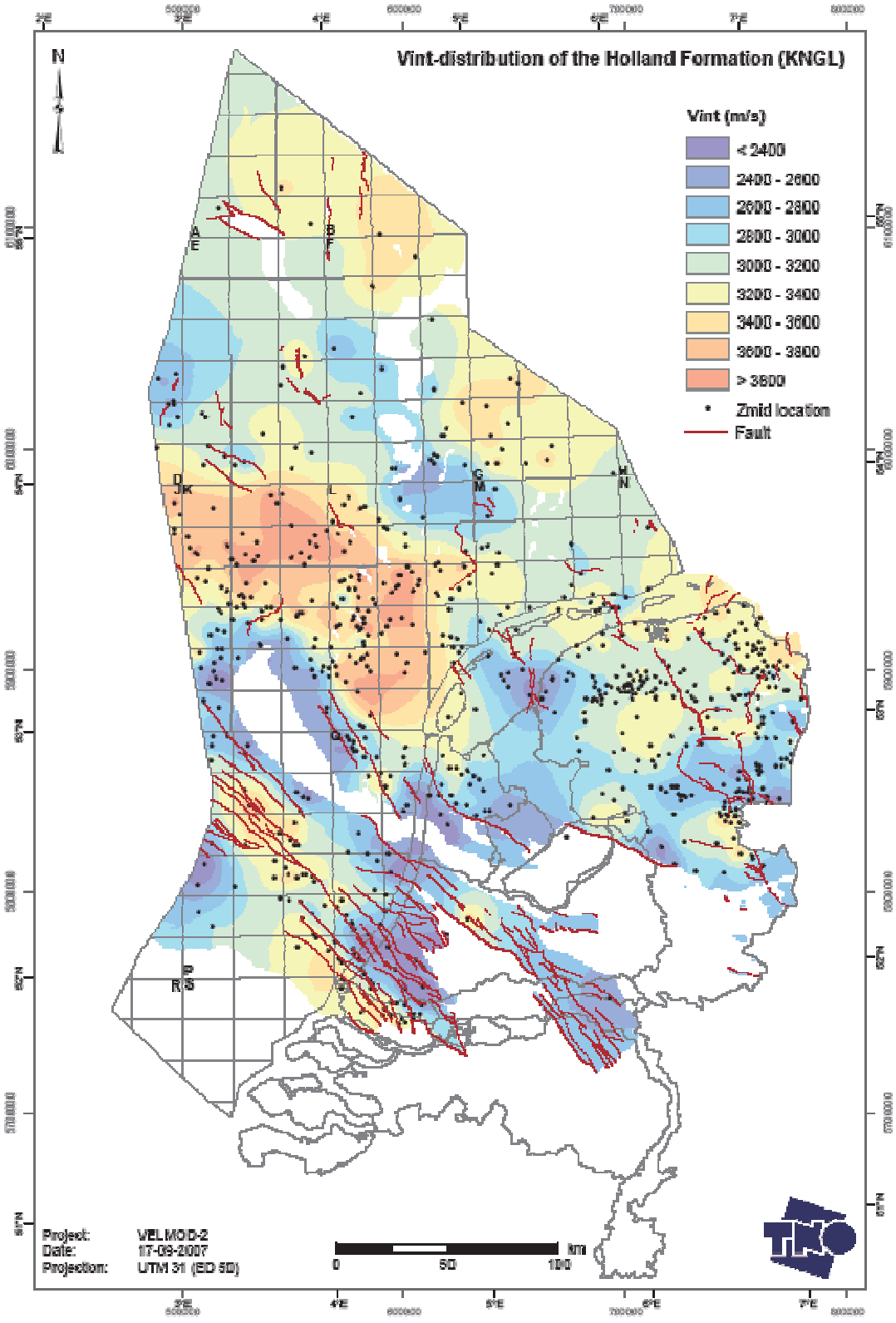

Goody 1-3a V_{int}-distribution of the layer of the Holland Formation (KNGL)

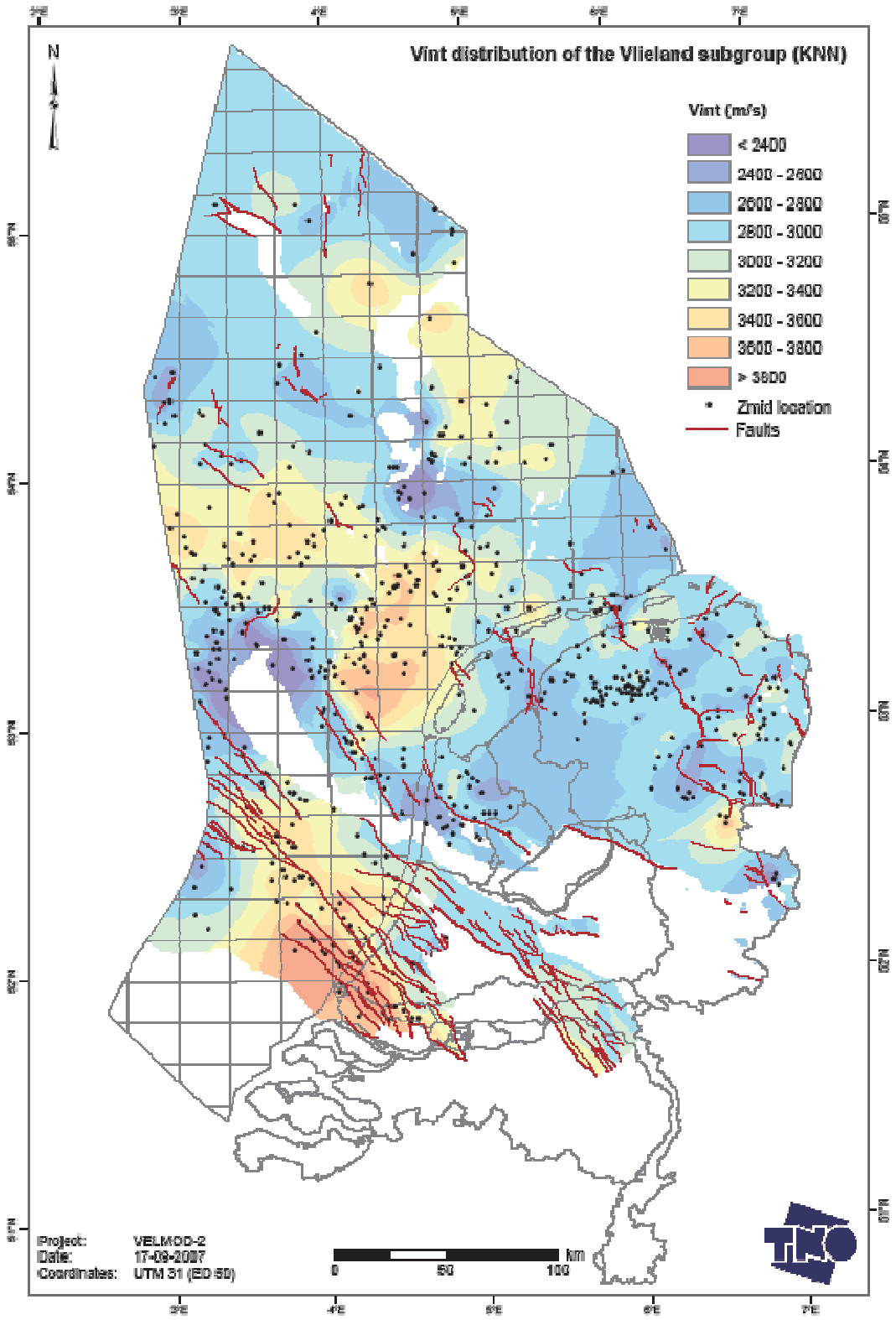

Goody 1-3b V_{int}-distribution of the layer of the Vlieland subgroup (KNN)

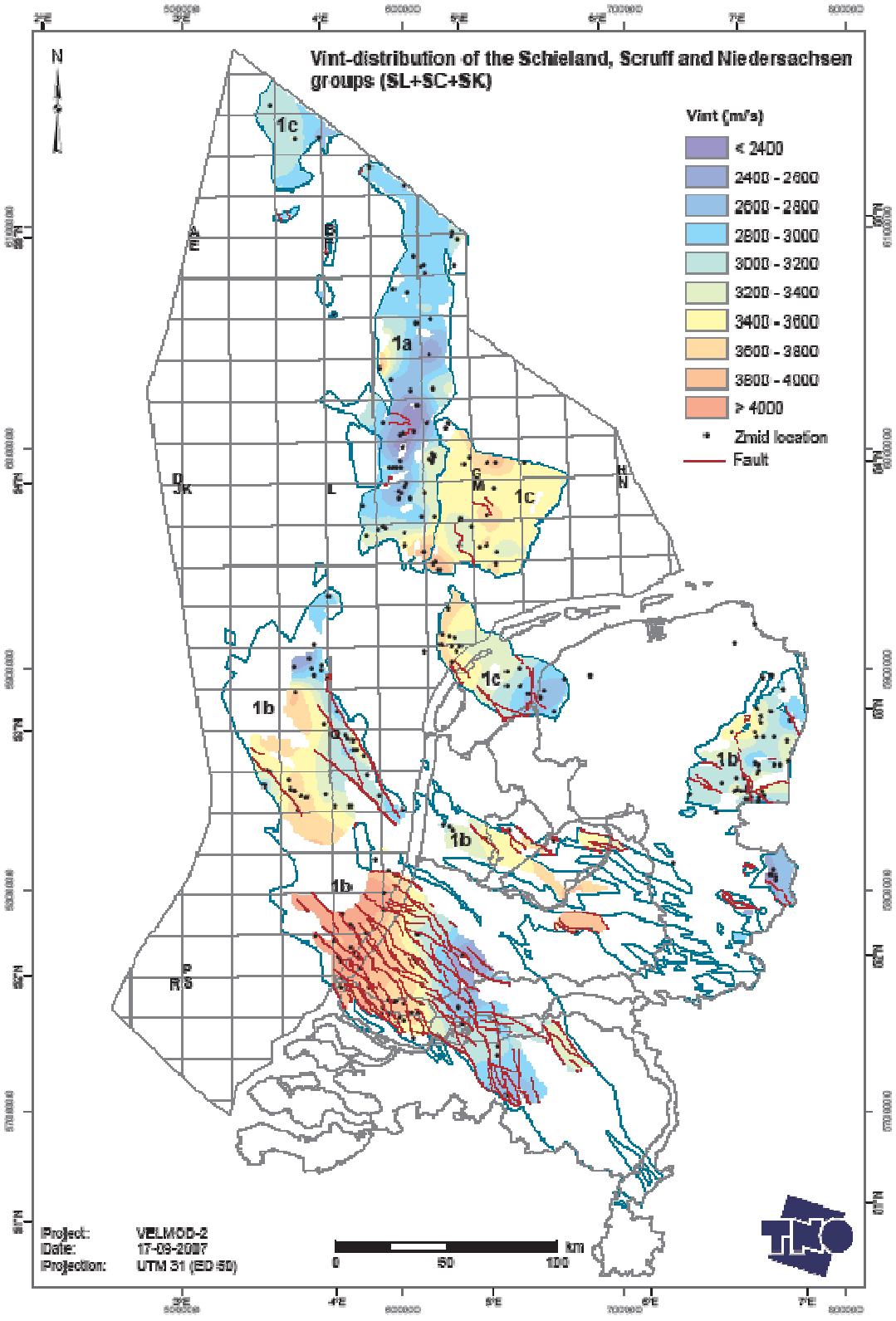

Goody 1-4 V_{int}-distribution of the layer of the Schieland, Scruff and Niedersachsen groups (SL+SG+SK)

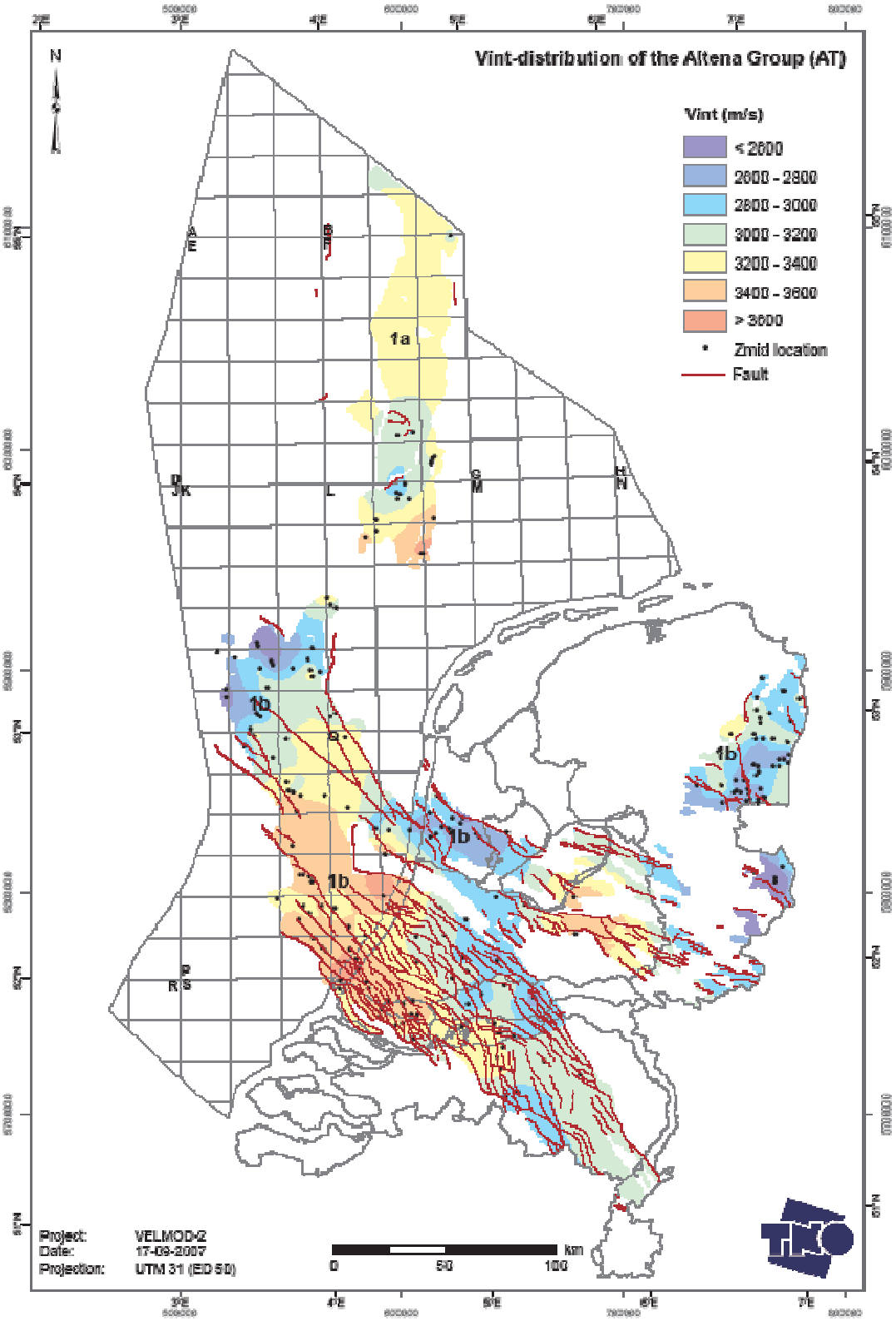

Goody 1-5 V_{int}-distribution of the layer of the Altena Group (AT)

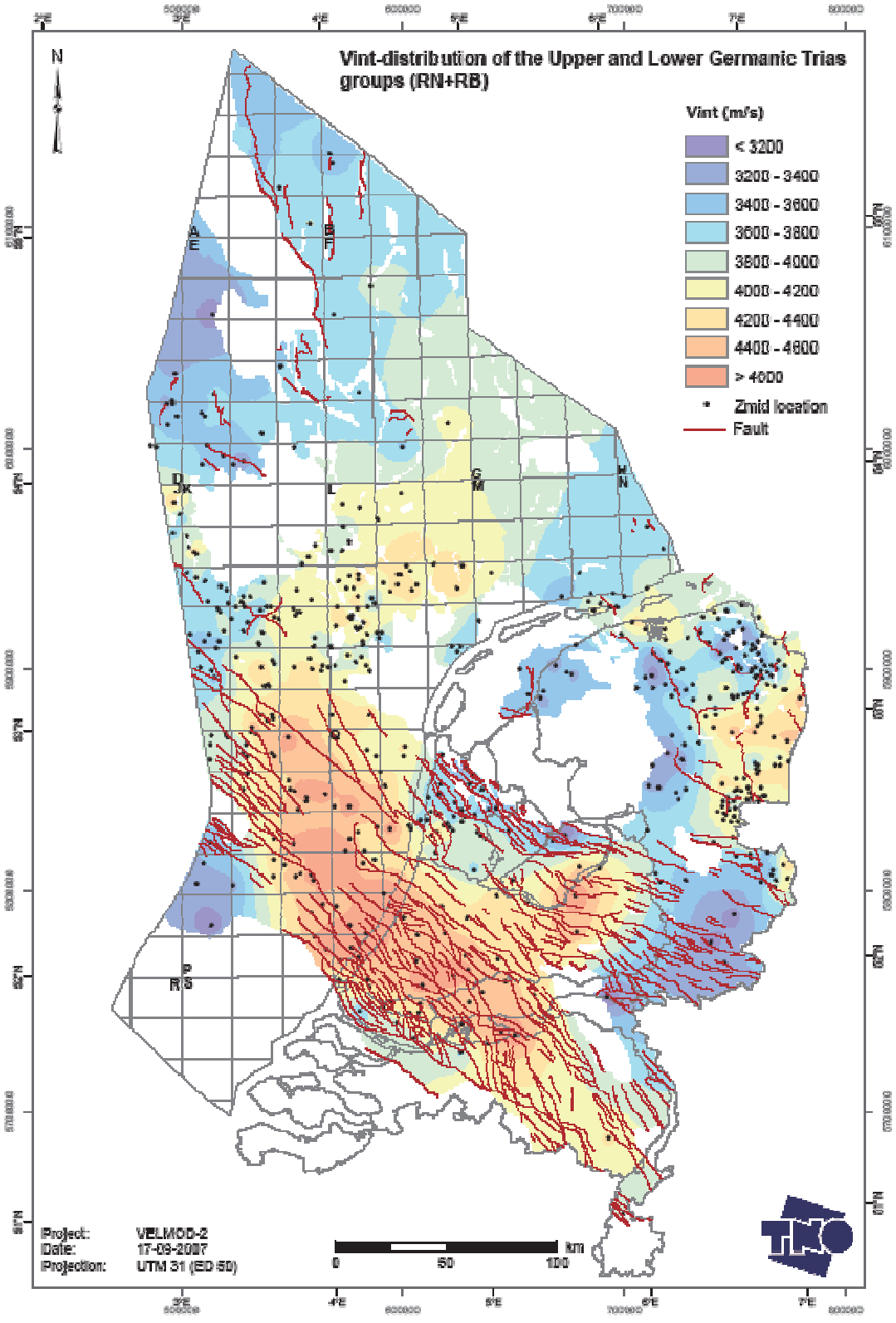

Goody 1-6 V_{int}-distribution of the layer of the Upper and Lower Germanic Trias groups (RN+RB)

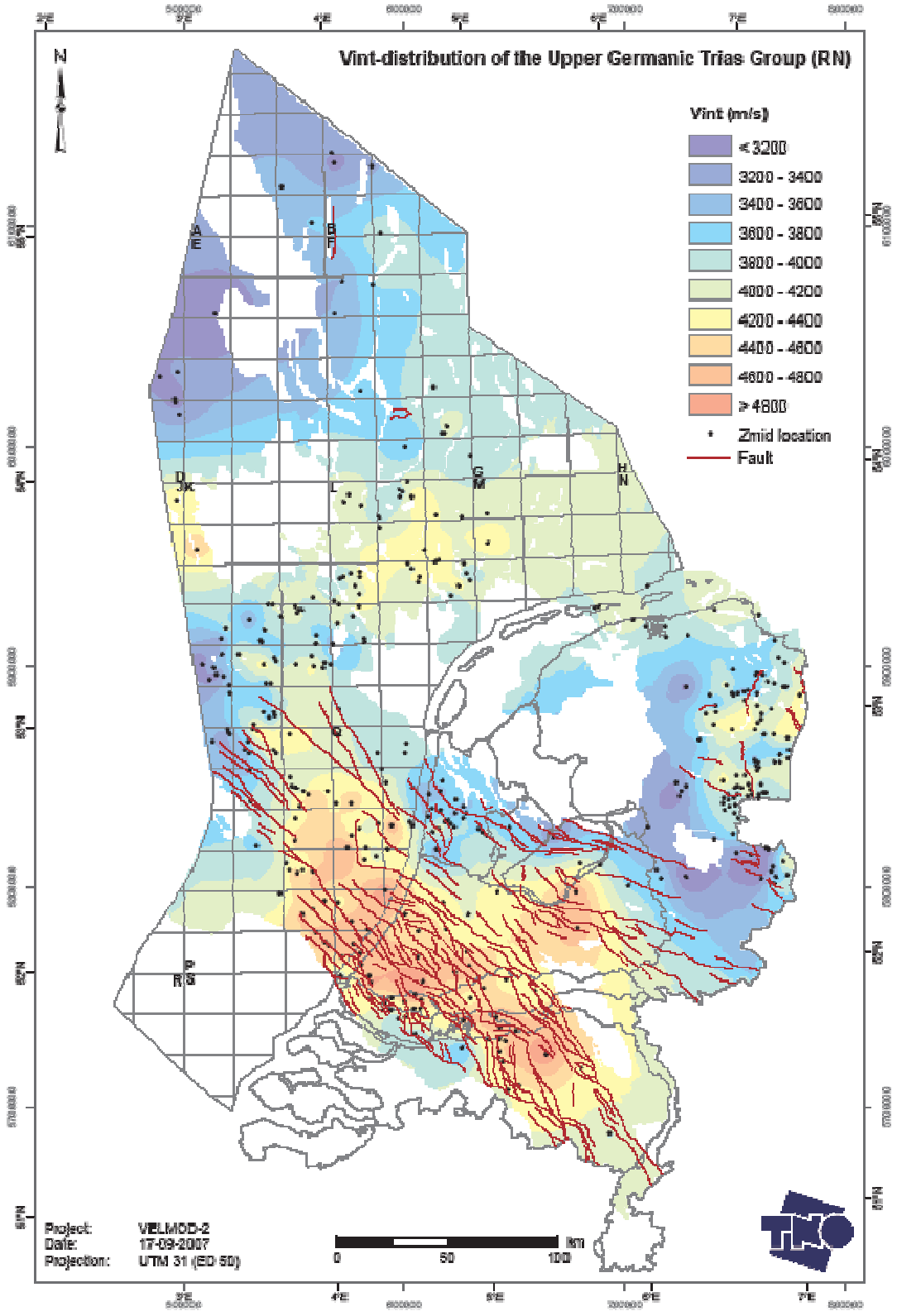

Goody 1-6a V_{int}-distribution of the layer of the Upper Germanic Trias Group (RN)

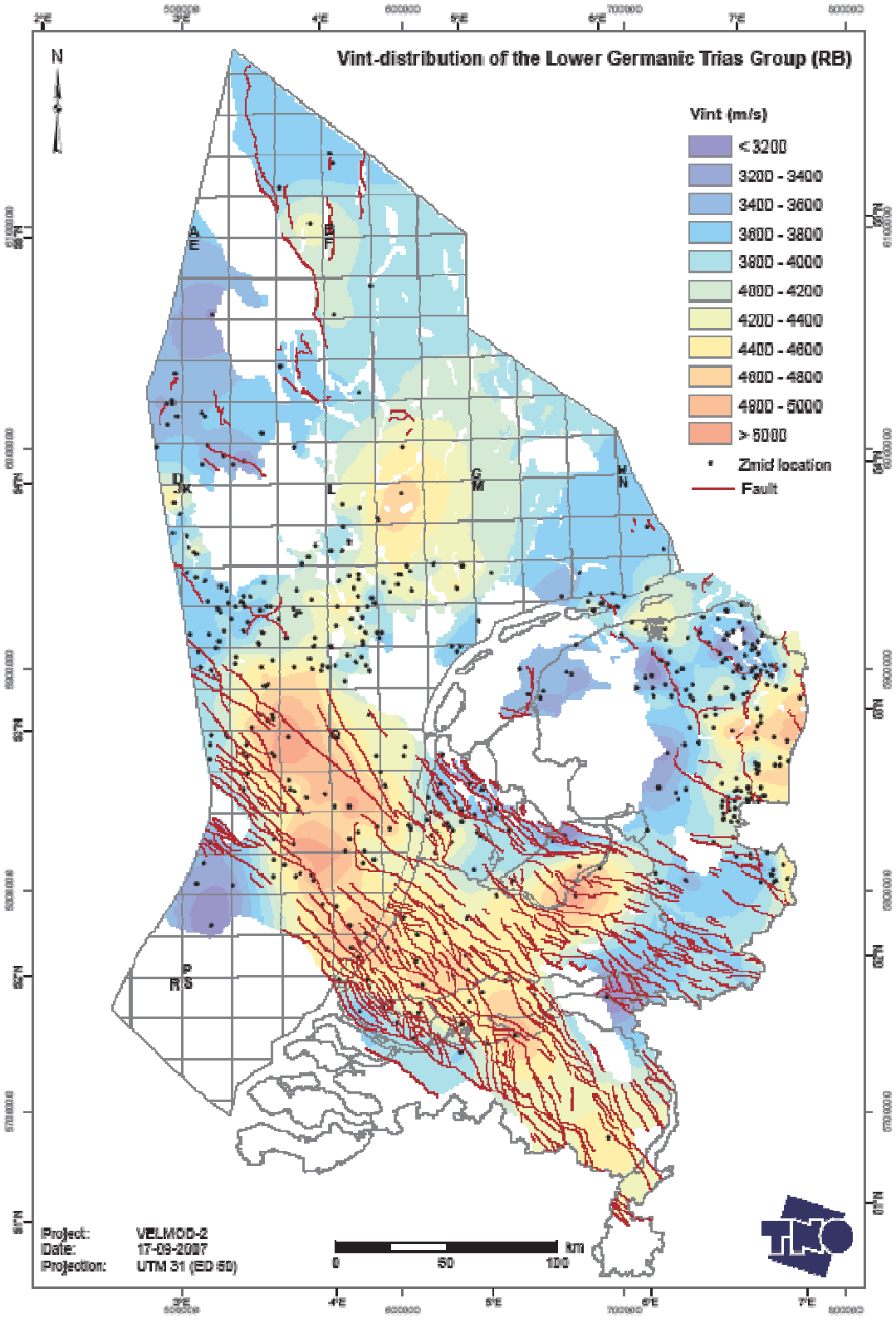

Goody 1-6b V_{int}-distribution of the layer of the Lower Germanic Trias Group (RB)

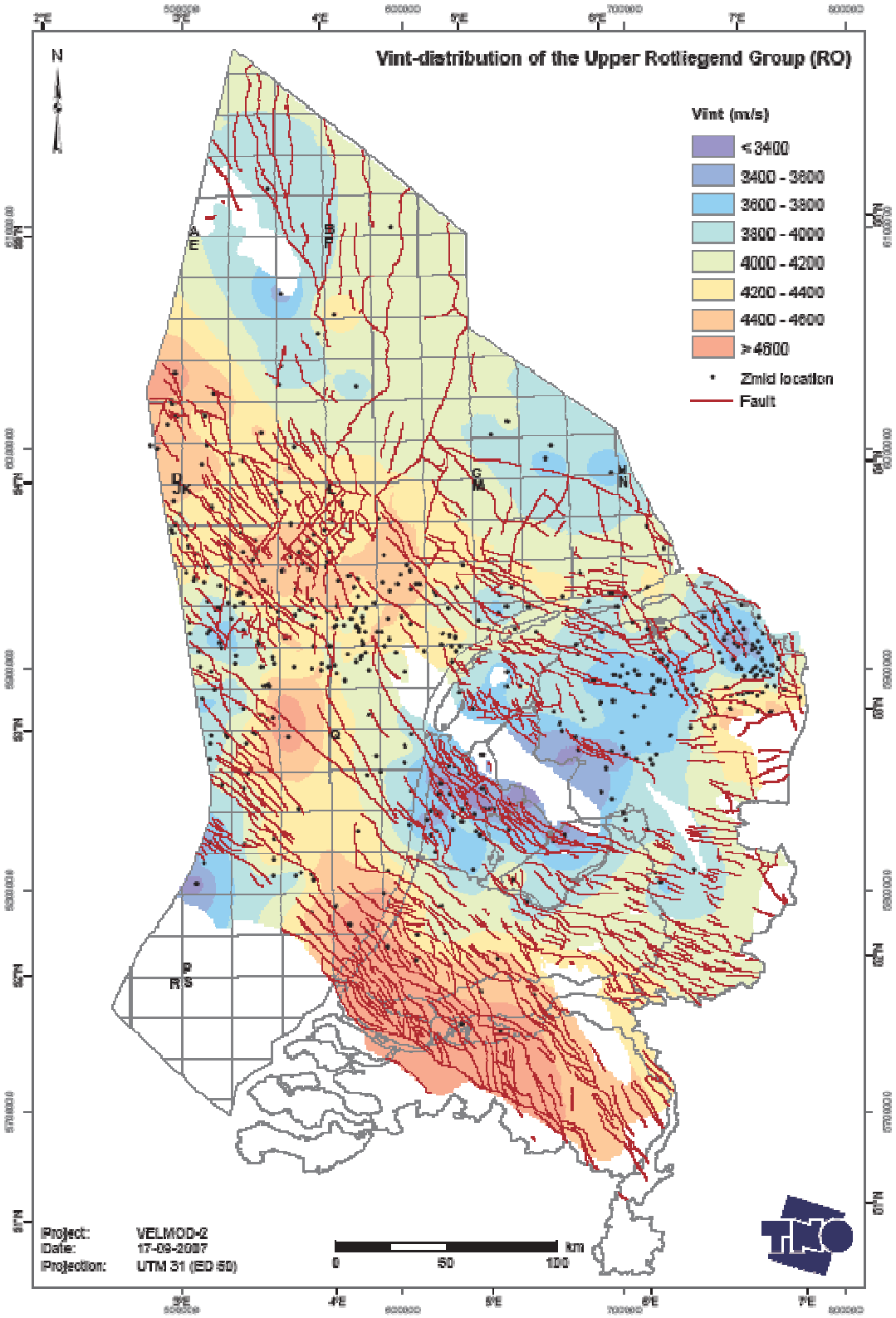

Goody 1-8 V_{int}-distribution of the layer of the Upper Rotliegend Group (RO)

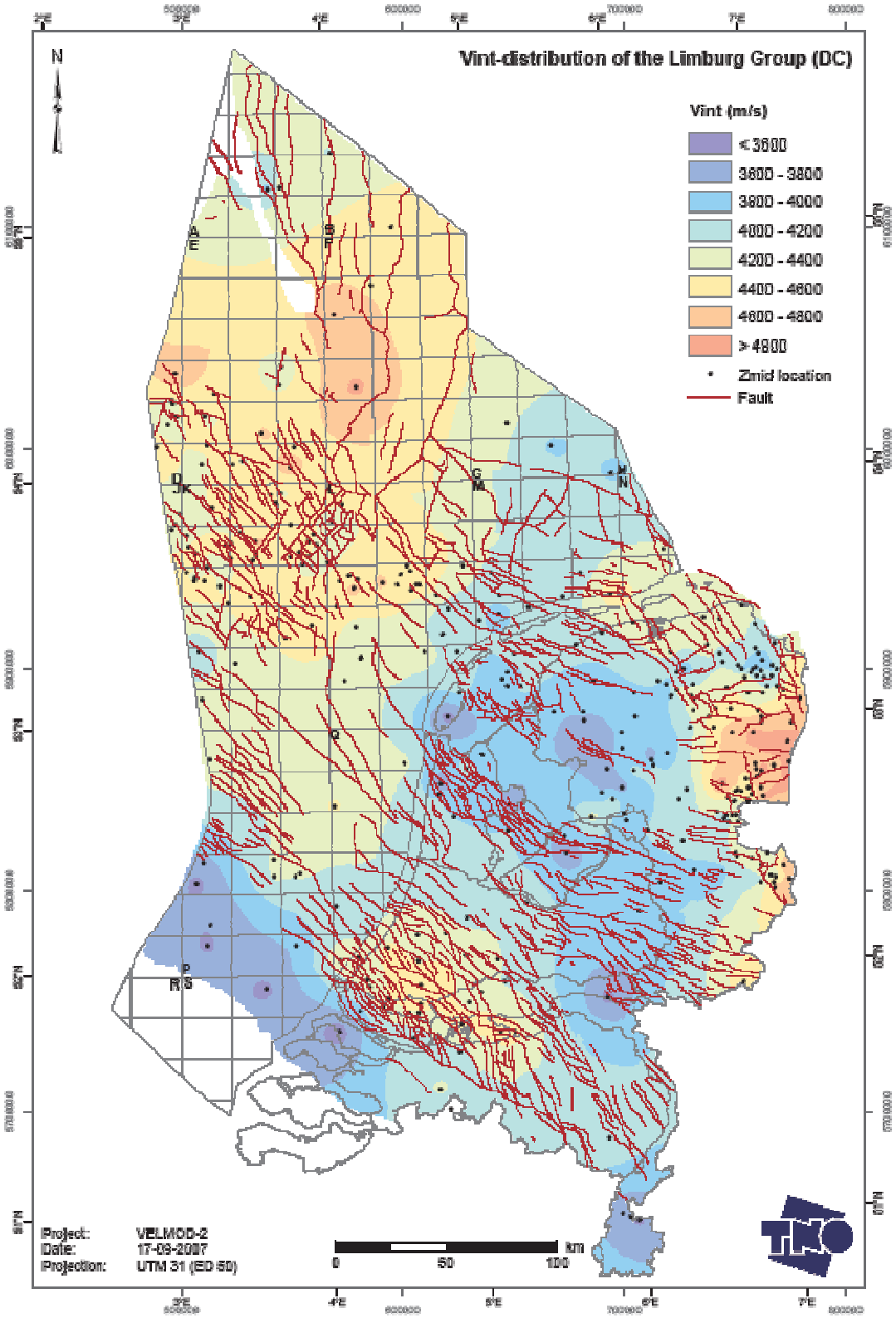

Goody 1-9 V_{int}-distribution of the layer of the Limburg Group (DC)

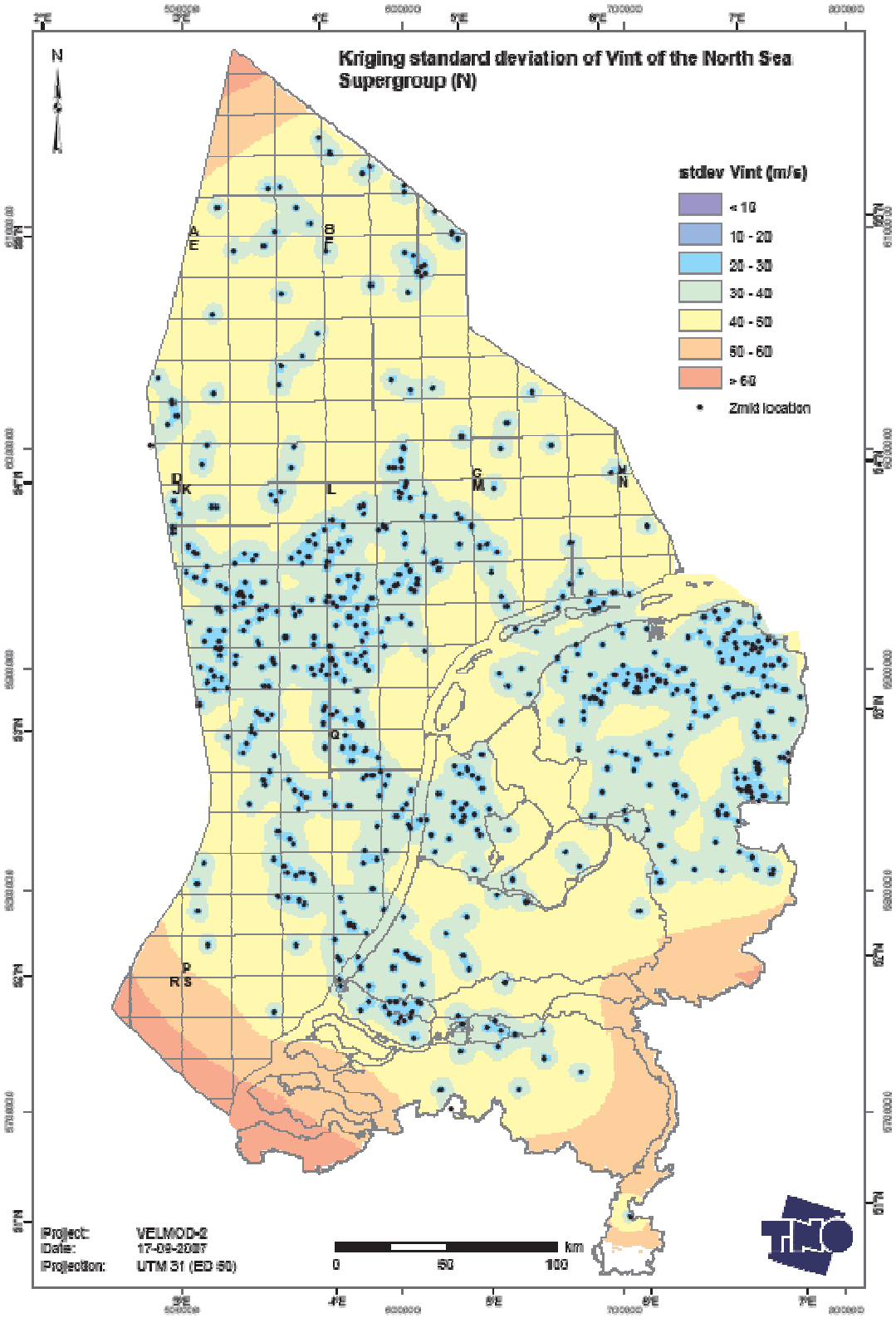

Goody 2-1 Kriging standard deviation of V_{int} for the layer of the North Sea Supergroup (NU+NM+NL)

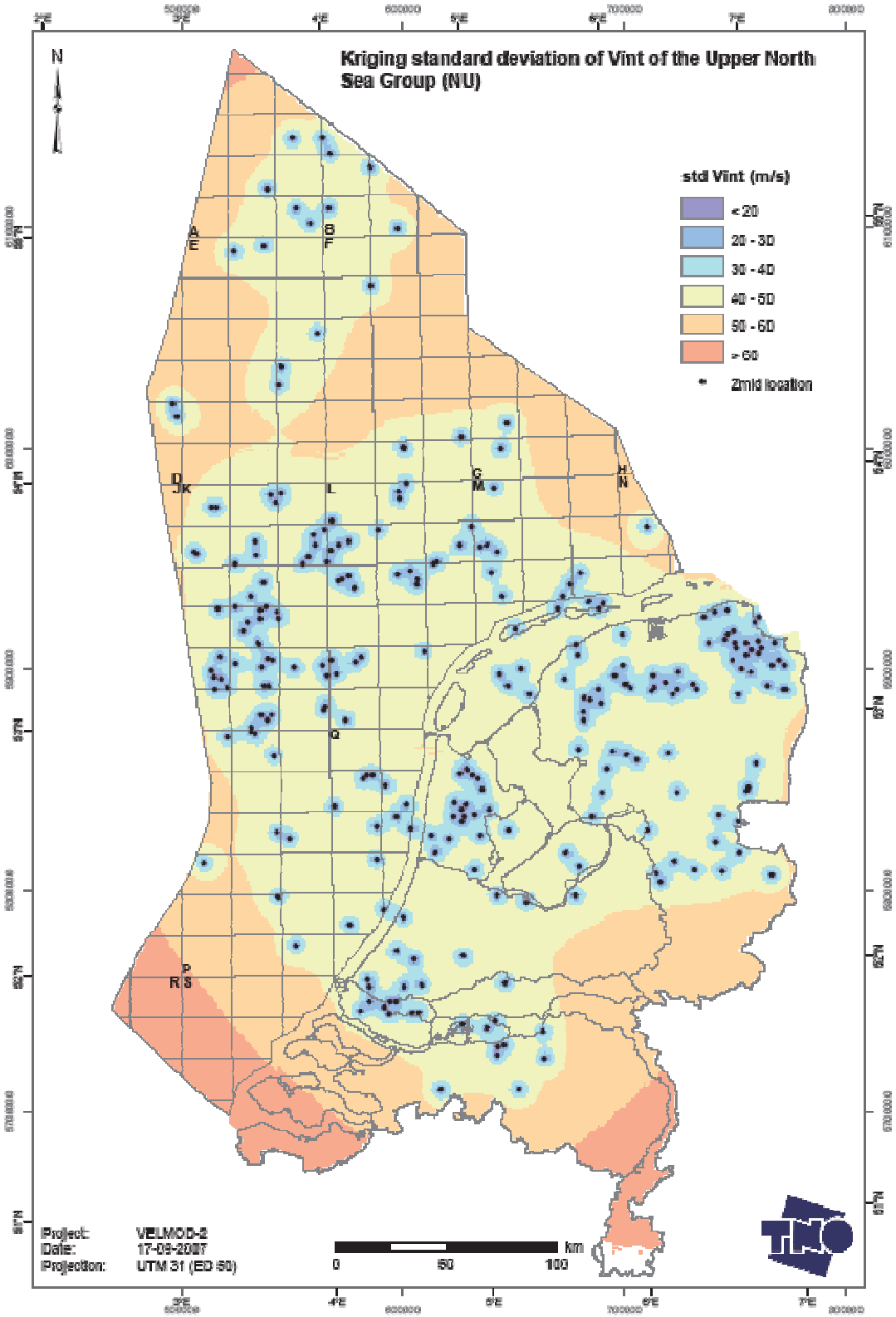

Goody 2-1a Kriging standard deviation of V_{int} for the layer of the Upper North Sea Group (NU)

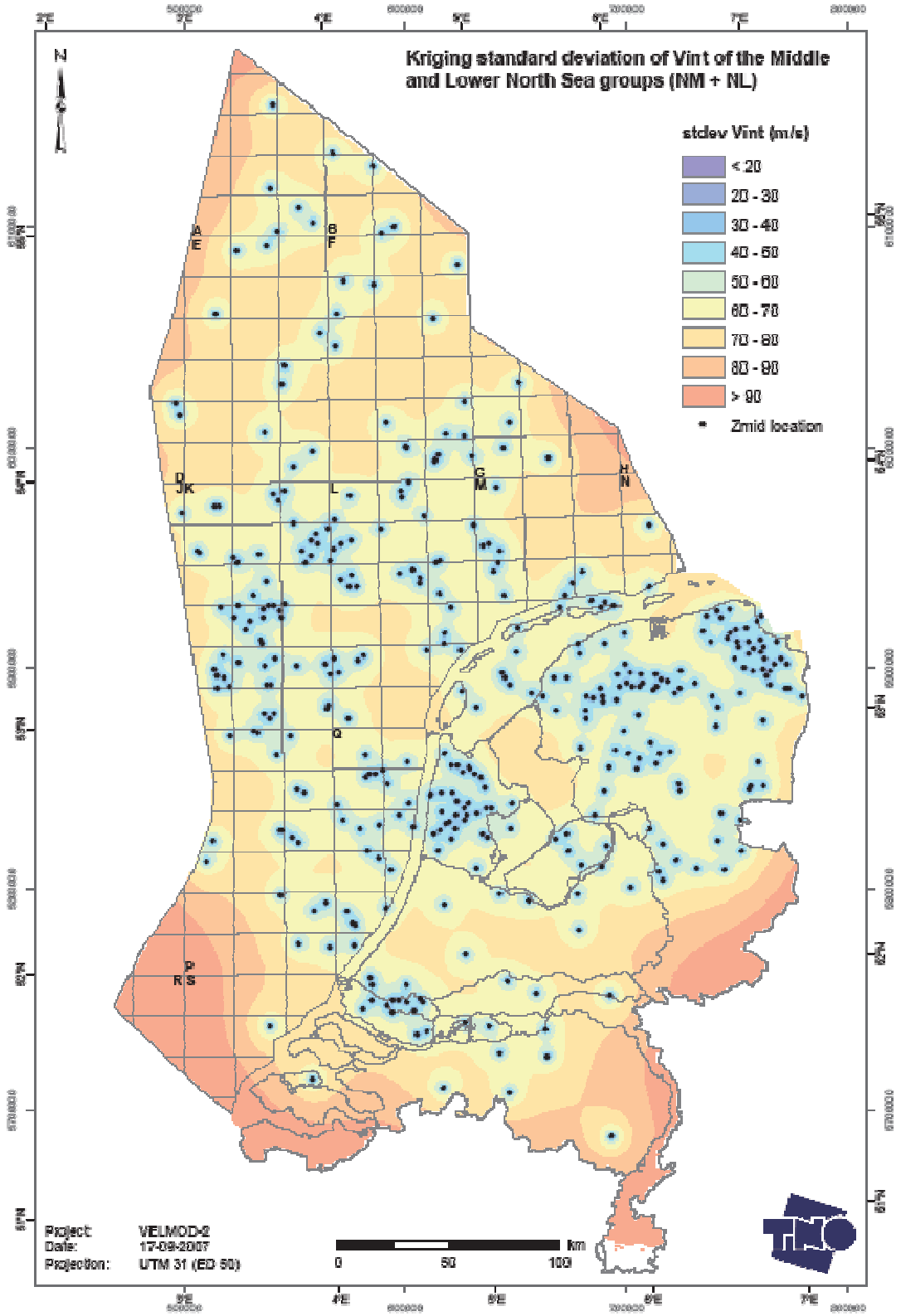

Goody 2-1b Kriging standard deviation of V_{int} for the layer of the Middle and Lower North Sea groups (NM+NL)

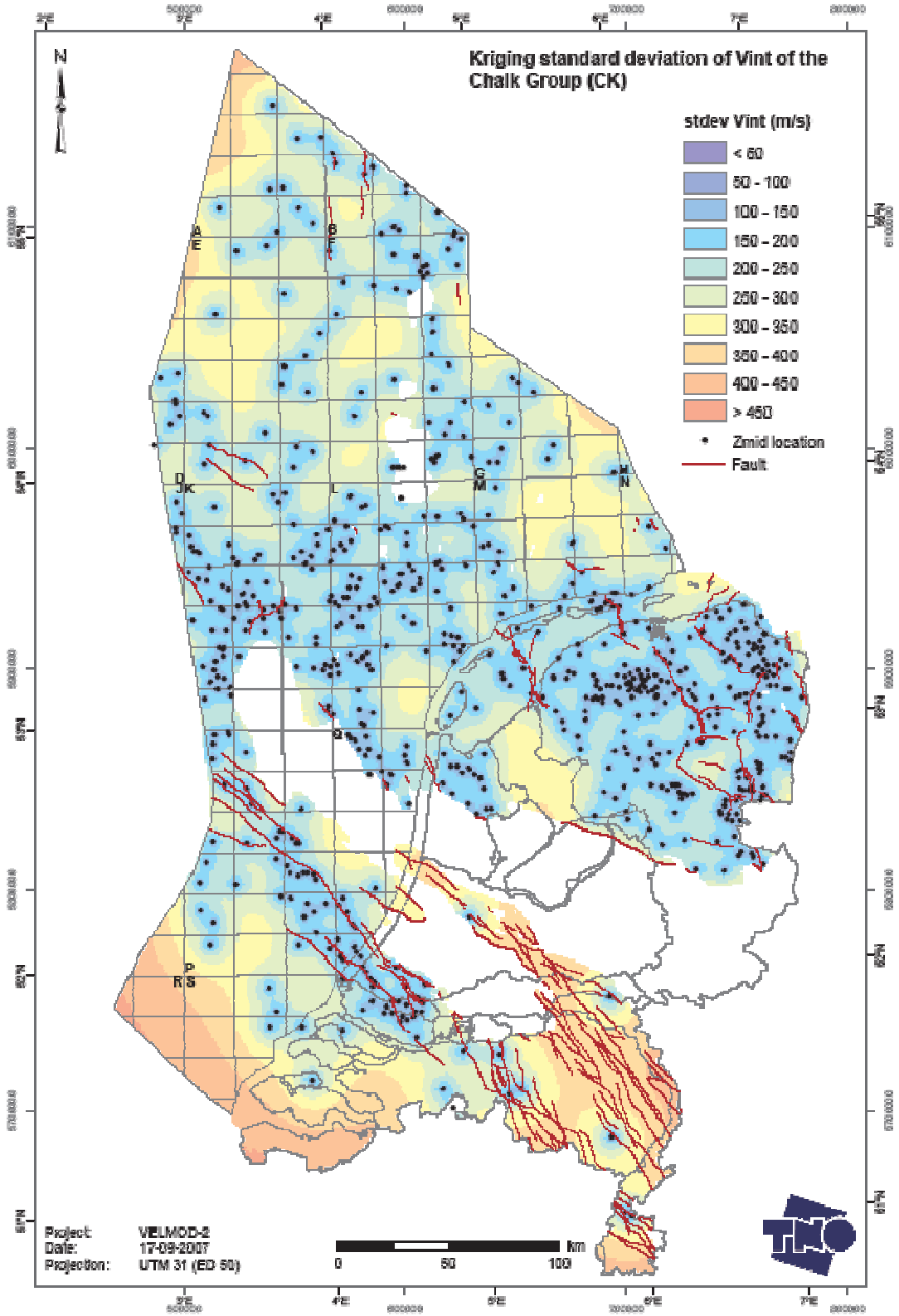

Goody 2-2 Kriging standard deviation of V_{int} for the layer of the Chalk Group (CK)

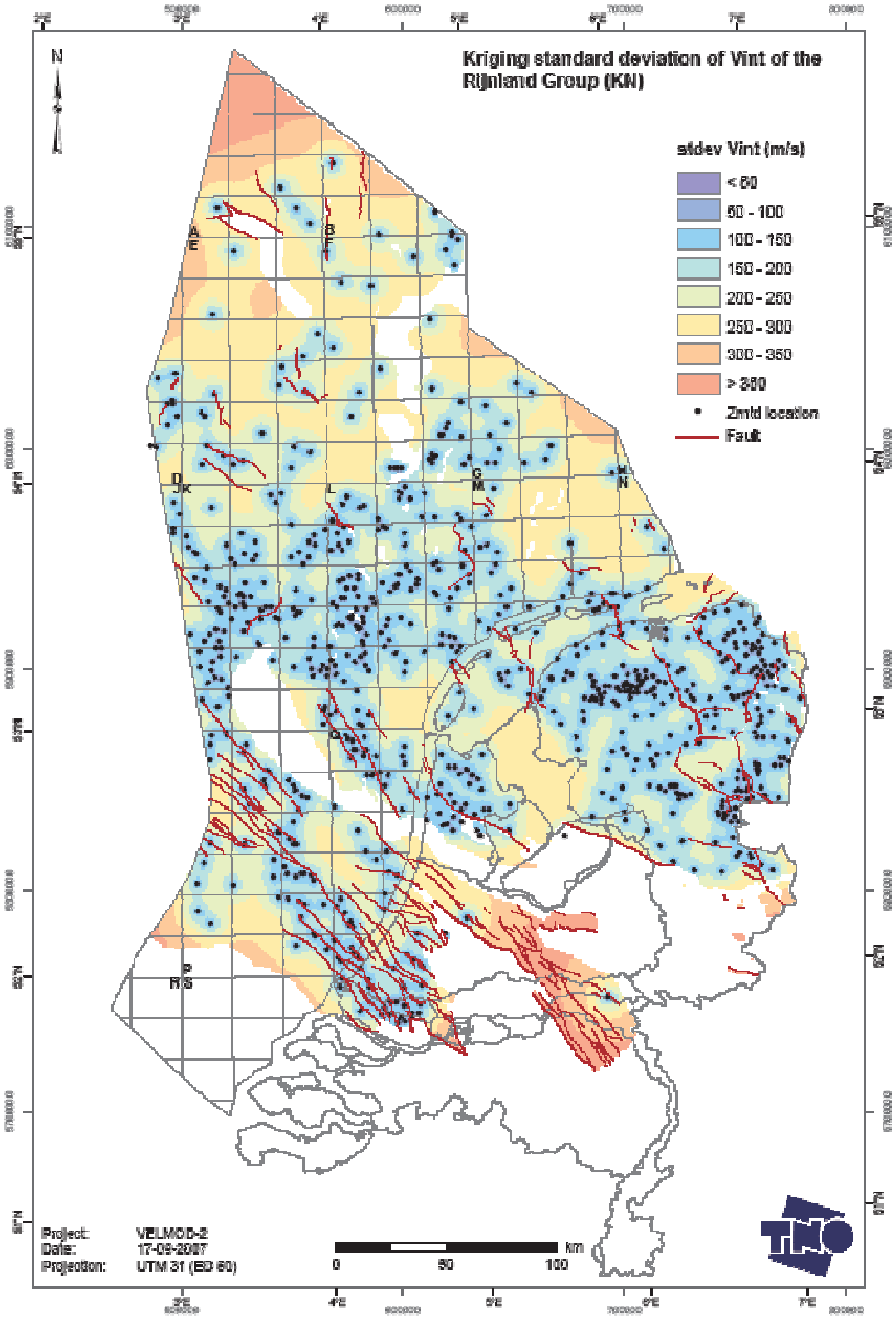

Goody 2-3 Kriging standard deviation of V_{int} for the layer of the Rijnland Group (KN)

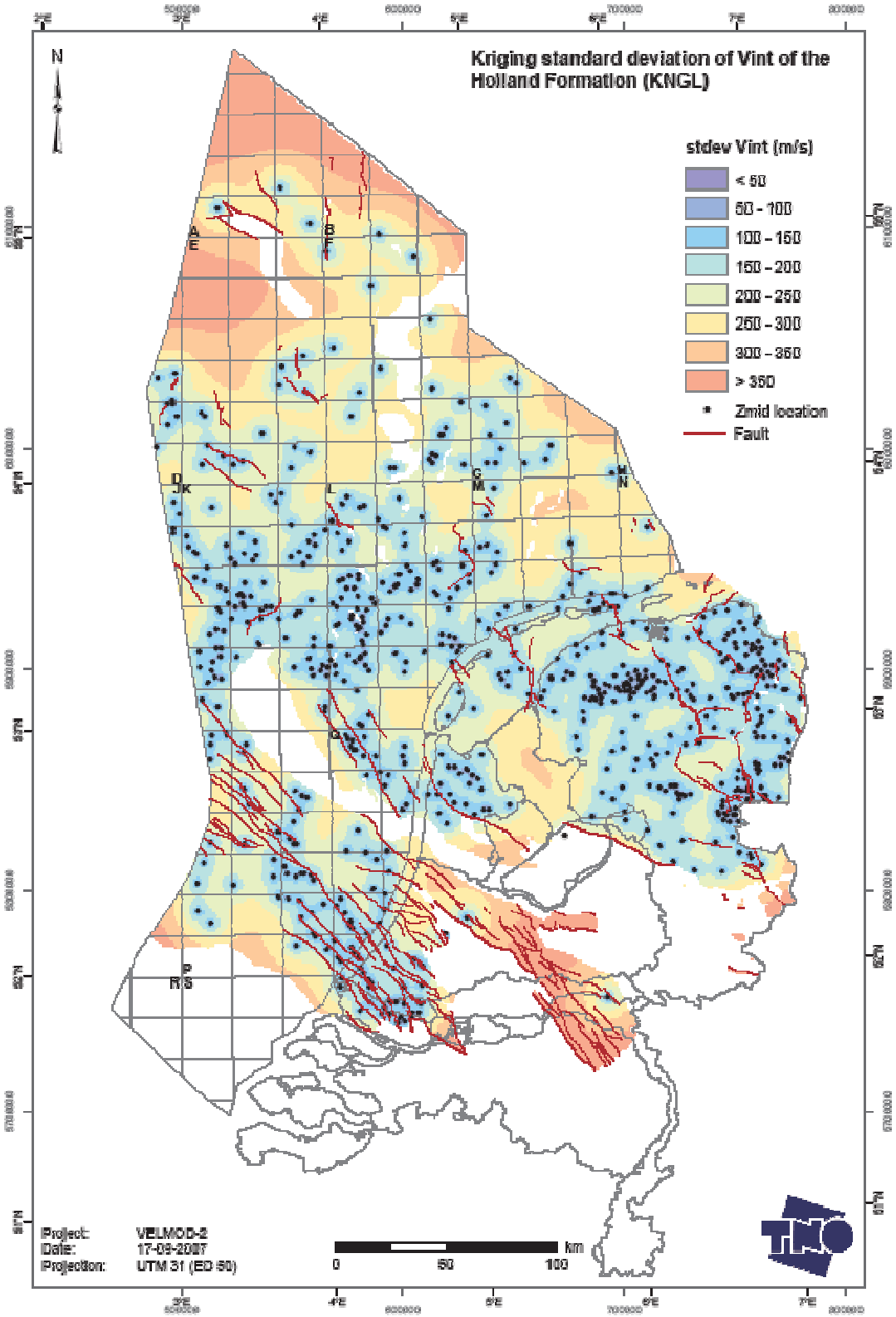

Goody 2-3a Kriging standard deviation of V_{int} for the layer of the Holland Formation (KNGL)

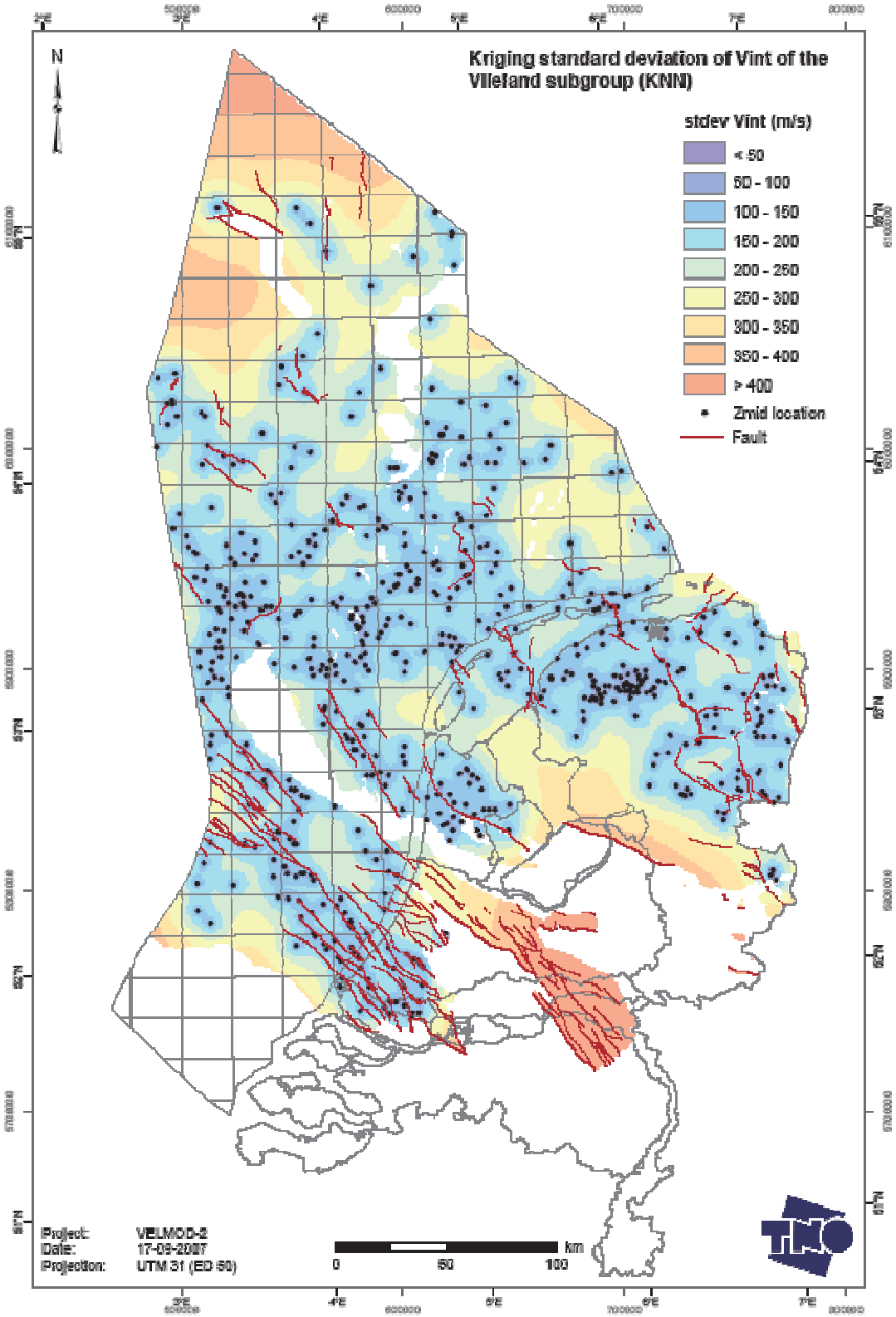

Goody 2-3b Kriging standard deviation of V_{int} for the layer of the Vlieland subgroup (KNN)

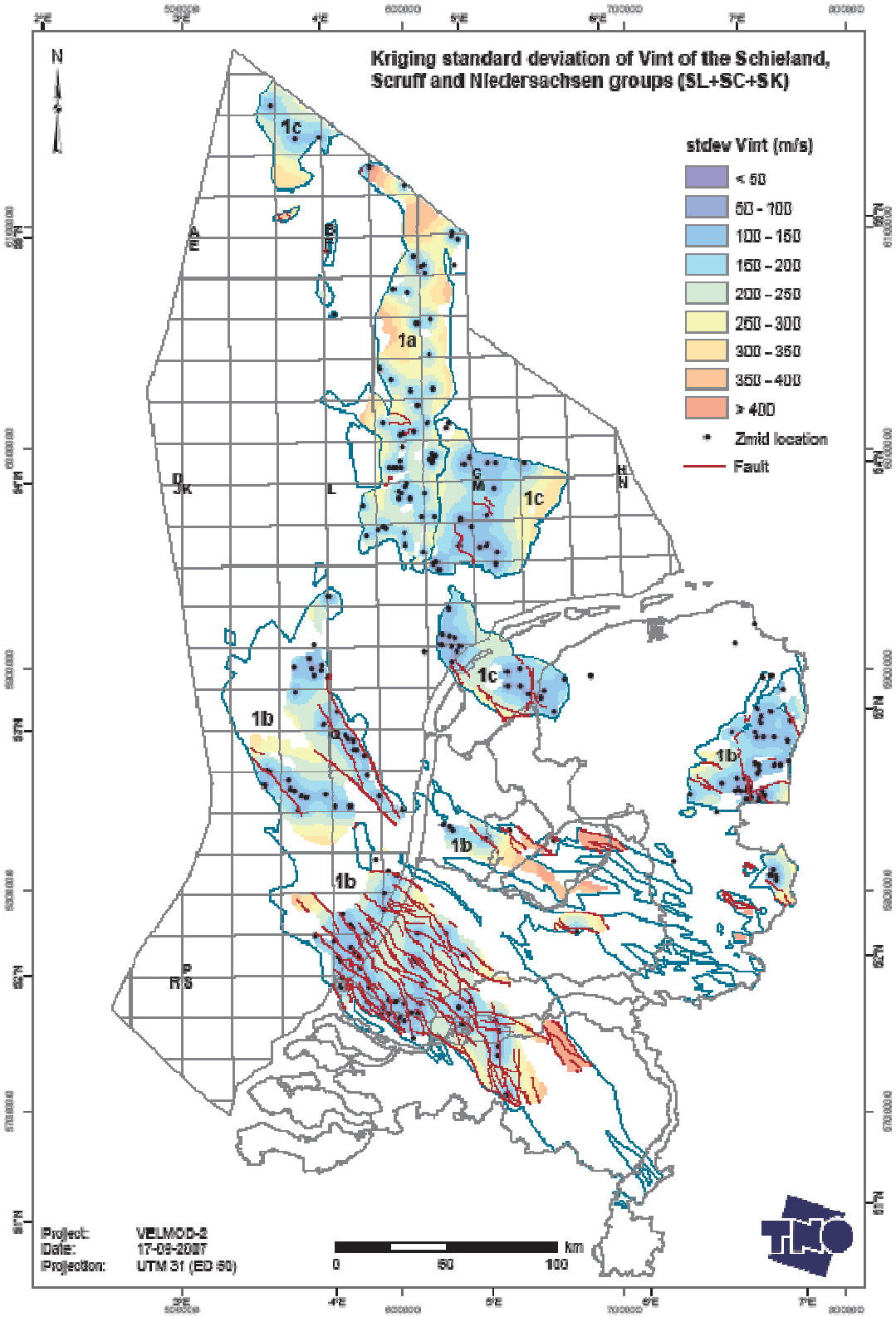

Goody 2-4 Kriging standard deviation of V_{int} for the layer of the Schieland, Scruff and Niedersachsen groups (SL+SG+SK)

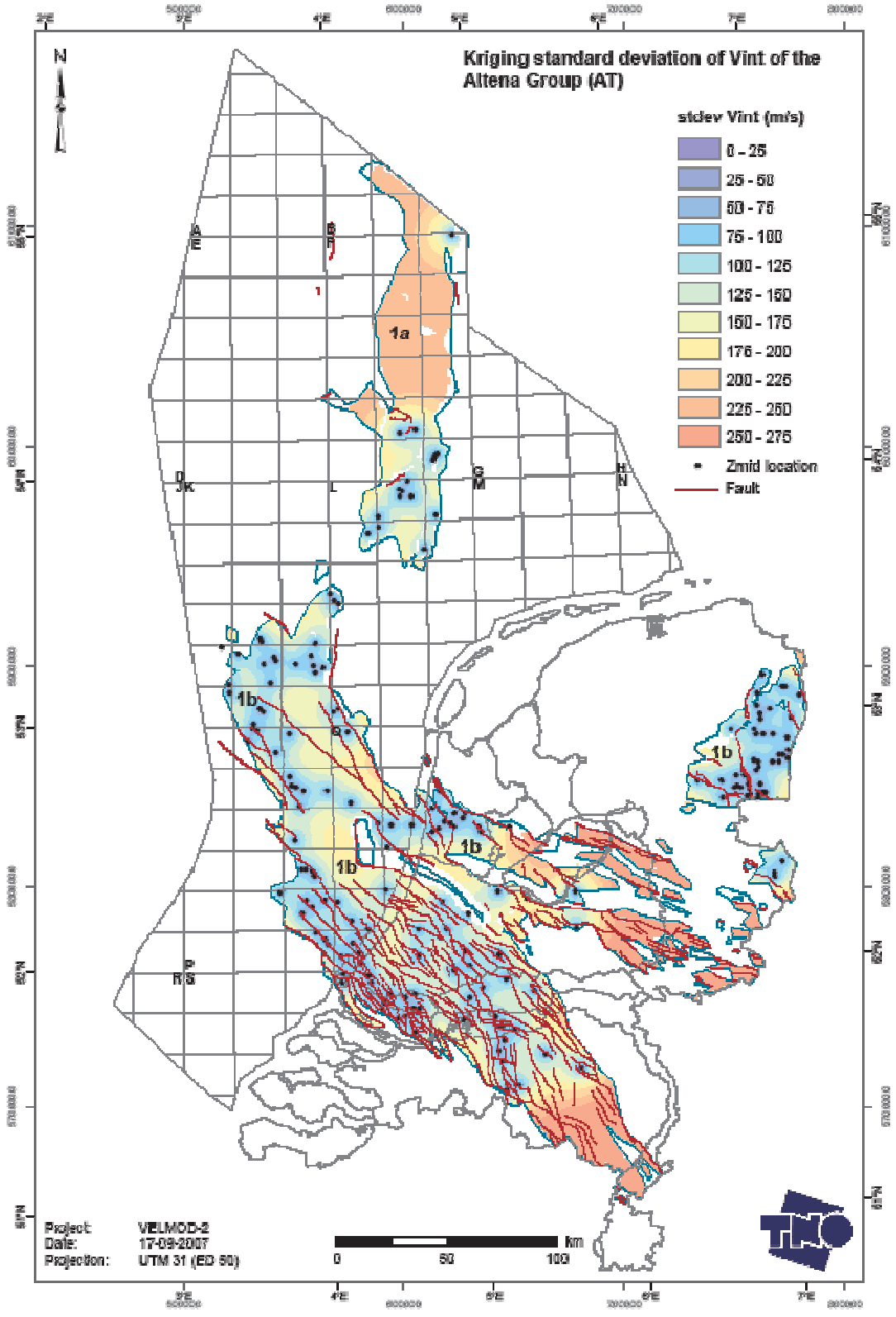

Goody 2-5 Kriging standard deviation of V_{int} for the layer of the Altena Group (AT)

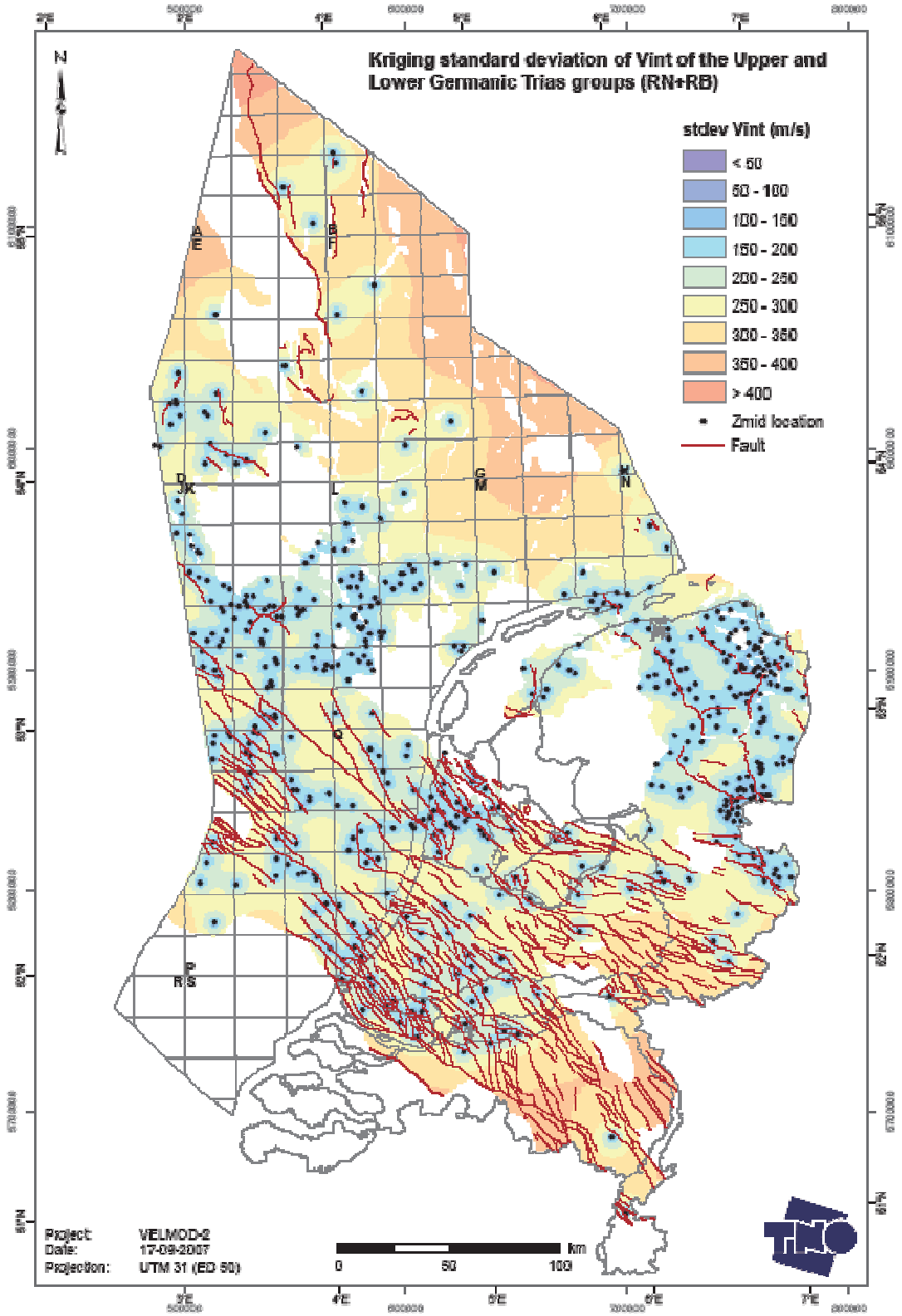

Goody 2-6 Kriging standard deviation of V_{int} for the layer of the Upper and Lower Germanic Trias groups (RN+RB)

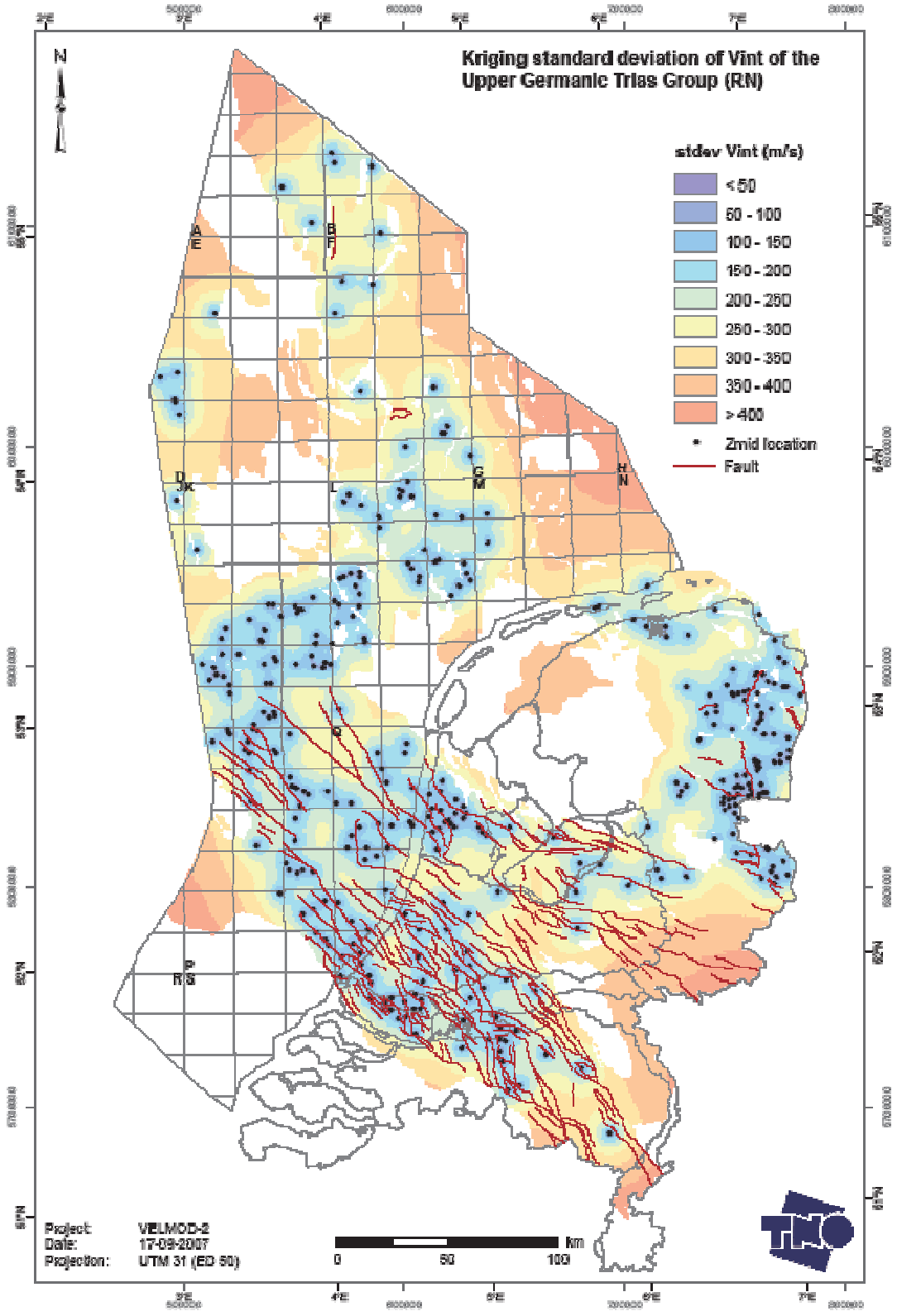

Goody 2-6a Kriging standard deviation of V_{int} for the layer of the Upper Germanic Trias Group (RN)

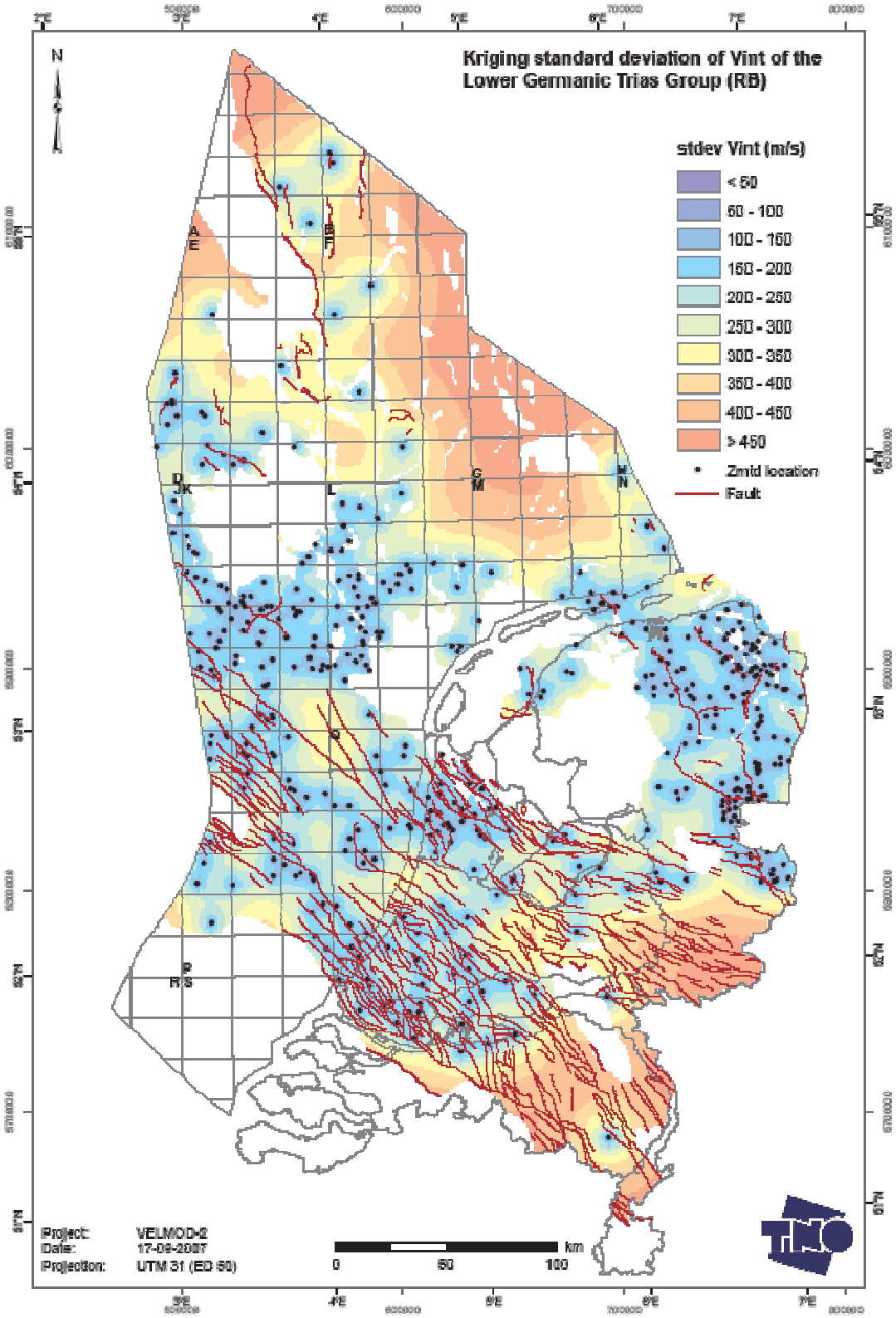

Goody 2-6b Kriging standard deviation of V_{int} for the layer of the Lower Germanic Trias Group (RB)

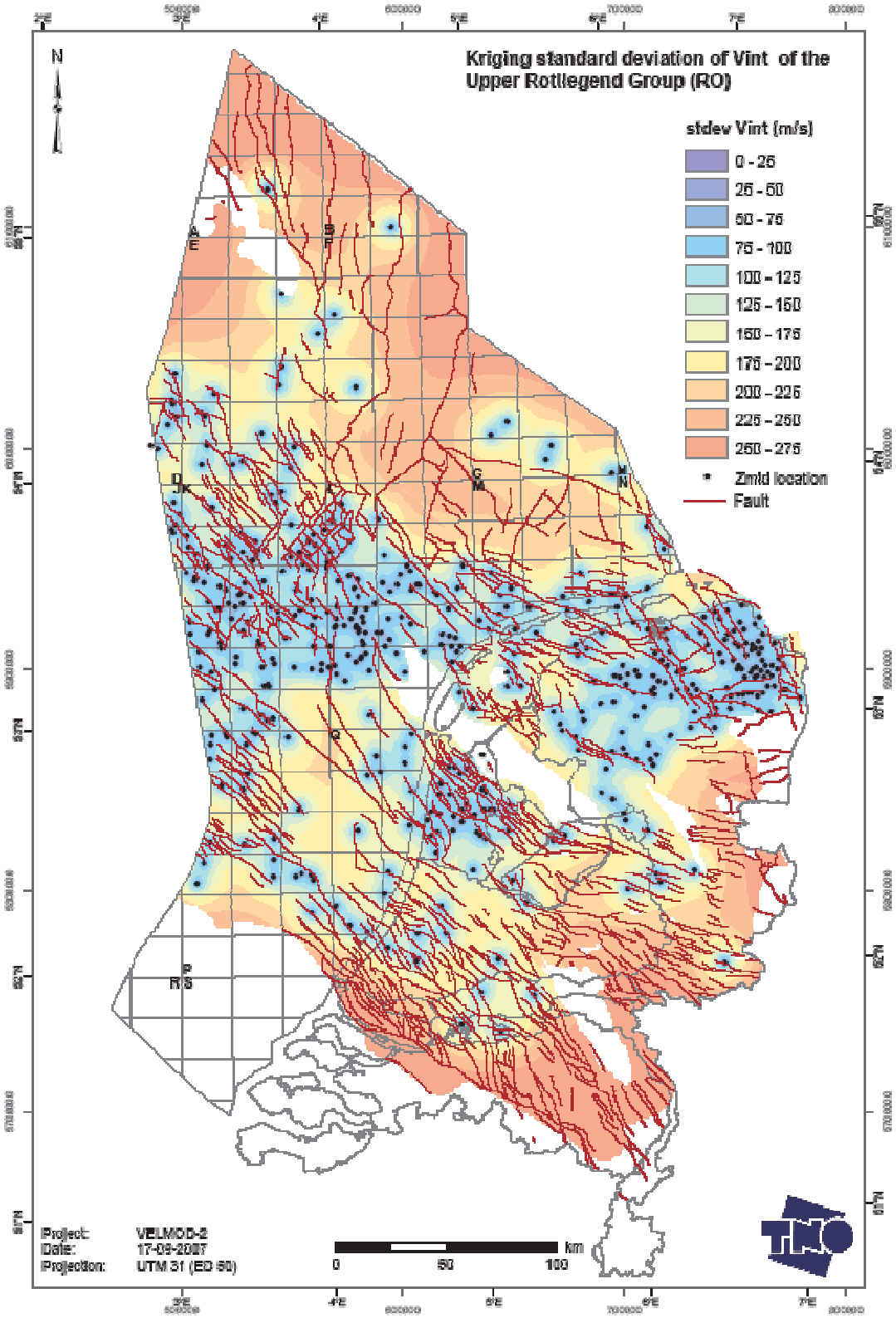

Goody 2-8 Kriging standard deviation of V_{int} for the layer of the Upper Rotliegend Group (RO)

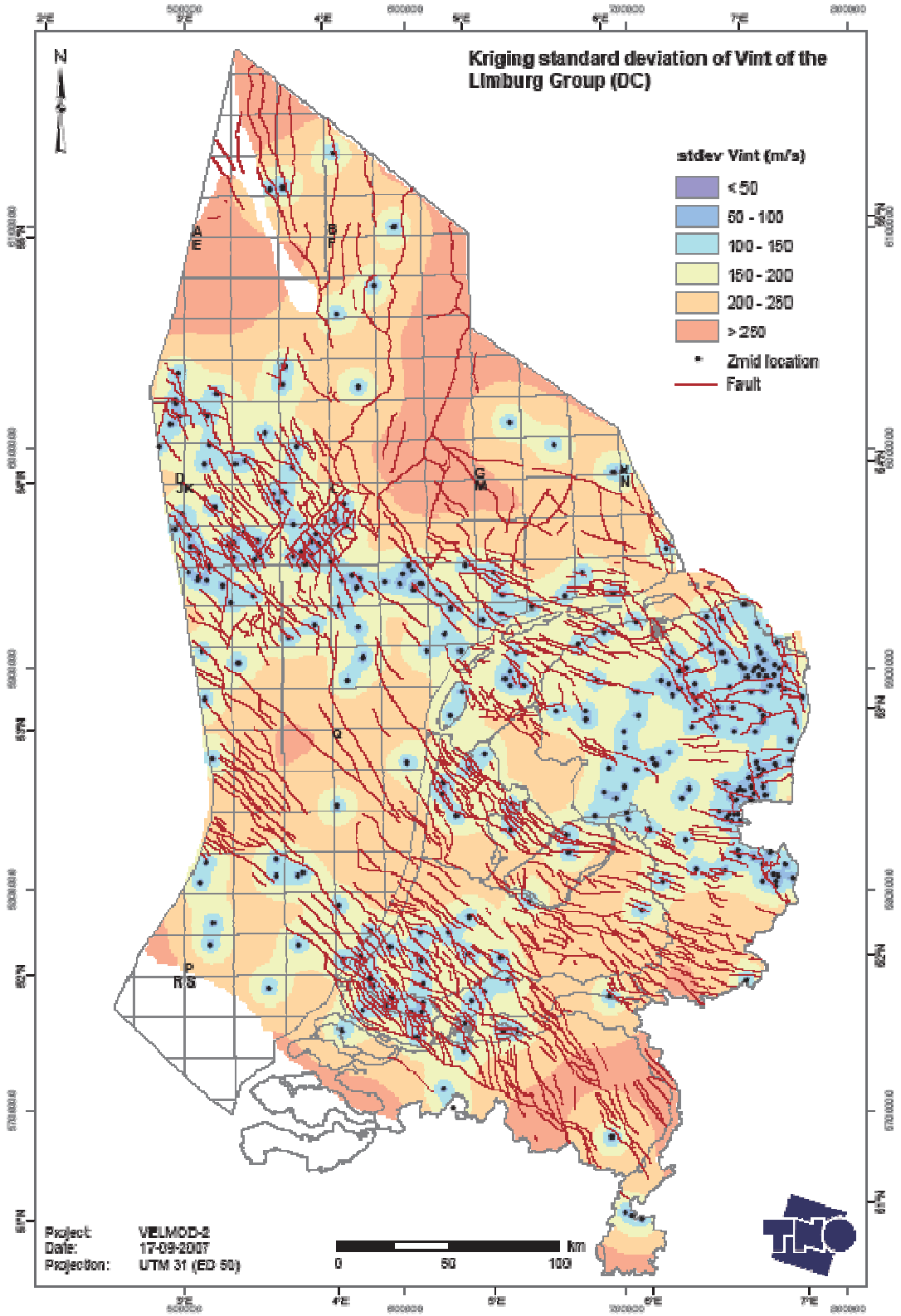

Goody 2-9 Kriging standard deviation of V_{int} for the layer of the Limburg Group (DC)

Goody 3 Variogram models of the V_{int}-values for the compacting main layers and sublayers of VELMOD-2

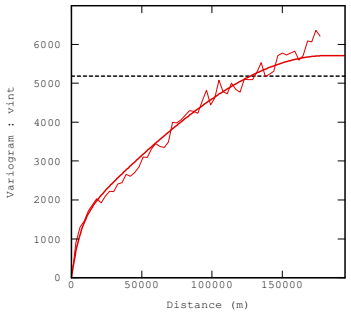

North Sea Supergroup (N)

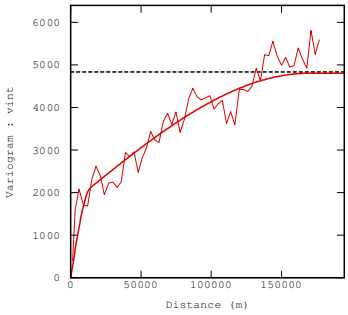

Upper North Sea Group (NU)

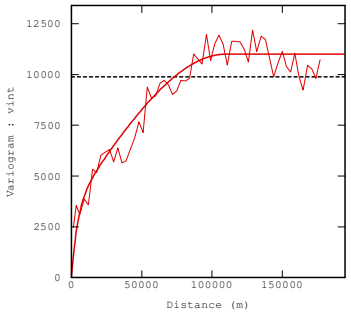

Lower and Middle North Sea groups (NM + NL)

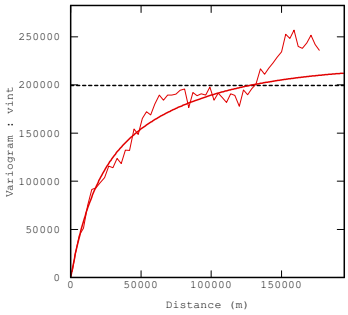

Chalk Group (CK)

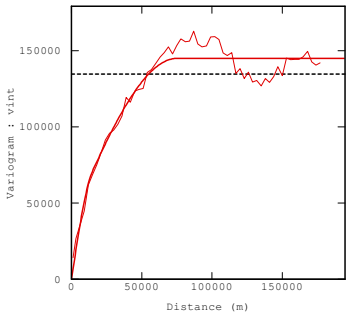

Rijnland Group (KN)

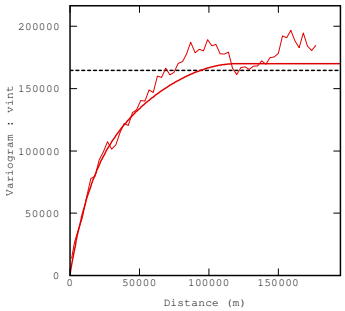

Holland Formation (KNGL)

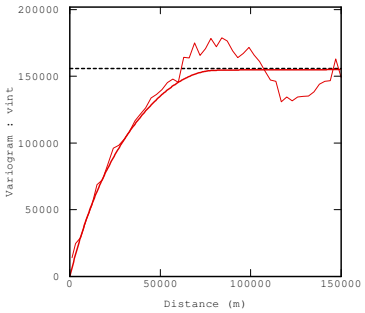

Vlieland subgroup (KNN)

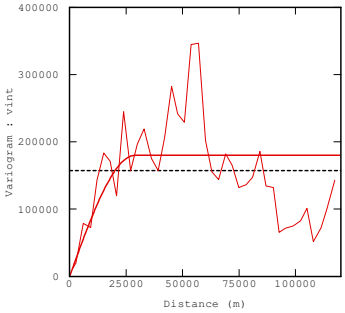

Schieland, Scruff and Niedersachsen groups (S), region 1a

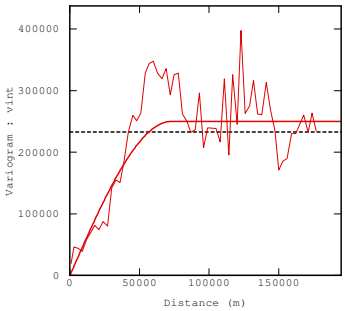

Schieland, Scruff and Niedersachsen groups (S), region 1b

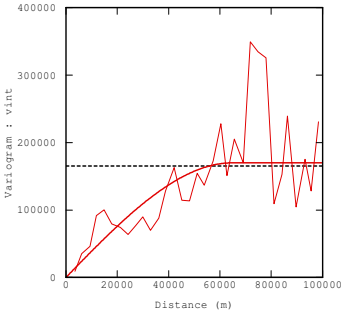

Schieland, Scruff and Niedersachsen groups (S), region 1c

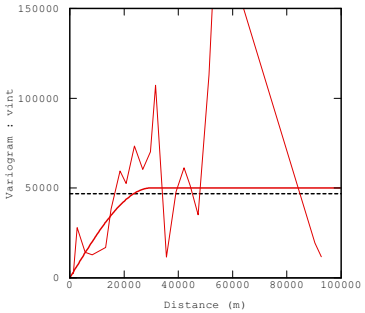

Altena Group (AT), region 1a

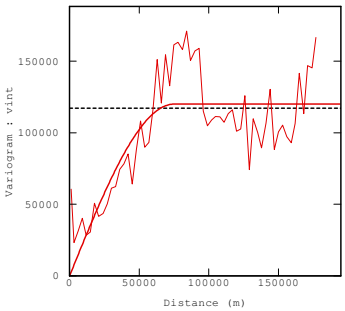

Altena Group (AT), region 1b

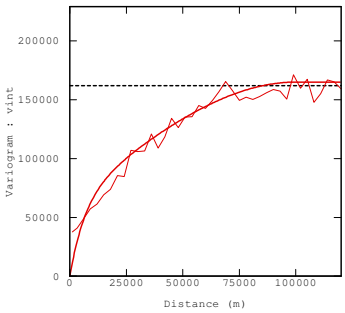

Upper and Lower Germanic Trias groups (RN+RB)

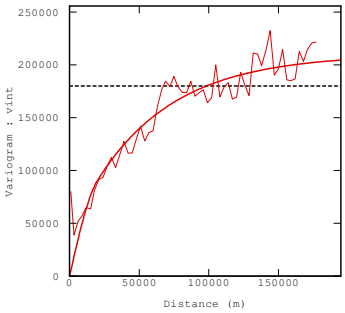

Upper Germanic Trias Group (RN)

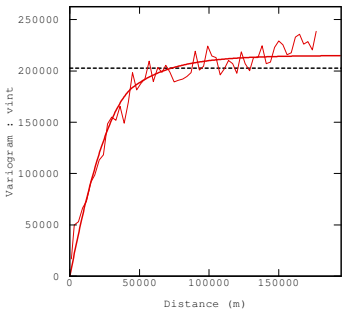

Lower Germanic Trias Group (RB)

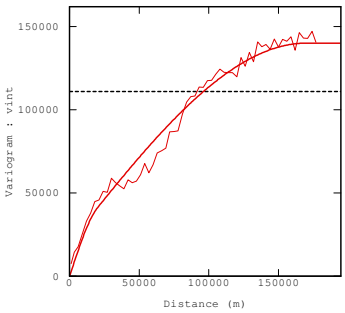

Upper Rotliegend Group (RO)

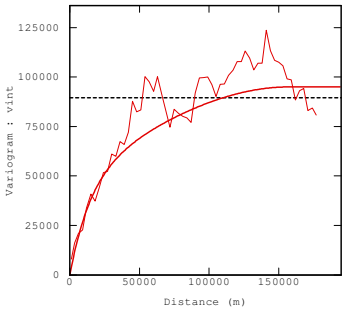

Limburg Group (DC)